UNIVERSITÀ
DEGLI STUDI
DI PADOVA

HOME INSTITUTION: UNIVERSITA' DEGLI STUDI DI PADOVA

DIPARTIMENTO DI SCIENZE DEL FARMACO

DOCTORAL DISSERTION IN :

MOLECULAR AND CELLULAR PHARMACOLOGY

XXV CICLE

METABOLIC AND MITOCHONDRIAL REMODELLING IN CISPLATIN RESISTANCE: STUDIES ON OVARIAN CANCER CELLS AND DERIVED CYTOPLASMIC HYBRIDS

Director: Ch.mo Prof. Pietro Giusti

Coordinator: Ch.mo Prof. Pietro Giusti

Supervisor :Ch.mo Prof. Laura Caparrotta

DOCTORAL CANDIDATE: Daniela Catanzaro

INDEX

ABSTRACT 1

RIASSUNTO 3

ABBREVIATIONS 5

INTRODUCTION: 9

1. OVARIAN CANCER 9

1.1 Etiology 9

1.2 Classification of ovarian neoplasms 11

1.3. Current treatments of ovarian cancer 14

2. CISPLATIN 15

2.1 Mechanism of action 15

2.2 Cisplatin resistance 19

2.3 Cisplatin and Mitochondria 23

3. ENERGETIC METABOLISM IN HEALTHY CELLS 25

4. METABOLIC REPROGRAMMING IN CANCER CELLS 28

3.1 The Warburg Effect 29

3.2 Lipogenic Phenotype 30

3.3 Key Regulators of the Metabolic Reprogramming 31

5. TRANSMITOCHONDRIAL HYBRIDS 34

AIM 37

MATERIALS AND METHODS: 39

1. Cell lines 39

1.1 Human ovarian carcinoma cell lines 39

1.2 206-ρ° cell line 39

1.3 Transmitochondrial cybrid cell lines 39

2. Cell viability assays 40

2.1. MTT assay 40

2.2 Trypan blue exclusion assay 40

2.3 Annexin V/propidium iodide staining. 40

3. ATP-luciferase assay 41

4. Oxygen consumption 42

5. Mitochondrial membrane potential (ΔΨ) and mitochondrial mass 42

5.1 Flow ytometry 42

5.2 In live cells confocal microscopy 43

6. Mitochondrial DNA analysis 43

6.1 qRT-PCR 43

6.2. Genome sequences 44

7. ^{1}H-NMR spectroscopy 44

8. Lipid droplet content 45

8.1 Flow cytometer 45

8.2. Confocal microscope 45

9. Immunoblot assay 46

10. qRT-PCR analysis 46

11. Liquid Chromatography-Mass Spectroscopy (LC-MS) 47

12. Data analysis and statistics of metabolomic results 48

12.1 Metabolite identification 49

13. Statistical analyses 49

RESULTS: 51

1. Phenotyping Of Ovarian Carcinoma Cells Sensitive (2008) And Resistant (C13) To Cisplatin 52

1.1 Oxygen Consumption 52

1.2 Effect of Galactose and Rotenone on Cell growth and ATP production 52

1. 3 Mitochondrial Mass and Membrane Potential 54

1.4 mtDNA content 56

1.5 Mitochondrial DNA Sequences 57

1.6 ^{1}H-NMR 58

1.7 Nile Red Neutral Lipid Staining 60

2. Phenotyping of Transmitochondrial Hybrids derived from 2008 and C13 Cells 61

2.1. Cell viability and apoptosis following CDDP treatment 61

2.2 Oxygen consumption 62

2.3. Effect of galactose and rotenone on Cell Growth 63

2.4 Mitochondrial Mass and Membrane Potential 64

2.5 mtDNA content 66

3. Metabolic reprogramming 67

3.1 Nuclear transcription factors and target genes 67

3.2 LC-MS 68

3.3. Effect of glutamine deprivation on cell viability 72

DISCUSSION 73

REFERENCES 77

ABSTRACT

The onset of resistance to cisplatin still limits its use in the chemotherapy of ovarian cancer and, despite several mechanisms of resistance have been discovered, they are not exhaustive. The aim of this study was to identify which other pathways are exploited by cancer cells to escape cisplatin cytotoxicity, to possibly prevent or overcome the phenomenon with new pharmacological approaches. The increase of anaerobic glycolysis, even in the presence of oxygen (Warburg effect), is the first observation indicating the alteration of energetic metabolism used by tumor cells as a strategy to adapt and grow independently from the availability of the substrate. This evidence suggested us to investigate the hypothesis that a similar metabolic strategy might be of relevance in resistance to cisplatin. Recently it has been shown that only approximately 1% of intracellular platinum is bound to nuclear DNA, while the great majority of the intracellular drug is available to interact with other nucleophilic sites including but not limited to phospholipids, cytosolic, cytoskeletal and membrane proteins, RNA and mitochondrial DNA. mtDNA, unlike nDNA, does not possess efficient repair systems and is therefore more susceptible to the onset of mutations often associated to cancer development, loss of tumor suppressor, activation of oncogenes and mitochondrial dysfunctions often related with an increase of glycolytic activity. Therefore, the aim of this study was to investigate the energetic metabolism and the mitochondrial function of cisplatin-resistant (C13) and sensitive (2008) ovarian cancer cells with different experimental approaches. Results revealed that resistant cells present a significant reduced respiratory chain activity correlated to a lower mitochondrial mass, altered mitochondrial morphology as well as a metabolomic profile typical of a lipogenic phenotype. To investigate the role of mtDNA and nDNA in the mitochondrial and metabolic remodeling of cisplatin-resistant line, cancer cells (2008-C13) were used to generate transmitochondrial hybrids (H2008-HC13). Mitochondrial DNA of parental and hybrid cells was sequenced, showing similar, almost non pathological, polymorphisms. Interestingly, investigating the energetic metabolism and the mitochondrial structure of hybrids, no differences were observed between H2008 and HC13. These data demonstrated that the metabolic reprogramming of C13 cells was not dependent from mtDNA, but was controlled by nuclear factors. Having regard to these data, the activity of some nuclear transcription factors (HIF-1α, and c-Myc) involved in the metabolic reprogramming of tumor cells, has been evaluated and it has been highlighted a different expression of some of their target genes involved in the glycolytic flux. Finally, the metabolic profile of 2008-C13 cells has been outlined by LC-MS which evidenced some interesting differences in aminoacids, phospholipids and antioxidants content.

RIASSUNTO

L'utilizzo del cisplatino nel trattamento del cancro all'ovaio è tutt'oggi limitato dall'insorgenza di chemioresistenza. Nonostante siano stati evidenziati numerosi meccanismi implicati nella resistenza al cisplatino, questo fenomeno non è ancora stato del tutto chiarito. Lo scopo di questo studio è stato quindi quello di identificare quali altre strategie vengano sfruttate dalle cellule tumorali per sfuggire alla citotossicità indotta dal cisplatino in modo da prevenire o superare la resistenza attraverso l'utilizzo di nuovi approcci farmacologici. L'aumento della glicolisi anaerobica, anche in presenza di alte concentrazioni di ossigeno (effetto Warburg), è la più nota e meglio conosciuta alterazione del metabolismo energetico utilizzato dalle cellule tumorali come strategia per adattarsi e crescere in modo indipendente dalla disponibilità del substrato. Queste evidenze scientifiche ci hanno suggerito di indagare l'ipotesi che una simile strategia possa essere rilevante nell'insorgenza della resistenza al cisplatino. Recentemente è stato dimostrato che solo ~1% del platino intracellulare si lega al DNA nucleare, mentre la gran parte del farmaco interagisce con altri siti nucleofili tra cui fosfolipidi, proteine di membrana, RNA e DNA mitocondriale. Il mtDNA, a differenza del nDNA, non possiede sistemi di riparazione efficaci ed è quindi più suscettibile all'insorgenza di mutazioni e trasformazioni oncogeniche spesso associate allo sviluppo del cancro, perdita di oncosoppressori, attivazione di oncogeni e ad alterazioni della funzionalità mitocondriale correlata ad aumento dell'attività glicolitica. Pertanto, l'obiettivo di questo studio è stato quello di studiare il metabolismo energetico e la funzione mitocondriale delle cellule di cancro ovarico sensibili (2008) e resistenti (C13) al cisplatino utilizzando diversi approcci sperimentali. I risultati hanno evidenziato che le cellule resistenti presentano una significativa riduzione dell'attività della catena respiratoria correlata ad una minore massa mitocondriale, alterata morfologia mitocondriale nonché un profilo metabolico tipico di un fenotipo lipogenico. Per studiare il ruolo del mtDNA e del nDNA nel rimodellamento metabolico e mitocondriale osservato nella linea resistente al cisplatino, le cellule tumorali (2008-C13) sono state utilizzate per generare ibridi transmitocondriali (H2008-HC13). Il DNA mitocondriale delle cellule parentali e degli ibridi citoplasmatici è stato quindi sequenziato, mostrando polimorfismi simili, ma non patologici. È interessante notare che, le differenze metaboliche e mitocondriali evidenziate nelle linee tumorali, non vengono mantenute nei rispettivi cibridi dimostrando che la riprogrammazione metabolica delle cellule C13 non è influenzata dal mtDNA, ma è controllata da fattori nucleari. Alla luce di tali dati, è stata quindi valutata l'attività di alcuni noti fattori di trascrizione (HIF-1α e c-Myc) coinvolti nella riprogrammazione metabolica delle cellule tumorali ed è stata evidenziata una diversa espressione di alcuni dei loro geni target implicati nel flusso

glicolitico. Infine il profilo metabolico delle linee 2008-C13 è stato delineato mediante LC-MS da cui sono emerse interessanti differenze nel contenuto lipidico, amminoacidico e di alcuni noti agenti antiossidanti.

ABBREVIATIONS

Abs	Absorbance
ACLY	ATP citrate lyase
BrdU	Bromodeoxyuridine
BSO	Buthiomine Sulfoximine
CA-125	Cancer Antigen 125
CDDP	Cis-diamminedichloroplatinum II
CL	Cardiolipin
DMEM	Dulbecco's modified Eagle's medium
ERCC1	Excision Repair Cross-Complementation 1
EtBr	Ethidium Bromide
FAs	Fatty Acids
FAS	Fatty Acid Synthase
FBS	Fetal Bovine Serum
FDG-PET	^{18}F-deoxyglucose Positron Emission Tomography
FIGO	International Federation of Gynecology and Obstetrics
F6P	Fructose-6-phosphate
gDNA	Genomic DNA
GOG	Gynecologic Oncology Group
G6P	Glucose-6-phosphate
G6PD	Glucose-6-phosphate dehydrogenase
Grx	Glutaredoxin
GSH	Glutathione
HGSC	High-grade Serous Carcinomas
HIF	Hypoxia Inducible Factor

HK2	Hexokinase 2
Hsp90	Heat shock protein 90
IDH	Iisocitrate dehydrogenase
LC-MS	Liquid Chromatography–Mass Spectrometry
LGSC	Low-grade Serous Carcinomas
LKB1	Liver kinase B1
MEF	Mouse Embryonic Fibroblasts
MFI	Mean Fluorescence Intensity
ML	Mobile lipid
MMR	mismatch repair
mRNA	Messenger RNA
MRP	Multi-drug Resistance Protein
MOA	Mechanism of Action
MT	Metalothioneins
mtDNA	Mitochondrial DNA
MTG	MitoTracker Green
MTT	[3-[4,5-dimethyl-thiazol-2-yl]-2,5-diphenyltetrazolium bromide
NAO	10-Nonyl bromide acridine orange
nDNA	Nuclear DNA
NEAA	Not essential Aminoacid
NER	Nucleotide Excision Repair
NMR	Nuclear Magnetic Resonance
OC	Ovarian Cacinoma
OXPHOS	Rational Treatment Strategies Combating Mitochondrial Oxidative Phosphorylation
PEG	Polyethylene glycol

Pen/Strep	Pennicilin-streptomycin
PBS	Phosphate buffered saline
PC	Phosphacholines
PCA	Principal Component Analysis
PDH	Pyruvate Dehydrogenase
PE	Phosphaethanolamines
PFK1	Phosphofructokinase 1
PPP	Pentose phosphate pathway
PS	Phosphatidylserine
PVDP	Polyvinylidene fluoride
qRT-PCR	Quantitative Real-time Polymerase Chain Reaction
Rh123	Rhodamine-123
RNAi	RNA interference
ROS	Reactive Oxygen Species
R5P	Ribose-5-phosphate
SDS	Sodium dodecyl sulfate
Ser/Thr	Serine/Threonine
TCA	tricarboxylic acid
TK-	Tyrosin-kinase deficient
TMRM	Tetramethyl Rhodamine Methyl Ester
Trx	Thioredoxin
VHL	Von Hippel-Linau
WHO	World Health Organization

INTRODUCTION

1. OVARIAN CANCER

Ovarian cancer (OC) is one of the most aggressive and lethal gynecological cancers [Jemal A. et al., (2007)] with a 5-year survival rate of approximately 45%. Around the world, more than 200.000 women are estimated to develop ovarian cancer every year and about 100.000 die from the disease. Epithelial ovarian cancer occurs most commonly in white women in the developed word and the mean age of occurrence is 56 years old [Green A. E. and Garcia A. A., (2012)].

The symptoms related to ovarian cancer, including abdominal pain, swelling or indigestion are quite vague and not disease specific [Lim M.C et al., (2009); Lim M.C. et al. (2010)] and although serum tumor markers, such as CA-125, and transvaginal ultrasonography can detect ovarian cancer, only fewer of 25% of ovarian cancer are found in the early stages and in the most cases the disease has already spread beyond the ovaries at the time of the diagnosis [Andersen M.R. et al., (2008)].

1.1 Etiology

Despite considerable efforts aimed at elucidating the molecular mechanisms of ovarian carcinoma (OC), the origin and the pathogenesis of this disease are still poorly understood [Kurman R.J. and Shih I. M., (2010)], however several risk and contributing factors have been identified.

Reproductive factors. The protective effect of parity on ovarian cancer risk is well-documented. Women who have been pregnant have a 50% decreased hazard for developing ovarian cancer compared with nulliparous women and multiple pregnancies seem to offer an increasingly protection [Whittemore A.S. et al., (1992)]. These findings support the idea that the ovarian cancer incidence is correlated with the number of ovulations and two theories regarding this relationship have been proposed. The incessant ovulation theory suggests that repeated mitotic activity required to repair the epithelial trauma caused by follicular rupture results in genetic alterations that can lead to malignant transformation [Murdoch W.J., (2003)]. The gonadotropin theory proposes that persistent stimulation of the ovaries by gonadotropins, coupled with local effects of endogenous hormones, increases surface epithelial proliferation and subsequent mitotic activity. Thus, factors that decrease the ovulatory cycles, such as pregnancy, lactation and the use of oral contraceptives, usually might have a protective role in the appearance of ovarian

cancer, while nulliparity and hormone therapies against infertility may lead to an increased ovarian cancer risk [Rossing M.A. et al. (2004); Morch L.S. et al. (2009)].

Genetic factors. The greatest risk factors of ovarian cancer are the family history and the associated genetic syndromes that are involved in the 10% of the cases. The hereditary component of ovarian cancer appears to be due to BRCA (BRCA1-BRCA2) mutations in hereditary breast-ovarian cancer syndrome [Yoshida and Miki (2004); Yang et al., (2011)] and to hMLH1 and hMLH2 mutations in hereditary non-polyposis colorectal cancer syndrome (HNPCC or Lynch II) [Bonadonna et al. (2011)]. The risk of a woman with a BRCA1 mutation developing ovarian cancer is between 36% and 46%; that of a woman with a BRCA2 mutation is estimated between 10% and 27% [Rebbeck T.R. et al., (2009)]. Both genes play important roles in genomic stability and integrity, in cell cycle control and in the apoptosis. Specifically, both genes are essential for DNA repair and activation of cell cycle checkpoint control (**Figure 1**). Repair-deficient cells (without BRCA genes) may accumulate molecular and chromosomal changes with consequent development and progress of cancer.

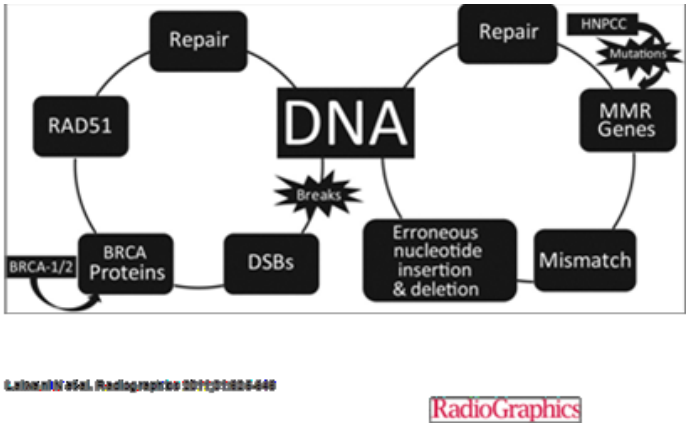

Fig. 1: Diagram illustrates the role of BRCA and mismatch repair (MMR) genes in DNA repair and in the pathogenesis of hereditary cancers.

Even if BRCA germline mutations are the most frequent in ovarian cancer, data indicate that each of the histologic OC subtypes is characterized by distinct histogenetic signatures and a unique complement of chromosomal abnormalities. High-grade serous (HGSC) and possibly endometrioid carcinomas most probably arise from surface epithelial inclusion glands with TP53 mutations and dysfunction of BRCA1 and/or BRCA2 [Kolasa et al., (2006); Salani et al., (2008)]. In contrast, low-grade serous ovarian carcinomas (LGSC) harbour alterations in KRAS, BRAF and/or HER-2 genes, implying a different route of carcinogenesis [Singer et al., (2003)]. Mucinous carcinomas arise via

an adenoma–borderline tumor–carcinoma sequence with mutations in KRAS while the characteristic genetic alterations of endometrioid carcinomas are mutations of the catenin gene (CTNNB1), PTEN and TP53.

Others factors. Although the incidence rate of ovarian cancer in Japan is significantly lower than in western countries, a remarkable change in lifestyle after World War II has increased the mortality rate by almost 4 fold [Li X.M. et al., (2003)]. This observation suggests that lifestyle may play a role in the etiology of ovarian cancer. There is some evidence that smoking, physical activity, diet, alcohol consumption and the exposure to certain environmental agents (talc, pesticides, and herbicides) may affect ovarian cancer risk. Some studies have suggested that animal derived food, such as red meat, milk, and eggs may increased serum gonadotropins (FSH and LH), which may increase the risk of ovarian cancer by directly stimulating cell proliferation and inhibiting apoptosis in the ovarian surface epithelium [Konishi I. et al., (1999)], but most studies have not identified a role for dietary fat and galactose intake in the development of ovarian cancer. Nonetheless, some studies have suggested that saturated fat consumption may result in an increased risk of epithelial ovarian cancer [Huncharek M. and Kupelnick B., (2001)]. A case-control study in Italy has shown that starch was directly associated with the risk of ovarian cancer and that unsaturated fatty acids were inversely associated with ovarian cancer risk [Bidoli E. et al.,(2002)].

1.2 Classification of ovarian neoplasms

The origin of ovarian cancer lies in the cells that constitute the ovaries including surface epithelial cells 85-90%), sex cord-stromal cells (~6%) and germ cells (<1%). The classification of ovarian epithelial tumors currently used, is based entirely on tumor cell morphology. Because of their complicated histological structure, ovaries produce several subtypes of malignant and benign tumors [Soslow R.A., (2008)]. The most common ovarian neoplasm is epithelial cancer which is traditional thought to arise from epithelium covering the ovaries. Five main histologic subtypes, which classification is entirely based on cell morphology, arise in the epithelial lining of the cervix, uterus, and fallopian tube, as follows: serous (fallopian tube); endometrioid (endometrium); mucinous (cervix); clear cell (mesonephros); Brenner.

Serous cystadenocarcinoma. This type is the most common, accounting for 40-50% of cases [Heintz A.P. et al., (2001); Quirk J.T.and Natarajan N., (2005)]. Most HGSCs arise de novo from tubal-ovarian epithelium, do not appear to be associated with macroscopic precursors and manifest with widely disseminated disease at presentation. LGSCs arise in a stepwise fashion from

cyst-adenomas and serous borderline tumors and are commonly diagnosed in the early stages of disease [Lalwani N. et al., (2011)].

Endometrioid adenocarcinoma. These tumors are malignant in 80% of cases, and represent 25% of all ovarian cancers and they have a strong association with both pelvic and ovarian endometriosis [De Priest P.D. et al., (1992)].

Mucinous cystadenocarcinoma. Traditionally they accounted for approximately 10% of all ovarian cancers, although this rate is now thought to be lower. Overall they have a relatively favorable prognosis probably because they are mostly confined in the ovary.

Clear Cell adenocarcinoma. They represent approximately 5% of ovarian cancers [Heintz A.P. et al., (2001); Quirk J.T.and Natarajan N., (2005)]; they are strongly associated with pre-existing endometriosis [Kennedy E.W. et al., (1989)] and they tend to present earlier in comparison with the other subtypes. Low response rate to chemotherapeutic drugs is typical for clear cells carcinoma.

Undifferentiated carcinomas. A significant number of epithelial ovarian cancers (5-25%) are termed unclassified or undifferentiated because their cells are so underdeveloped that is not possible to tell where they have originated.

Epithelial ovarian cancer are also classified based on their grade and stage. Historically, the most commonly used grading systems have been those proposed by the International Federation of Gynecology and Obstetrics (FIGO), the World Health Organization (WHO), and the Gynecologic Oncology Group (GOG) [Cho K.R. and Shi I.M., (2009)]. The FIGO classification of ovarian carcinoma staging (1989) is shown in **Table 1**.

TABLE 1: FIGO staging system for ovarian cancer

Stage	Characteristics
I	Growth limited to the ovaries
IA	Growth limited to one ovary; no ascites; no tumor on the external surfaces, capsule intact
IB	Growth limited to both ovaries; no ascites; no tumor on the external surfaces, capsule intact
IC	Tumor either stage IA or IB but on the surface of one or both ovaries; capsule ruptured; ascites-containing malignant cells present; or positive peritoneal washings
II	Growth involving one or both ovaries with pelvic extension of disease
IIA	Extension of disease and/or metastases to the uterus and/or fallopian tubes
IIB	Extension of disease to other pelvic tissues
IIC	Tumor either stage IIA or IIB but on the surface of one or both ovaries; capsule(s) ruptured; ascites-containing malignant cells present; or positive peritoneal washings
III	Tumor involving one or both ovaries with peritoneal implants outside the pelvis and/or positive retroperitoneal or inguinal nodes; superficial liver metastasis equals stage III; tumor is limited to the true pelvis but with histologically verified malignant extension to the small bowel or omentum
IIIA	Tumor grossly limited to the true pelvis with negative nodes but with histologically confirmed microscopic seeding of abdominal peritoneal surfaces
IIIB	Tumor of one or both ovaries; histologically confirmed implants on abdominal peritoneal surfaces, none > 2 cm in diameter; nodes negative
IIIC	Abdominal implants > 2 cm in diameter and/or positive retroperitoneal or inguinal nodes
IV	Growth involving one or both ovaries with distant metastases; if pleural effusion is present, there must be positive cytologic test results to allot a case to stage IV; parenchymal liver metastasis equals stage IV

FIGO = International Federation of Gynecology and Obstetrics

1.3 Current treatments of ovarian cancer

In the last decades, survival of patients with ovarian cancer has improved due to new cytostatic agents and to advances in surgical strategies. Treatment and prognosis depend on the type of ovarian cancer and how far it has spread at the time of the diagnosis [Cho K.R. and Shi I.M., (2009)]. Surgery, whose aim is to confirm the diagnosis, define the extent of disease, and resect all visible tumor, is the initial treatment of choice, but only a small percentage of women with epithelial ovarian cancer can be treated with surgery alone. These include patients with stage IA grade 1 and stage IB grade 1 serous, mucinous, endometrioid, and Brenner tumors. Clear-cell carcinomas are associated with a significantly worse prognosis in stage I, and patients with this histologic subtype should be considered for chemotherapy at all stages. The standard treatment of advanced ovarian cancer involves surgical resection followed by cycles of adjuvant chemotherapy with a combination of taxane and platinum compounds [Bookman M., (2005)]. Radiation has not been widely accepted as a routine treatment modality in the initial treatment of patients with epithelial ovarian cancer, despite reports of efficacy for higher-risk stage I and II disease and in stage III disease where small-volume residual disease is present after surgery. In selected cases, pelvic diseases may respond to palliative dosing regimens with minimal toxicity. Currently, the first-line treatment for ovarian cancer is a combination chemotherapy: usually a platinum-based drug, such as cisplatin or carboplatin, coupled with paclitaxel [Joerger M. et al., (2007); Vella N. et al., (2011)]. The mechanism of action (MOA) of paclitaxel is to stabilize microtubules and as a result it induces mitotic arrest and apoptosis [Xiao H. et al., (2006)]; instead, the MOA of carboplatin is to bind DNA and to form intra-strand crosslinks, inhibiting DNA replication and transcription [Wang D. et al, (2005)]. Despite high initial response rates, a large proportion of patients relapse or develops chemoresistance, resulting in a therapeutic challenge. [Fung-Kee M. et al., (2007)]. Unraveling the underlying mechanisms causing chemoresistance is crucial for personalized therapy and the improvement of patients long-term survival.

2. CISPLATIN

Cis-diamminedichloroplatinum II, best known as cisplatin (CDDP), is one of the most potent anticancer agents used in the treatment of various solid tumors including testicular, ovarian and lung cancer [Galanski M., (2006)]. Although the synthesis and the characterization of cisplatin was first reported by Peyrone in 1845, its anticancer properties was casually discovered in the middle of 1960s, when Rosenberg and co-workers studied the effects of electric fields on Escherichia coli growth [Rosenberg B. et al., (1965)]. Cisplatin cytotoxicity is believed mainly due to the ability to form inter- and intra-strand nuclear DNA crosslinks that, hindering both RNA transcription and DNA replication, can lead to cell cycle arrest and apoptosis [Wang D. et al., (2004)]. Even if the clinical benefits of cisplatin are largely recognized, the therapeutic effectiveness of the drug is limited by the severity of its side effects (ototoxicity, nephrotoxicity and neurotoxicity) [Pasetto L.M. et al., (2006)], and by the potential progression of tumor cells to a cisplatin-resistant state [Koberle B. et al., (2010)].

2.1 Mechanism of action

Cisplatin is a relatively simple planar compound consisting of a platinum atom complexed by two ammine groups and two chloride ions (**Fig. 2**).

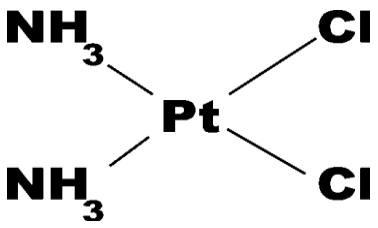

Fig. 2: cis-diamminedichloroplatinum II

Drug Accumulation. Once CDDP is intravenously administered to the patient, it rapidly diffuses into tissues and is highly bound to plasma proteins. Binding of cisplatin to plasma proteins is a result of the strong reactivity of platinum against sulphur of thiol groups of amino acids such as cysteine. Hence, near 90 % of the platinum in the blood is bound to albumin and other plasma proteins (es. gamma-globulins and transferrin) leading to inactivation of a great amount of cisplatin molecules [Judson I. and Kelland L.R., (2000)]. In blood, where the chloride concentration is relatively high (~100 mM), cisplatin exists mainly in the dichloro neutral form. Loss of the chloride groups from the cisplatin molecule is required for intracellular CDDP activity. When the neutral compound enter the cell, the relatively low chloride concentration (2-30 mM) favours the replacement of one or both chloride leaving groups by water, resulting in a positively charged molecule mono and diaquo species ($[Pt(H_2O)Cl\ (NH_3)_2]^+$ and $[Pt(H_2O)_2(NH_3)_2]^{2+}$ cations) that reacts with nucleophilic molecules such as DNA,RNA and proteins [Kartalou, M. and Essigmann, J. M. (2001)].

The biochemical mechanism by which cisplatin crosses the cell membrane still remains unclear. Early studies reported that cisplatin uptake was not inhibited by their structural analogues and the entry into the cell did not seem to be dependent on an optimum pH [Binks S.P. et al. (1990)]. On the other hand, it has been demonstrated that the uptake can clearly be modulated both by a variety of pharmacologic agents that do not cause general permeabilization of the membrane, and by activation of some intracellular signal transduction pathways. Thus, it has been proposed that ~50% of the initial rate of uptake is due to passive diffusion and the remaining 50% to facilitated diffusion through a gated channel [Gately D. P. and Howell S. B., (1993)] and growing evidences indicate that a copper transporter is involved [Ishida S. et al., (2002)], leading to propose an active transport for cisplatin in addition to passive diffusion (**Fig. 3**).

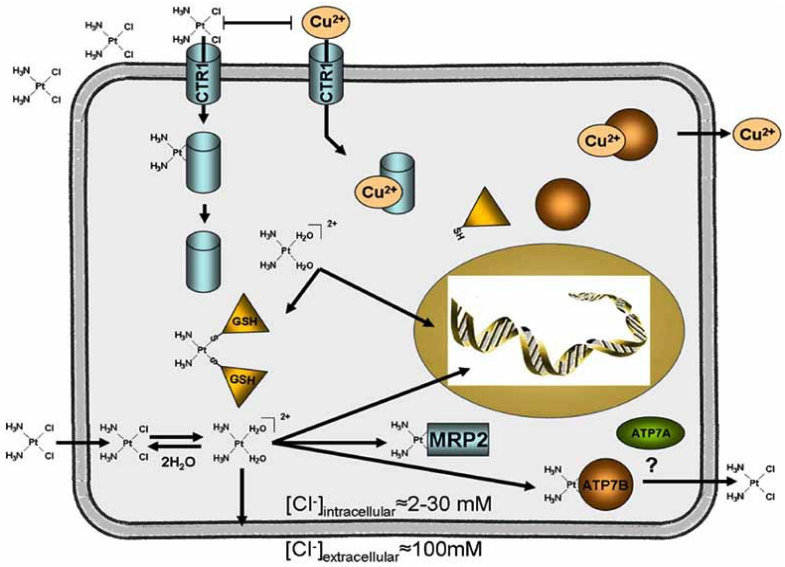

Fig. 3: Schematic cisplatin uptake and efflux and binding to nuclear DNA. In addition to passive diffusion, cisplatin is also actively uptaked through the copper transporter CTR1. Copper-transporting P-type adenosine triphosphate (ATP7B) is involved in cisplatin efflux. Both copper and *cis*-DDP show the ability to decrease the import of the other and can induce the degradation and delocalization of CTR1. Once *cis*-DDP is in the cytoplasm, it may be inactivated by gluthathione (GSH) or may bind to its main cellular target, nuclear DNA.

Binding to DNA. Experimental data accumulated over the last 35 years, indicate that DNA is the preferential and cytotoxic target of cisplatin blocking DNA replication, inducing G2 cell cycle arrest, inhibiting RNA transcription and finally promoting cell death through apoptosis [Zorbas H. and Keppler B.K., (2005), Eastman A., (1999)]. When binding to DNA, CDDP favors the N7 atoms of the imidazole rings of guanosine and adenosine, that are the most accessible and nucleophilic reactive sites for platinum coordination to DNA. As shown in **Fig. 4**, cisplatin may form several

types of lesions on purine bases of DNA: monoadducts and bifunctional adducts called intrastrand or interstrand crosslinks [Payet D.G. et al.; (1993)].

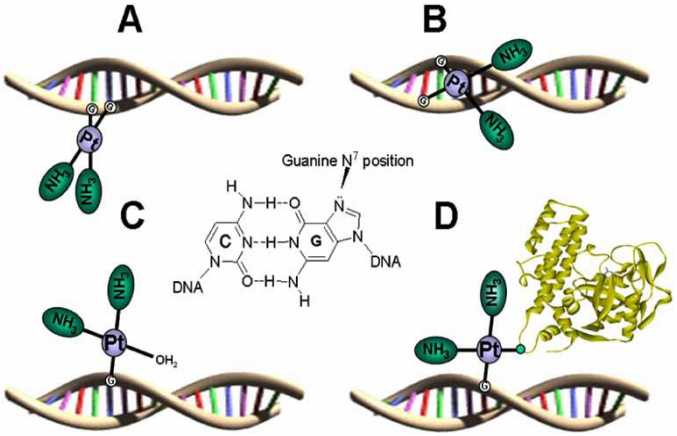

Fig. 4: Main adducts formed after binding of cis-DDP to DNA. (A) 1,2-intrastrand cross-link, (B) interstrand cross-link, (C) monofunctional adduct, and (D) protein-DNA cross-link. The main site of attack of cis-DDP to DNA (N7 of guanine) is shown in the central panel

Monoadducts are the first formed, however, greater than 90% of monoadducts then react to form crosslinks. Almost 60-65% of these crosslinks are 1,2-d(GpG) intrastrand while 20-25% are 1,2-d(ApG) intrastrand cross-links. It has been recently shown that the minor 1,3-d(GpTpG) intrastrand cross-link could be also important in the mechanism of action of cisplatin. In fact, the minor 1,3-d(GpTpG) intrastrand cross-link adduct induces in nucleosomes an asymmetric arrangement of the DNA in relation to the histone octamer, which affects the translational positioning of the DNA. All crosslinks result in contortion of the DNA [Fuertes M.A. et al., (2003)]. Both 1,2-d(GpG) and 1,2-d(ApG) intrastrand crosslinks unwind DNA by 13°, while the 1,3-d(GpXpG) intrastrand lesion unwinds DNA by 34°. Interstrand lesions induce even more steric changes in DNA, with extrusion of the cytosines at the crosslinked d(GpC)d(GpC) sites, bending of the double helix toward the minor groove by 20-40°, and extensive DNA unwinding of up to 80°.

Binding to non-DNA targets. When the drug passes through the cell membrane, the cis-Pt(II) center may coordinate to some constituents of the lipidic bilayer, which contain nitrogen and sulphur atoms including phospholipids and phosphatidylserine [Speelmans G. et al., (1997)]. In the cytoplasm many cellular components that have soft nucleophilic sites such as cytoskeletal microfilaments, RNA and thiol-containing peptides and proteins may react with cisplatin [Jordan P. and Carmo-Fonseca M., (2000); Arnesano F. and Natile G., (2008)]. Hence, of interest is the observation that only 5-10% of covalently bound cell-associated cisplatin is found in the gDNA

fraction, whereas 75-85% of the drug binds to proteins and other cellular constituents. The most important non-DNA target of cisplatin is probably the tripeptide glutathione (GSH) which is present in cells at high concentrations (0.5-10 mM). GSH and other thiol-containing biomolecules such as metalothioneins (MT) bind quickly to platinum. Cisplatin binding to GSH and MT has primarily been associated with negative pharmacological properties, including the development of resistance and toxicity. On the other hand, cisplatin may alter the activity of enzymes, receptors, and other proteins through coordination to sulfur atoms of cysteine and/or methionine residues and to nitrogen atoms of histidine residues [Arnesano F. and Natile G., (2008)]. In fact, binding of cisplatin to *N*-terminal methionine (Met1) and histidine (at position 68) of ubiquitin may inhibit the ubiquitin-proteasome pathway of selective degradation of cellular proteins, which ends up in cytotoxic events [Peleg-Shulman T. and Gibson D. J., (2001)]. In addition, it has been found that cisplatin, besides inhibiting in vitro the activity of heat shock protein 90 (Hsp90), an ATP-binding chaperone, efficiently and specifically blocks its C-terminal ATP binding site. The C-terminal of Hsp90 via its ATP hydrolytic function is involved in the correct folding of proteins which play a role in signal transduction and cell cycle regulation [Soti C. et al., (2002)].

Signaling cascades and transcription factors. A number of additional properties of cisplatin are now emerging including activation of signal transduction pathways leading to apoptosis. Firing of such pathways may originate at the level of the cell membrane after damage of receptor or lipid molecules by cisplatin, in the cytoplasm by modulation of proteins via interaction of their thiol groups with cisplatin or finally from DNA damage via activation of the DNA repair pathways [Boulikas T. and Vougiouka M., (2003)]. It was found that AKT, c-Abl, p53, MAPK/JNK/ERK/p38 and related pathways respond to presence of DNA lesions [Cepeda V. et al. (2007); Wang D. and Lippard S.J., (2005)]. AKT molecule, as most important Ser/Thr protein kinase in cell survival, protects cells from damage induced by different stimuli as well as by cisplatin [Datta S.R. et al., (1999)]. Cisplatin downregulates XIAP protein level and promotes AKT cleavage resulting in apoptosis in chemosensitive but not in resistant ovarian cancer cells [Fraser M. et al., (2003); Dan H. C. et al., (2004)]. Recently published data about synergistic effect of XIAP, c-FLIP, or NFkB inhibition with cisplatin are mainly mediated by AKT pathway [Viniegra J.G. et al. (2002)]. Protein marked as the most important in signaling of the DNA damage is c-Abl which belongs to SRC family of non-receptor tyrosine kinases [Cepeda V. et al. (2007); Wang D. and Lippard S.J., (2005)]. This molecule acts as transmitter of DNA damage triggered by cisplatin from nucleus to cytoplasm [Shaul Y., (2000)]. Moreover, sensitivity to cisplatin induced apoptosis is directly related with c-Abl content and could be blocked by c-Abl overexpression [Wang D. and Lippard S.J., (2005)].

Cisplatin induces oxidative stress and is an activator of stress-signaling pathways especially of the mitogen activated protein (MAP) kinase cascades. Cisplatin induces caspase activation in enucleated cells (cytoplasts lacking a cell nucleus) in a mechanism associated with rapid induction of cellular reactive oxygen species and increases in Ca^{2+}, induces clustering of Fas/CD95 in the plasma membrane, long-term growth arrest ("premature cell senescence"), and mitotic catastrophe [Havelka et al, (2007)]. Cisplatin induced E-cadherin cleavage resulting in disconnection of the actin cytoskeleton and accumulation of E-cadherin and beta-catenin in the cytoplasm.

2.2 Cisplatin resistance

Acquired resistance due to mutations and epigenetic events hinders the effectiveness of platinum drugs in the treatment of cancer, causing cancer relapse, failure of subsequent treatments and eventual death of patients. As shown in **Fig. 5**, resistance to cisplatin is generally considered a multifactorial phenomenon, which is mainly due to: 1. reduced drug accumulation; 2. inactivation by thiol containing species; 3. increased repair of platinum-DNA adducts; 4. increase of cisplatin adducts tolerance and failure of cell death pathways [Rabik C.A. and Dolan M.E., (2007); Boulikas T. et al., (2007)]. These mechanisms are cell line-dependent so that a particular tumor may exhibit one, two or even all the above-mentioned mechanisms [Kelland L.R. et al., (2000)].

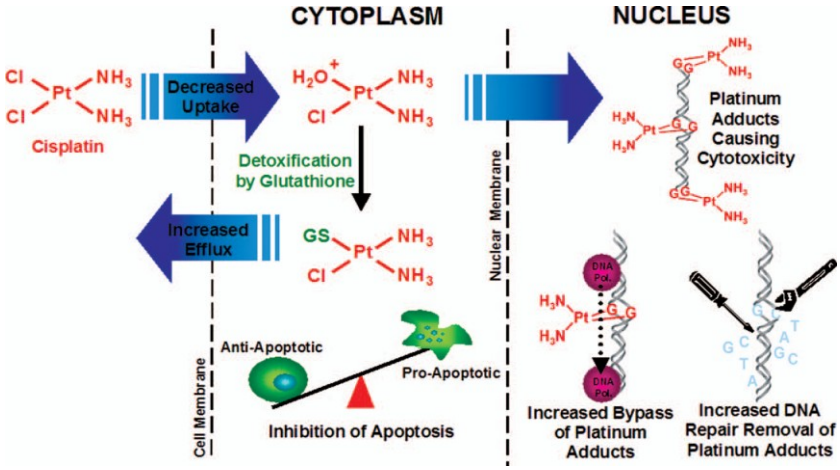

Figure 5. Cisplatin resistance mechanisms. Cisplatin is a neutral complex which on entering the cell becomes positively charged, and so able to interact with many molecules including DNA and proteins. Many mechanisms may contribute to cisplatin resistance including reduced uptake, increased efflux, increased detoxification, inhibition of apoptosis, increased ability to replicate past DNA adducts and increased DNA repair. GS–Glutathione, Pol–Polymerase.

Reduced drug accumulation. The major mechanism of resistance to cisplatin is a decreased effective concentration of intracellular drug, reduced from 20-70% [Siddik Z.H., (2003)]. This can be due either to decreased influx or increased efflux. It has long been presumed that cisplatin is taken up passively by the cell, as uptake is not saturable, nor is it inhibited by structural analogs. Interestingly, however, ouabain, a small molecule which inhibits the membrane sodium/potassium ATPase pump, blocks cisplatin import, indicating that cisplatin uptake may be dependent on the membrane potential of the cell [Andrews P.A. et al., (1988)]. Additionally, benzaldehyde and similar aldehyde molecules decrease intracellular accumulation of cisplatin by inhibiting uptake, thought to occur through formation of Schiff bases with integral membrane transport proteins [Dornish J.M. et al., (1985); Dornish J.M. et al., (1986); Dornish J.M. et al., (1989); Pettersen E.O. et al. (1986)].

Cisplatin, at plasma concentrations, not only prevents copper from being transported by the high-affinity copper transporter Ctr1, but also downregulates protein expression of Ctr1 in human ovarian carcinoma cell lines [Holtzer A.K. et al., (2004)]. More evidence for the role of copper transport in cisplatin sensitivity is based on the observation that cisplatin and copper are competitive inhibitors for the transport of the other molecule into the cell [Holtzer A.K. et al., (2004)]. Mouse embryonic fibroblasts (MEF) null for CTR1 provide 3.2-fold increased resistance as compared with transfected cells. Two other copper transporters have also been implicated in resistance to cisplatin: ATP7A/B shuttle copper between the Golgi and the plasma membrane. ATP7B was first proposed to be involved in cisplatin resistance when Komatsu *et al.* overexpressed this transporter in human epidermoid carcinoma cells and observed that these cells gained approximately 60% resistance to cisplatin more than cells transfected with empty vector [Komatsu M. et al., (2000)]. In human ovarian tumors, SKOV3, OMC6, and PA1 cells exhibit high ATP7B expression levels and SKOV3 cells, exhibiting the highest level of ATP7B expression, also showed the highest resistance to cisplatin [Nakayama K. et al, (2001)]. Additionally, eighty-two primary ovarian carcinomas were profiled for expression of several known resistance genes including ATP7B, MDR1, MRP1, MRP2, LRP, and BCRP [Nakayama K. et al, (2002)]. With the exception of ATP7B, none were indicators for resistance of ovarian cancer to cisplatin. Patients, whose carcinomas expressed high levels of ATP7B, had a significantly poorer prognosis than patients with tumors that expressed low levels of ATP7B [Nakayama K. et al, (2001)]. Additionally, it has been shown that at least one additional resistant ovarian cell line, IGROV-1/CP exhibited increased expression of ATP7B [Katano K. et al., (2002)]. ATP7A is able to sequester into vesicles not only cisplatin, but also both carboplatin and oxaliplatin. Increased expression of ATP7A in the 2008 line (2008/MNK) leads to increased resistance to all three of these agents; interestingly, overexpression leads to increased sequestration of platinating agents and not to decreased total

accumulation [Samimi G. et al., (2004)]. ATP7A is overexpressed as measured by protein levels in some cisplatin-resistant ovarian carcinoma cell lines [Katano K. et al., (2002)]. In two cell lines, A2780/CP and 2008/C13*5.25 overexpression of ATP7A was shown to be causative for resistance to cisplatin. In addition to the copper transporters, the multi-drug resistance protein (MRP) is thought to function as an ATP-dependent pump for many drugs, including cisplatin [Ishikawa T. Ishikawa T. and Ali-Osman F., (1996); Lautier D. et al., (1996)]. In rat hepatocyte cell lines treated with cisplatin, MRP-2 protein and mRNA levels increased approximately 3-fold upon treatment with cisplatin [Schrenk D. et al., (2001)]. Cisplatin also slightly increased the mRNA expression of MRP3, but did not affect MRP1 expression [Ishikawa T. et al., (1996); Schrenk D. et al., (2001)]. Using sensitive and resistant melanoma cell lines, MRP2 expression was shown to be upregulated in the cisplatin-resistant cell lines as compared to the sensitive line [Liedert B. et al., (2003)].

Drug Inactivation by thiol containing species. In the cytoplasm, platinating agents becomes aquated, which then enables them to react with thiol-containing molecules, including glutathione (GSH) and metallothioneins. Increased concentrations of these compounds are known to induce resistance against cisplatin [Siddik Z.H. et al., (2003)].

Glutathione itself acts as an antioxidant of the cell; it helps to maintain the redox environment while maintaining reduced sulfhydryl groups. Cisplatin is detoxified by glutathione through adduct formation [Rudin C.M. et al., (2003)]. Several ovarian cell lines known to be resistant to cisplatin showed a correlation between the degree of resistance and the levels of GSH, likely due to increased d-glutamylcysteine synthetase [Godwin A.K et al., (1992)]. In bladder carcinoma cisplatin-resistant, exposure to buthiomine sulfoximine (BSO), an inhibitor of glutathione synthesis, resulted in a significant enhancement in cisplatin cytotoxicity [Byun S.S. et a., (2005)]. Additionally, indomethacin significantly decreases cellular concentrations of GSH and sensitizes bladder carcinoma cells to cisplatin treatment [Byun S.S. et a., (2005)]. However, neither of these treatments sensitizes these cells to the level of their parent sensitive strain, indicating that glutathione is only one component of cisplatin resistance [Byun S.S. et a., (2005)].

Thioredoxin (Trx), similar to glutathione, regulates the oxidation reduction environment of the cell [Amer ES. J. et al., (2001)] and also, it is involved in the regulation of transcription factors, apoptosis, and DNA synthesis, among others. Trx is reduced by thioredoxin reductase (TrxR), which involves the oxidation of NADPH [Witte A.B. et al., (2005).]. In clinical samples, Trx levels correlate with cisplatin resistance in bladder, prostate, liver, gastic, and colon cancer cells [Amer ES. J. et al., (2001)]. No study has shown that glutaredoxin (Grx), the analogous enzyme to TrxR in the glutathione system, is inhibited by cisplatin; however, the glutathione-cisplatin adduct (GS-Pt) is also able to inhibit both mammalian TrxR1 and Grx [Amer ES. J. et al., (2001)].

Metallothioneins (MT) are very low molecular weight proteins comprised of several cysteine and aromatic amino acid residues [Siegsmund M.J. et al., (1999)]. MT are thought to be involved in controlling levels of copper and zinc, as well as protecting cells from oxidative stress and toxicities associated with heavy metals, including copper, cadmium, and zinc [Siegsmund M.J. et al., (1999); Toyoda H. et al., (2000)]. High levels of MTII have been described in cisplatin-resistant cell lines, and cisplatin-resistant bladder cancer lines exhibit cross resistance to cadmium [Siegsmund M.J. et al., (1999)]. Human bladder cancer xenografts [Toyoda H. et al., (2000)] and esophageal [Hishikawa Y. et al., (1999)] and transitional cell primary carcinomas [Siu L.L. et al., (1998)], that express high levels of MT, exhibit less of a clinical response to cisplatin. In head and neck cancers, cisplatin induces metallothionein expression [Muramatsu Y. et al., (2000)], while in germ cell and testicular tumors, no relationship between MT and cisplatin was observed [Meijer C. et al., (2000)]. Therefore the association of MT levels with cisplatin resistance may be tissue specific and may play a minor role depending on the cellular environment.

Increased repair of platinum-DNA adducts**.** Alteration in the structure of the DNA molecule, leads to cellular DNA damage recognition and repair, resulting in platinum resistance. It appears that tumor cells can have intrinsic differences in DNA repair mechanisms when compared with their normal counterparts, although alterations may also be acquired. The role that DNA repair pathways play in mediating platinum resistance has been studied for many years, first in the preclinical, and more recently, in the clinical setting, and this knowledge has been used prospectively in the clinical arena [Cobo M. et al., (2007)].

Platinating agent adduct repair occurs primarily through Nucleotide Excision Repair (NER) [Rabik C.A. et al., (2007)]. NER is an ATP-dependent multiprotein complex that recognizes the binding induced on DNA by 1,2-intrastrand cross-links, and subsequently excises the DNA that includes as 27- to 29-base-pair oligonucleotides. The gap that remains is then filled by DNA polymerase [Chaney S.G. and Sancar A. J.; (1996)]. However all three types of intrastrand crosslinks (1,2-d(ApG), 1,2-d(GpG), and 1,3-d(GpNpG)) are recognized by the NER mechanism, the 1,2 intrastrand crosslinks are repaired less efficiently than the 1,3 intrastrand crosslinks, supporting the hypothesis that the 1,2 intrastrand crosslinks are the cytotoxic lesion [Zamble D.B. et al., (1996); Moggs J.G. et al., (1997)]. The excision repair cross-complementation group 1 (ERCC1) protein plays a key role in nucleotide excision repair. ERCC1 dimerizes with xeroderma pigmentosum complementation group F, and this complex is required for the excision of the damaged DNA. One of the most impressive and important successes of cisplatin-based therapy is in its role in treating metastatic testicular cancer which has resulted in >90% of patients achieving cure [Bosl G.J. and Motzer R.J., (1997)]. Studies of testicular carcinoma cell lines were notable for

exquisite cisplatin sensitivity in comparison with cell lines derived from other cancers [Welsh C. et al., (2004)]. Further in vitro study showed a deficiency in nucleotide excision repair in these cell lines, and in particular, reduced levels of ERCC1 and xeroderma pigmentosum complementation group F DNA repair proteins [Welsh C. et al., (2004); Koberle B. et al., (1999)]. This finding has also been shown in multiple studies with human ovarian cancer cell lines, including cell lines with intrinsic cisplatin resistance which showed increased sensitivity to cisplatin after antisense RNA inhibition of ERCC1 [Selvakumaran M. et al., (2003)]. In addition, cell lines that develop resistance in vitro after exposure to cisplatin chemotherapy were found to have increased expression of ERCC1 [Ferry K.V. et al., (2000)].

Mismatch repair (MMR) is a highly conserved, strand-specific repair pathway which follows a stepwise process, initiated with the recognition of DNA damage [Kunkel T.A. and Erie D.A., (2005); Jascur T. and Boland C.R., (2006)]. The mismatch repair system involves at least five proteins (MLH1, MSH2, MSH3, MSH6 and PMS2) and functions as a repair mechanism that needs ATP [Fishel R., (2001)]. Platinum complexes interfere with normal MMR activity and prevent a repair from being completed. Inability to complete the repair of the DNA damage leads to apoptosis. When MMR is deficient, cells can continue to proliferate in spite of DNA damage caused by platinating agents, and are thus resistant [Peltomaki P., (2003)] Tumor cells deficient in MMR are 2-3 fold more resistant to cisplatin treatment compared to cells proficient in MMR [Stojic L. et al., (2004)]. Defects in MMR may be inherited, as in the case of hereditary nonpolyposis colorectal carcinoma or may occur through epigenetic silencing of an essential MMR gene [Peltomaki P., (2003); Suzuki H. et al., (1999); Esteller M., (2000)]. Epigenetic silencing of MMR seems to occur most often through Mut L homologue 1 (hMLH1) promoter hypermethylation, as has been shown in ovarian, endometrial, gastric, and colorectal carcinoma, among others [Peltomaki P., (2003); Geisler J.P. et al., (2003); Bignami M. et al., (2003)]

2.3 Cisplatin and Mitochondria

While most investigations of cisplatin cytotoxicity have been focused on interactions between cisplatin and nuclear DNA, only approximately 1% of intracellular platinum is bound to nuclear DNA, with the great majority of the intracellular drug available to interact with other nucleophilic sites on other molecules, including but not limited to phospholipids, cytosolic, cytoskeletal and membrane proteins, RNA, and mitochondrial DNA [Fuertes M.A. et al., (2003); Gonzalez V.M. et al., (2001)].

Mitochondria are subcellular organelles involved in critical cellular processes, from energy production to apoptosis. They are rod-shaped structures that are enclosed within two membranes each composed of a phospholipid bilayer. The two membranes are quite distinct in appearance and in physico-chemical properties, thus determining the biochemical function of each membrane. The inner membrane encloses and convolutes into the mitochondrial matrix, forming cristae. This serves to increase the surface of the inner membrane, which carries the main enzymatic machinery of oxidative phosphorylation. The outer membrane is a simpler structure, containing protein called porins which permit the interchange of molecules such as ions, nutrient molecules, ATP and ADP. On contrary, the inner membrane is freely permeable only to oxygen, carbon dioxide, and water. Its structure is highly complex and includes all the complexes of the electron transport system, the ATP synthetase complex, and transport proteins. The membranes create two compartments: the intermembrane space that has an important role in oxidative phosphorylation [NelsonD.L and Cox M.M, (2002)]. The oxidative processes of cells use to degrade fuel molecules yield NADH and FADH2 which are used as electron donors for the electron transport chain. These are the basis of chemiosmotic theory that postulates the coupling of respiration and ATP synthesis in mitochondria [Mitchel P., (1965)]. The free energy of electron transport is conserved by the proton gradient, which is built up by the enzymatic complexes of the electron transport chain. These complexes pump protons from the matrix to the intermembrane space and create an electrochemical gradient across the inner membrane. This gradient then enables the ATPase to synthesize ATP. The electrochemical gradient, resulting in a negative charge within mitochondria, may play a role in the accumulation of positively charged cisplatin in this organelle [Cullen K. J. et al., (2007)].

Mitochondria contain their own DNA (mtDNA) that is transcribed and translated to synthesize 13 proteins of the mitochondrial electron transport chain [Fernandez-Silva P. et al. (2003)]. Cisplatin may crosslink also mitochondrial DNA that, lacking nucleotide excision repair, is significantly more sensitive than nDNA to the damage [Preston T.J. et al., (2001)]. Indeed, mitochondria are thought to be a major target for cisplatin in cancer cells [Tacka, K. A. et al., (2004)] and alterations in mitochondrial function (reduced mitochondrial respiration and ATP production) have been investigated in cancer cell resistance [Harper M. E. et al., (2002)]. Recent findings has shown that cells depleted of mtDNA show significant resistance to cell death induced by cisplatin [Park S.Y. et al., (2004); Montopoli M. et al., (2009)], confirming that mtDNA is a major target of CDDP.

Furthermore mitochondrial damage by cisplatin has been increasingly studied as a mediator of systemic toxicity such as gastrointestinal toxicity, ototoxicity [Devarajan P. et al., (2002)] and nephrotoxicity [Park M.S. et al. (2003)].

3. ENERGETIC METABOLISM IN HEALTHY CELLS

In normal cells a large amount of ATP is required to replicate all cellular contents: glucose participates with two ATP molecule synthesis through glycolysis and up to 36 ATPs through its complete catabolism by the TCA cycle and OXPHOS (oxidative phosphorylation). The large requirements for nucleotides, amino acids, and lipids are provided by intermediate metabolites of these pathways. In addition to glucose, glutamine is catabolized in appreciable quantities for most mammalian cells growing in culture. Therefore glucose and glutamine both supply carbon, nitrogen, free energy, and reducing equivalents necessary to support cell growth and division. This means that glucose, in addition to being used for ATP synthesis, should also be diverted to macromolecular precursors such as acetyl-CoA for fatty acids, glycolytic intermediates for non-essential amino acids, and ribose for nucleotides to generate biomass.

Glycolytic pathway. Glucose enters the cell through glucose transporters (GLUTs) and thereafter it is phosphorylated to glucose-6-phosphate (G6P) by hexokinase 2 (HK2). Phosphoglucose isomerase catalyzes G6P to fructose-6-phosphate (F6P), which yields fructose-1,6-biphosphate by phosphofructokinase 1 (PFK1), and then pyruvate and ATP by pyruvate kinase (PK) in the final step of glycolysis. Pyruvate is converted to acetyl-CoA, which enters the TCA cycle. Ultimately, glycolysis produces two ATP molecules and six NADH molecules per glucose. In normal tissues, most of the pyruvate is directed into the mitochondrion to be converted into acetyl-CoA by the action of pyruvate dehydrogenase (PDH) or transaminated to form alanine (**Figure 6**).

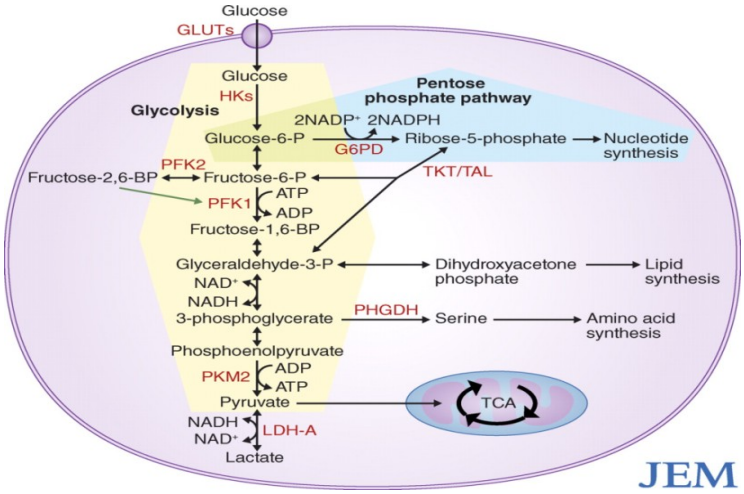

Fig. 6: Metabolic pathways involved in glucose metabolism

Pentose phosphate pathway (PPP). This is a metabolic pathway that generates NADP and pentose sugars from G6P. The enzyme that governs the entry of G6P into this pathway is glucose-6-phosphate dehydrogenase (G6PD), which is regulated by the availability of its substrate and the NADPH to $NADP^+$ ratio [Saiati L.M. and Amir-Ahmady B., (2001)]. G6P is converted to ribose-5-phosphate (R5P) while producing two molecules of NADPH (**Figure 6**). NADPH is both a major cellular antioxidant, maintaining glutathione in a reduced state to prevent oxidative damage, and a required cofactor in the reductive biosynthesis of fatty acids, nucleotides, and amino acids. NADH is also used in mitochondrial OXPHOS.

Tricarboxylic acid (TCA) cycle. Pyruvate produced by glycolysis is converted to acetyl-CoA, which enters the TCA cycle, and citrate, α-ketoglutarate, succinyl-CoA, fumarate, malate, and oxaloacetate are produced as intermediate products (**Figure 7**). Most of the carbon for fatty acids derives from acetyl-CoA synthesized in the mitochondrial matrix. However, acetyl-CoA cannot cross the inner mitochondrial membrane, but intramitochondrial acetyl-CoA and oxaloacetate combine to form citrate, which is transported out of the mitochondria and broken back down into its constituents by ATP citrate lyase (ACLY). Acetyl-CoA is converted to malonyl-CoA by acetyl-CoA carboxylase, and acetyl-CoA and malonyl-CoA are then both used by the multi-subunit enzyme fatty acid synthase (FAS) for the synthesis and elongation of fatty acid chains. Oxaloacetate is used for the synthesis of non-essential amino acids. Cytosolic and nuclear acetyl-CoA is also a precursor for the post-translational modification of proteins (for example, histones) by acetylation. Similarly to citrate, malate produced in the TCA cycle leaves the mitochondria, and it is converted to pyruvate plus NADPH. Citrate might also be converted to isocitrate and then to α-ketoglutarate, generating another molecule of NADPH by the action of isocitrate dehydrogenase 1 (IDH1).

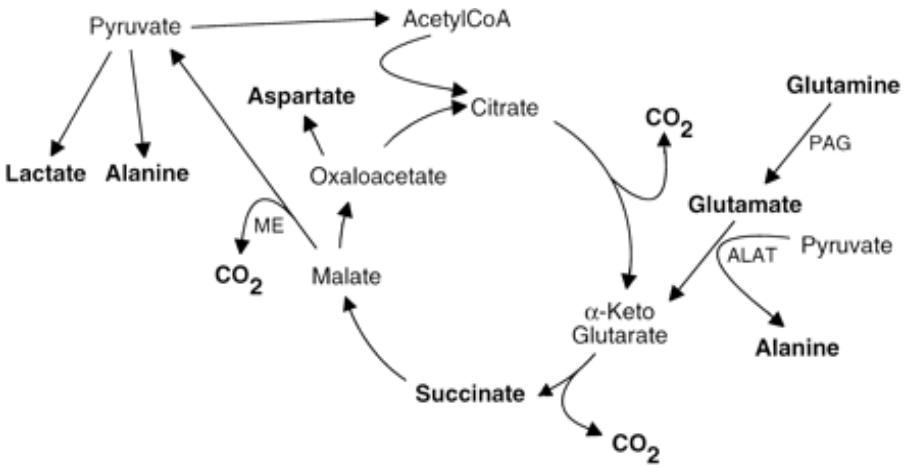

Fig. 7: TCA cycle and glutamine metabolic pathways.

Glutaminolysis. After glutamine is taken into the cell, a mitochondrial-associated enzyme, glutaminase-1 (GLS), converts it to glutamate. Glutamate is converted to α-ketoglutarate and enters the TCA cycle in the mitochondria (**Fig. 7**). Glutamate can also be converted to aspartate, which contributes to nucleotide synthesis. The excessive quantity of glutamine used by the cells results in alanine and ammonium secretions. Furthermore glutamine contributes both to the substrate needs of a dividing cell and of redox potentials through the NADH synthesis of.

4. METABOLIC REPROGRAMMING IN CANCER CELLS

The uncontrolled cell proliferation that characterizes the essence of neoplastic disease, involves not only deregulated control of cell proliferation, but also corresponding adjustment of energy metabolism in order to fuel cell growth and division [Hanahan D. and Weinberg R.A.; (2011)]. This means that, in contrast to normal cells, cancer cells metabolism appears to be adapted to facilitate the up-take and the incorporation of nutrients needed to generate a new cell [Vander Heiden M.G. et al., (2009)]. Indeed, several altered oncogenes and tumour suppressor genes, directly control and activate metabolic pathways that maintain and enhance an efficient wiring between glycolysis, oxidative phosphorylation, the pentose phoshate pathway and glutamine metabolism, that allows for both NADPH production and Acetil-CoA flux to the cytosol for lipid synthesis [Menedez J.M.; (2010)]. Several important hallmarks of the metabolic reprogramming include an increase of protein and DNA synthesis and the functionally relationship between the glycolytic pathway and the increased de novo fatty acids synthesis [Kuhajda F.P; (2000)]. By shifting from oxidative to glycolytic metabolism cancer cells catabolize glucose at a rate that exceeds bioenergetic need [Shaw R.J., (2006); Bui T. and Thompson C.B., (2006)]. In this scenario tumor cells can redirect the excess glycolytic intermediates toward the novo fatty acids synthesis (**Figure 8**) [Menendez J.M. and Lupu R., (2007)].

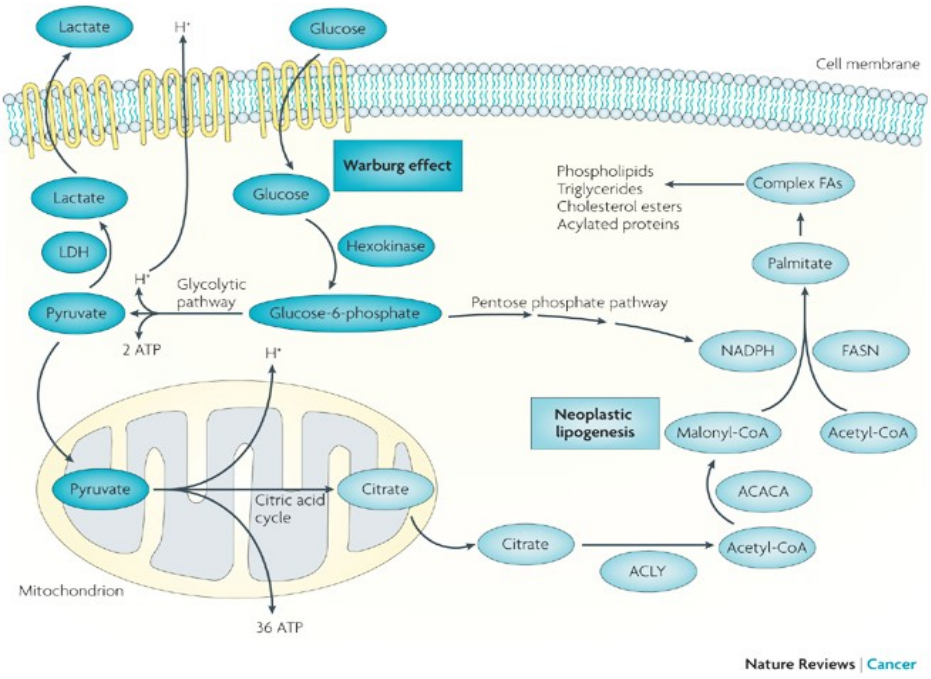

Fig. 8: Connecting glucose metabolism and fatty acid biosynthesis pathways in tumor cells.

4.1 The Warburg Effect

In the first half of the 20th century Otto Warburg observed that cancer cells exhibited significant alterations in energy metabolism and mitochondrial respiration compared to normal cells [Warburg O. et al., (1927)] He showed that tumor cells preferentially use glycolysis for ATP generation, even in the presence of sufficient oxygen, postulating the shift from OXPHOS to glycolysis as a consequence of a respiratory injury (mitochondrial dysfunction) leading to increased aerobic fermentation, a critical event for the origin of cancer [Warburg O., (1956)]. Since then the Warburg effect has been demonstrated in different types of tumors and the increase in glucose uptake through 18F-deoxyglucose positron emission tomography (FDG-PET), positively correlated with poor prognosis and higher metabolic potential in clinical setting [Gatenby R.A. and Gillies R.J., (2004); Kroemer G. and Pouyssegur J., (2008)], supporting the theory that alterations in cellular metabolism may contribute to the malignant phenotype.

Since the glycolysis generates only 2 ATPs per molecule of glucose, whereas oxidative phosphorylation generates up to 36 ATPs upon complete oxidation of one glucose molecule (Lehninger A.L. et al., (1993)], there is some debate about the why cancer cells decide to use the less efficient glycolysis rather than OXPHOS. One compelling idea is that the altered metabolism of cancer cells confers a selective advantage for survival and proliferation in the unique tumor microenvironment. Initial work focused on the concept that glycolytic metabolism arises as an adaptation to hypoxic conditions during the early avascular phase of tumor development, as it allows for ATP production in the absence of oxygen [Guppy M. et al., (1993)]. Another explanation is that the high levels of lactic acid produced during glycolysis may activate metallo-proteinases and matrix remodeling enzymes, thus promoting cancer invasion and metastasis [Berardi M.J. and Fantin V.R., (2011); DeBerardinis R.J. et al., (2008)]. Others proposed that tumor cells develop defects in mitochondrial function, and aerobic glycolysis is therefore a necessary adaptation to cope with a lack of ATP generation by OXPHOS. However, it was later appreciated that mitochondrial defects are rare [Frezza C. and Gottlieb E., (2009)] and that most tumors retain the capacity for oxidative phosphorylation and consume oxygen at rates similar to those observed in normal tissues [Weinhouse S., (1976)]. Finally it has been proposed that the aerobic glycolysis provides a biosynthetic advantage for tumor cells, and that a high flux of substrate through glycolysis allows an increased intermediate generation providing building blocks and precursors for the synthesis of DNA and fatty acids and for redox regulation [DeBerardinis R.J. et al., (2008); Vander H. et al., (2009)]. For instance, glucose6phosphate, the product of the first glycolytic reaction, can be channeled to the pentose phosphate pathway (PPP) to generate ribose5phosphate and NADPH, key intermediates in nucleotide biosynthesis and in redox

homeostasis respectively. NADPH and 3 carbon intermediates are also important for lipid biosynthesis.

It is known that glucose and glutamine supply the carbon, nitrogen, free energy and reducing equivalents necessary to support cell growth and division. Thus, in cancer cells there is an increasing of glucose uptake that is transported into cells by facilitative transporters and then trapped intracellularly by glucose phosphorylation [Berg J.M. et al., (2002)]. The hexose phosphate is further phosphorylated and split into three-carbon molecules that are converted to glycerol for lipid synthesis or sequentially transformed to pyruvate. Pyruvate in normal cells is preferentially converted to acetyl-CoA in the tricarboxylic acid (TCA) cycle, while in cancer cells can also be transaminated to alanine or become lactate, particularly under hypoxic conditions. Formation of citrate from acetyl-CoA and oxaloacetate permits a new round of TCA cycling, generating high-energy electrons, CO2, and carbon skeletons that could be used for biosynthesis or anaplerosis. Citrate itself could be extruded into the cytosol and then converted to acetyl-CoA by ATP citrate lyase (ACLY) for fatty acid synthesis and generation of biomembranes. Glucose, through the pentose phosphate pathway (PPP), generates ribose for nucleic acid synthesis and NADPH for reductive biosynthesis. Most of the carbon for fatty acid synthesis is derived from glucose, but also glutamine uptake appears to be critical for lipid synthesis in that it supplies carbon in the form of mitochondrial oxaloacetate to maintain citrate production in the first step of the TCA cycle [Wise D.R. et al., (2011); Metallo C.M. et al., (2012); Mullen A.R. et al. (2012)]. Thus, metabolism of both glutamine and glucose is orchestrated to support the production of acetyl-CoA and NADPH needed for fatty acid synthesis.

4.2 Lipogenic Phenotype

Development and progression of cancer are frequently associated with an increased rate of *de novo* lipid synthesis compared with their normal counterparts [Ookhtens M. et al., (1984); Rashid A. et al., (1997)]. This metabolic change occurs as a result of common oncogenic insults and is mediated by the activation of multiple lipogenic enzymes. In support of this hypothesis, blockade of lipogenesis by chemical inhibitors or RNA interference (RNAi)–mediated silencing of lipogenic enzymes or their regulators, attenuate cell proliferation and ultimately lead to cell death [Kinlaw W.B. et al., (2006); Pizer E.S. et al., (1996)]. Increased lipids not only supply energy through β-oxidation, but more importantly serve as precursor of membrane phospholipids, signaling and secondary messengers essential for a faster cell proliferation [Swinnen J.V. et al., (2006)].

Although lipogenic phenotype of cancer cells has been primarily attributed to an increased expression or aberrant activity of the major lipogenic enzyme fatty acid synthase (FAS) that is responsible for the terminal catalytic step in fatty acids synthesis [Kuhajida F.P., (2000); Kuhajida F.P., (2006); Swinnen J.V. et al., (2006)], other enzymatic mechanisms are involved. First, the net conversion of glucose to lipids is dependent on the ability of cells to produce cytosolic Acetyl-CoA from mitochondria-derived citrate trough the action of ATP citrate lyase (ACLY). Markedly increased ACLY expression and activity have been reported in cancer cells [Swinnen J.V. et al., (2006); Bauer D.E. et al., (2005); Hatzivassiliou G. et al., (2005)]. The relevance of ACLY-driven challenging of glucose into *de novo* lipid synthesis as an important component of cell growth and transformation is supported by the fact that ACLY inhibition, drastically limits the *in vitro* proliferation [Bauer D.E. et al., (2005)] and reduces tumorigenesis *in vivo* [Hatzivassiliou G. et al., (2005)]. Second, CoA carboxylase (ACACA), the rate limiting enzyme for the long Fas synthesis that catalyses the ATP-dependent carboxylation of Acetyl-CoA to malonil-CoA [Tong L., (2005)], has been shown to be overexpressed both at mRNA and protein levels, not only in advanced breast carcinomas, but also in preneoplastic lesions associate with increased risk for the development of infiltrating breast cancer [Milgraum L.Z. et al., (1997)].

4.3 Key Regulators of the Metabolic Reprogramming

Research over several decades has identified many oncogenes and tumor suppressors that are involved in the metabolic switch from OXPHOS toward an altered glycolysis of tumor cells. A substantial proportion of these oncogenes have been shown to stimulate genes encoding for proteins that mediate glycolysis and glutaminolysis.

AKT. The serine/threonine kinase AKT, a downstream effector of the insulin signaling, plays a major role in cell survival and proliferation and is an important promoter of glysolysis. In the majority of tumor cells, Akt is hyperactive and seems to drive addiction to glucose metabolism for survival and proliferation [Elstrom R.L. et al., (2004)]. The Akt glycolytic enhancer role is driven by stimulation of glucose uptake in response to insulin [Elstrom R.L. et al., (2004)]. Akt upregulates GLUT1 by enhancing its expression at transcription level. Moreover the AKT signaling enhances glucose metabolism within the cell by stimulating the association of HKII with the mitochondrial outer membrane, thus positioning it to phosphorylate glucose to glucose6phosphate for use in glycolysis and other metabolic pathways [Pastorino J.G. et al., (2005)]. Akt's ability to promote metabolism via glycolysis is also partly due to induced expression of glycolytic enzymes through the mTOR and HIF1 signaling [Hay N., (2004)].

mTOR. The mammalian target of rapamycin (mTOR) is an energy censor that promotes nutrient uptake and glycolysis. Deregulation of mTOR pathway is often found in cancer cells [Chapuis N. et al., (2010)]. Under nutrient deprivation, mTOR forms a stable complex with raptor, leading to an inhibition of mTOR kinase activity [Kim D.H. et al., (2002)]. Akt regulates mTOR through the inactivation of the protein tuberous sclerosis2 (TSC2). TSC2 and TSC1 associate and form a complex that suppresses mTOR activity [Crino P.B. et al., (2003)]. Activated AKT phosphorylates TSC2, thus affecting its interaction with the small G protein Rheb, which when loaded with GTP, activates mTORC1 [Kim D.H. et al., (2002); Inoki K. et al., (2002)]. The activation of mTORC1 increases glycolysis by increasing the translation of the mRNA encoding HIF-1α thus stimulating the expression of glycolytic enzymes [Duvel K. et al., (2010)]. Importantly, mTOR is regulated by liver kinase B1 (LKB1) and AMPK [Green A.S., et al., (2011)]. The mTOR energy sensor function is conferred in part by AMPK, a heterotrimeric serine/threonine kinase consisting of a catalytic subumit (α) and two regulatory subunits (β and ϒ) [Carling D. et al., (2008)]. Nutrient depravation causes cellular stress, leading to an increase of the AMP/ATP ratio, which promotes the binding of AMP to the ϒ regulatory subunit and triggers AMPK activation [Luo Z. et al., (2010)]. AMPK activation in turn induces TSC2 phosphorylation, leading to suppression of mTOR activity and inhibition of protein translation. The serine/threonine kinase LKB1 activates AMPK under low ATP conditions [Shackelford D.B. and Shaw R.J., (2009)]. Therefore, the LKB1/AMPK/mTOR axis serves as an important energy sensor that links energy status and the metabolic signaling pathways [Scholl C. et al., (2008)].

HIF. Hypoxia inducible factor 1, is an heterodimer protein complex that consists of HIF-1α and HIF-1β, has been implicated in the induction of key genes involved in cell proliferation, oxygen and nutrient delivery, and anaerobic energy metabolism [Patiar S. and Harris A.L., (2006)]. HIF-1α is degradated in normoxia: oxygen promotes prolyl hydroxylation, which stimulates the association of HIF-1α with the Von Hippel-Linau (VHL) tumor suppressor, thereby targeting HIF-1α for ubiquitination and proteosomal degradation. Hypoxia suppresses prolyl hydroxylation through a process involving mitochondria generated ROS [Brunelle J.K. Et al., (2005); Mansfield K.D. et al., (2005)]. HIF-1 α has been found highly expressed within hypoxic tumors and at low levels within normal tissue [Semenza G.L., (2003)]. As such, HIF-1 is considered as the master sensor that orchestrates cellular responses to changes in oxygen homeostasis: HIF-1 upregulates 9 of the 10 genes involved in glycolysis and, thus, plays a key role in switching glucose metabolism from OXPHOS to glycolysis when cells are in a hypoxic environment [Semenza G.L., (2003); Macheda M.L. and Rogers S. (2005)]. HIF promotes: 1) glucose uptake by upregulating the expression of the GLUT1; 2) glucose metabolism by upregulating hexokinase, the enzyme responsible of the first

glycolytic reaction; 3) LDHA expression [Pouyssegur J. et al., (2006); Semenza G.L., (2007)]; 4) upregulates PDK1 thus preventing the use of pyruvate by the mitochondria [Papandreou I. et al., (2006)]. HIF-1 expression is regulated by molecules such as FH and SDH: loss of function mutations of FH and SH lead to the accumulation of fumarate and succinate TCA cycle intermediates, resulting in inhibition of the α-ketoglutarate-dependent prolyl hydroxylase, thereby stabilizing HIF1 [Gottlieb E. and Tomlinson I.P., (2005)].

c-MYC. This oncogene affects many cellular functions including energy metabolism [Dang C.V. et al., (2009)]. c-Myc overexpression is estimated to be associated with at least 40% of all cancers [Wokolorczyk D. et al., (2008)]. Similar to HIF-1, c-Myc promotes glycolysis mainly through upregulation of glycolytic molecules including GLUT1, HKII, phosphofructokinase (PFK), enolase, and LDH [Bensaad K. et al., (2009)]. c-Myc also plays a major role in promoting glutamine use in cancer cells through the upregulation of glutamine transporters SLC5A1and SLC7A1 and of GLS1 by repressing the expression of miR-23A and miR-23B thus releasing the suppressive effect of these miRNAs on GLS1 expression.

p53. The tumor suppressor p53 is a stress sensor and cell cycle checkpoint regulator in mammalian cells that plays essential roles in cell cycle regulation, apoptosis, and genome stability [Aylon Y. and Oren M., (2007)]. The role of p53 in energy metabolism was recognized by Matoba et al. [Matoba S. et al., (2006)], demonstrating that loss of p53 diminishes the synthesis of cytochrome C oxidase, a nuclear DNA encoding gene whose product is necessary for the assembly of mitochondrial respiratory complex IV. Thus, this study directly links p53 to OXPHOS. The loss of p53 shifts the cellular ATP production from mitochondrial respiration to glycolysis. Moreover, 53 protein represses the expression of the GLUT1 and GLUT4 transporters. Thus, the loss of p53 enhances the expression of glucose transporters and further promotes glycolysis. Interestingly, Benssad et al. identified a p53 target gene known as TP53 induced glycolysis and apoptosis regulator (TIGAR), which is a potent glycolysis regulator [Bensaad K. et al., (2006)]. Expression of TIGAR decreases the intracellular level of fructose2,6-bisphosphate, which otherwise suppresses glycolysis by shunting glucose to the PPP [Chesney J. et al., (1999)] . In addition, p53 also affects energy metabolism by regulating AMPK, mTOR, PTEN, and IGF binding protein3 [Feng Z. and Levine A.J., (2010)].

Ras. Ras mutations are found in approximately 30% of all human cancers [Bos J.L., (1989)] and are important in promoting cancer initiation and progression [Friday B.B. and Adjei A.A., (2005)]. K-The most commonly mutated oncogenic Ras in pancreatic cancer, has been shown to affect the shape and function of the mitochondria during fibroblast transformation [Chiaradonna F. et al.,

(2006)]. Further studies showed that fibroblasts transformed by K-Ras activated attenuated OXPHOS by suppressing the activity of respiratory complex I, with a corresponding decrease in the expression level of complex I proteins [Baracca A. et al., (2010)]. Similarly, H-Ras transformed mouse fibroblasts exhibited low mitochondrial respiration, an increased dependency on glycolysis, a sensitivity to glycolytic inhibitors, and an insensitivity to OXPHOS inhibitors [Yang D. et al., (2010)]. However, K-Ras may affect the synthesis of the mitochondrial phospholipid cardiolipin and that the absence of led to K-Ras increased respiration [Chun S.Y. et al., (2010)], suggesting that the effect of K-Ras on mitochondrial respiration is likely complex and requires further study.

5. TRANSMITOCHONDRIAL HYBRIDS

Cancer cells adapt themselves to hypoxic and acidic conditions generated during progressive tumor cell growth by shifting the burden of energy metabolism from mitochondrial oxidative phosphorylation to glycolysis [Gatenby R.A. and Gillies R.J. (2004)] and it is not surprising that mitochondria might play a crucial role in this transition.

Mitochondria are multifunctional organelles that regulate metabolism, cellular energy production and cell death pathways, and are involved in free radical production. Human mitochondria contain their own circular DNA (mtDNA) that consists of 16,569 bp and encodes 13 oxidative phosphorylation (OXPHOS) subunits, 22 transfer RNAs (tRNAs), 2 ribosomal RNAs (rRNAs) and the displacement loop (D-Loop) [Taanman J.W., (1999)]. The remaining subunits of OXPHOS complexes are encoded by nuclear DNA and imported into the mitochondria. mtDNA is present as thousands of copies per cell and is not associated with histones. Because it is not protected by histones and due to its close proximity to reactive oxygen species (ROS) production, mtDNA is directly exposed to the damaging effects of ROS produced during OXPHOS. Additionally, because of a limited DNA repair system, mtDNA has a higher mutation rate than nuclear DNA. The effect of mtDNA in tumorigenesis or progression to malignancy can be achieved through a number of changes in mtDNA; first of all, by reducing the mtDNA content [Kulawiec M. et al., (2008)] Indeed, tumor-specific changes in the mtDNA copy number have been reported in human cancers. Reduced mtDNA content has been reported in breast [Yu M. et al., (2007); Mambo E. et al., (2005); Tseng L.M. et al., (2006)] prostate [Mizumachi T. et al., (2008) ovarian[Desouki M.M. et al., (2005)], renal [Selvanayagam P. and Rajaraman S., (1996)]; hepatocellular carcinoma [Lee H.C. et al., (2005); Yin PH. Et al., (2004)] and in gastric tumors [Wu C.W. et al., (2005)]. The second type of change through which tumorigenesis can be achieved is a decrease in mitochondrial gene expression [Weber K. et al., (2002)] or alteration in mitochondrial enzymatic activity [Espineda

C.E. et al., (2004);. Isidoro A. et al., (2004)]. The third type of change in mtDNA is somatic or germ line mtDNA mutations. However, a majority of these somatic mtDNA changes are in the noncoding D-loop regions or result in silent amino acid changes, that do not apparently affect mitochondrial function. Only a few mtDNA may harbor identifiable pathogenic mutations. In order to investigate the role of mitochondria and their involvement in the pathogenic mechanisms of cancer development, the effect of nuclear background must be excluded [Krishnamachary B. et al., (2003); Ohta S., (2006)] and transmitochondrial hybrids, generated by fusion of enucleated cell with cells deprived of mitochondria, represent an useful experimental model.

The technique of cytoplasts fusion with whole cells (**Fig. 9**) is based on the creation of mtDNA-depleted cells (ρ°) through prolonged treatment with 3.8-diamino-5-ethyl-6-fenilfenantridiniombromuro or ethidium bromide (EtBr) [King M.P. and Attardi G., (1989); King MP and Attardi G., (1996)]. EtBr is an intercalating agent selectively toxic for mtDNA that, differently from nDNA, hasn't efficient DNA repair systems [Goldring E.S., et al., (1970); Nagley P. and Ninnane A.W. (1970)].

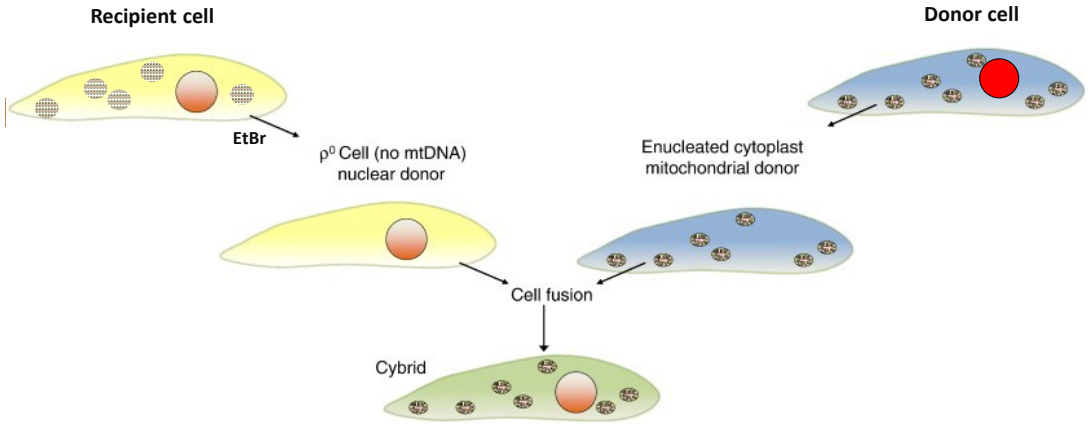

Fig. 9: cytoplasts fusion with whole cells

The ρ° cells derived from this step, are mtDNA-deficient and consequently their mitochondria are completely non-functional, nevertheless, they can survive by adding to the culture medium supplements ensuring a sufficient support of energy. Theoretically it is possible to create ρ° from any cell line; in practice 206-ρ° coming from the line TK^--143B are the most commonly used mtDNA deficient cells to create transmitochondrial hybrids. TK^- refers to the lack of the thymidine kinase enzyme normally deputy to the synthesis of thymidine monophosphate from thymidine. After checking that ρ° cells are completely devoid of mtDNA, ρ° are fused with vesicles containing

mitochondria from a donor cell. The fusion is, mediated by polyethylene glycol 1500 (PEG). The advantage of this experimental model is the fact that it allows to analyze different mtDNA in a nuclear DNA environment virtually identical, without any influence of their own nuclear DNA.

It has been shown that 206-ρ° cells are dependent from addition of uridine and pyruvate in the culture medium [King M.P. and Attardi G., (1996)]. The uridine dependence is due to the fact that the diidrooratato dehydrogenase enzyme, involved in the pyrimidines biosynthetic pathway, is localized in the inner mitochondrial membrane and its activity thus dependents from the membrane potential. In ρ° cells the potential is not present, and then the enzyme is inactive. Therefore it is necessary to provide a pyrimidine precursor in the form of Uridine. Instead, the pyruvate dependence, is an unexpected phenomenon. Indeed, the ρ° cells should be able to generate large amounts of pyruvate from glucose metabolism through the glycolytic pathway. The most widely accepted hypothesis is that the lack of the respiratory chain functionality prevents the oxidation of NADH produced in the cytoplasm, so the pyruvate reduction to lactic acid may be a way to elimenate the excess of NADH cytosolic. This would reduce the amount of pyruvate available to enter the tricarboxylic acid cycle (TCA) leading to the need of pyruvate addition.

According to the method of cybrids creation, after the merger, a long period of selections using the appropriate medium is necessary. The selection serves to eliminate from cell culture: ρ° cells who have not acquired mitochondria; donor cells; and residual cells that have acquired also the nuclear DNA (binucleate hybrids). Donor cells and hybrids binucleate can be removed using bromodeoxyuridine (BrdU) in the culture medium. This compound is an analogue of thymidine and therefore is recognized by the enzyme thymidine kinase and subsequently used in the synthesis of DNA creating lethal mutations. The cells TK^- (ρ° and cybrids) are not able to process the BrdU then that is not incorporated into DNA. By contrast, donor cells and binucleate hybrids possess at least one copy of the enzyme thymidine kinase, thus will be killed by the presence of BrdU. To delete ρ° cells, their dependence from uridine and pyruvates has been exploited. Therefore, a free uridine and pyruvate/DMEM, added with fetal serum dialyzed to 5%, was used.

AIM

The complex regulatory networks involving cancer genes and metabolic pathways need to be defined for specific cancer types so that the targeting of cancer cell metabolism could be strategically focused for specific genetic changes of particular cancers.The major goal of this investigation was to gain insights into the relevant processes and/or compensatory mechanisms that turn energetic metabolism specifically in cisplatin-resistant cancer, a phenomenon with clinical implications in chemotherapy. To this aim, we used a combination of genetics, biochemistry and metabolomics to identify different signatures of metabolic adaptations operating in cisplatin-sensitive (2008) and cisplatin-resistant (C13) human ovarian cancer cells. Mitochondria was studied using trans-mitochondrial hybrids derived from 2008 and C13 cells to establish the contribution of mitochondrial and nuclear DNA in cisplatin-resistance. More in detail, we aimed to identify, in the metabolomic fingerprint of cisplatin-resistant cells, possible targets useful to design pharmacological strategies to bypass the resistance.

The results generated will potentially lead to novel prognostic and predictive biomarkers for chemosensitization and/or novel therapeutic strategies for tumours resistant to cisplatin.

MATERIALS AND METHODS

1. Cell lines

1.1 Human ovarian carcinoma cell lines

2008 (wild type) and C13 (cisplatin-resistant) were grown in RPMI 1640 medium supplemented with 10% fetal bovine serum, 4 mM glutamine, 100 U/ml penicillin and 100 µg/ml streptomycin, in humidified condition at 5% CO_2 and 37° C. Cells were collected every 2 days with minimum amount of 0.25% trypsin-0.2% EDTA and seeded at $2x10^6$ density in 100mm dishes.

1.2 206-ρ° cell line

206-ρ° cells, obtained from mtDNA depletion of 143B-TK^- osteosarcoma cells, were cultured in high-glucose Dulbecco's modified Eagle's medium (Gibco), supplemented with 10% fetal bovine serum (FBS), mm L-glutamine, 100 U/ml penicillin and 100 µg/ml streptomycin, 1mM sodium-pyruvate, 1 % of a solution of not essential aminoacid (NEAA) and 0.05 mg/ml uridine in humidified condition at 5% CO_2 and 37° C.

1.3 Transmitochondrial cybrid cell lines

H2008 and HC13 were generated by polyethylene glycol fusion of enucleated 2008 and C13 with the mtDNA-less (ρ0) osteosarcoma (143B.TK-) cell line (kind gift of Andrea Martinuzzi) as previously described (King and Attardi, 1989). After fusion the cells were replated 24 hours in uridine-free DMEM supplemented with 100 µg/ml BrdU and 10% dialyzed FBS to allow selection of hybrids. Individual hybrid clones were isolated 10–20 days later using glass cylinders. Hybrid cell lines (H2008 and HC13) were cultured in high-glucose Dulbecco's modified Eagle's medium (DMEM, Cambrex-Lonza, NY, USA), supplemented with 10% fetal bovine serum (FBS), 2 mM glutamine, 100 U/ml penicillin and 100 µg/ml streptomycin, 1mM sodium-pyruvate and 1 % of a solution of not essential aminoacid (NEAA), in a humidified atmosphere of 95% air and 5% CO2 at 37°C.

2. Cell viability assays

2.1. MTT assay

MTT test, first described by Mosmann in 1983, is based on the ability of mitochondrial dehydrogenase enzyme from viable cells to reduce the tetrazolium ring of the pale yellow MTT [3-[4,5-dimethyl-thiazol-2-yl]-2,5-diphenyltetrazolium bromide into the dark blue formazan crystals. For the assay, 2500 cells/well were seeded in 96-well plates, allowed to attach overnight and exposed at different concentrations (0.1-100 µM) of cisplatin (Teva, Italy). After 24 hours 20 µL/well of a 5 mg/ml MTT solution (Sigma-Aldrich, St Louis, MO, USA) was added and cells incubated for 4 hrs at 37°C. The formazan crystals were dissolved by adding 200 µl of acidic isopropanol and the absorbance (Abs) was measured at 570 nm using a Victor3X multilabel plate counter (Wallac Instruments, Turku, Finland). CDDP IC50 values were extrapolated from concentration-response curves, calculated as the concentration causing a 50% reduction of Abs in comparison with untreated cells.

2.2 Trypan blue exclusion assay

This test measures the percentage of viable cells with the intact membrane thus excluding the blue dye, while dead cells take up the colouring agent. 6 wells plates were seeded with a constant number of cells and, following overnight incubation, were exposed to different treatments, according to experimental protocols. At the end of incubation the cells were washed, detached with 0.25% trypsin-0.2% EDTA and suspended in trypan blue (Sigma-Aldrich, St Louis, MO, USA), at 1:1 ratio in medium solution. Cell number was counted using a chamber Burker hemocytometer under the microscope.

2.3 Annexin V/propidium iodide staining.

Annexin V, belonging to the annexin proteins with anticoaugulant properties, has proven to be an useful tool in detecting apoptotic cells since, in the presence of Ca^{2+}, it preferentially binds to the negatively charged phospolipids like PS (phosphatidylserine). Phosphatidylserine is normally located on the cytosolic surface of the plasma membrane, but, in early apoptotic cells, it translocates to the extracellular surface to be recognised and phagocytised by macrophages.
Cells were seeded in 12 wells-plates, incubated overnight and treated with different concentrations of CDDP (1-10 µM). After 24 hrs of incubation cells were harvested by quick trypsinization and centrifugated at 1200 rpm for 5 minutes. The cell pellet was resuspended in 56 µL of a binding buffer [10 mM HEPES (Sigma-Aldrich), 140 mM NaCl; 2,5 mM $CaCl_2$; H_2O q.b.]

containing 80 nM of Alexa Fluor 488 annexin V and 33 µM of propidium iodide (PI) (Molecular Probes, Invitrogen, Carlsbad, CA, USA). The samples were incubated for 15 minutes at room temperature in the dark and, after dilution with the binding buffer, the fluorescence of stained cells was analysed by Epics XL flow cytometer (Coulter Systems, Fullerton, CA, USA) at laser excitation of 488 nm. The green emission signal of Annexin V was measured at 525 nm and the red emission signal of PI at 620 nm. The cell population separates into three groups: viable live cells show almost a negative fluorescence for both annexin V and PI, apoptotic cells show green fluorescence (Annexin V+/PI–), and dead cells show both red and green fluorescence (Annexin V+/PI+).

3. ATP-luciferase assay

Cells were seeded in 12 wells-plate, incubated overnight and treated according to the experimental protocols. After 24 hrs ATP levels were measured using the Luminescence ATP Detection Assay System (PerkinElmer) that is a bioluminescence assay for quantitative determination of ATP with recombinant firefly luciferase and its substrate D-luciferin. The assay is based on luciferase's absolute requirement for ATP in producing light (emission maximum ~560 nm at pH 7.8). The luminescence was read with Victor^{TM} X3 multilabel reader (Wallac Instruments, Turku, Finland) and normalized on the protein content of each sample.

4. Oxygen consumption

Oxygen consumption was measured in live cells ($3.5x10^6$) incubated in 1 ml glucose-free DMEM (Gibco, Invitrogen, Carlsbad, CA, USA) supplemented with 10% Na-pyruvate (Cambrex-Lonza, NY, USA) at 37°C, using a Clark-type oxygen electrode (Hansatech Instruments, King's Lynn, Norfolk, UK). Using the software Oxygraph plus v. 1.01 the oxygen consumption is detected by the time:

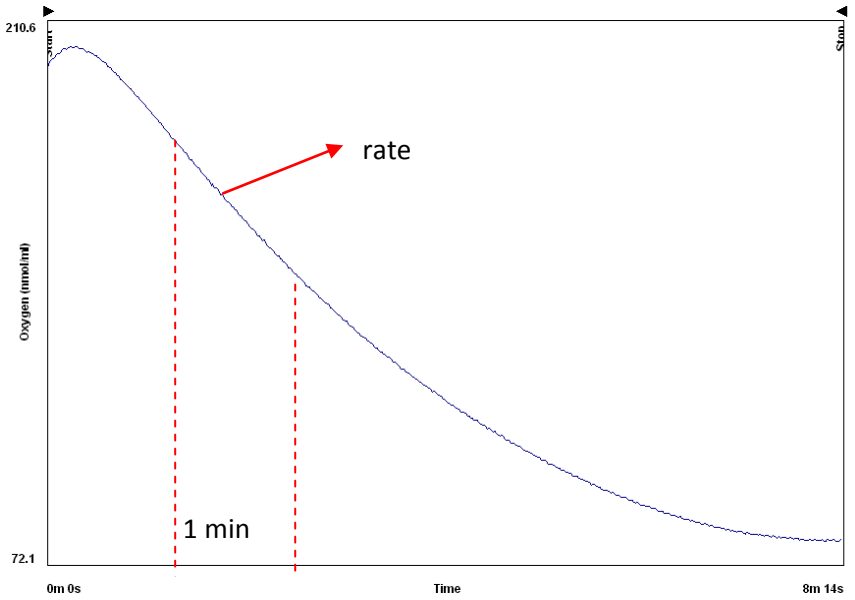

Data processing includes:

Fmol/c/min= (RATE/$3.5x10^6$)*1 million

Where:

fmol/c/min= femto moles of oxygen consumed by one cell every minute

RATE= slope of the curve of a range of one minute

$3.5x10^6$= number of cells

5. Mitochondrial membrane potential (ΔΨ) and mitochondrial mass

5.1 Flow ytometry

Mitochondrial transmembrane potential (ΔΨm) was probed by the cationic lipophilic, green-fluorescent rhodamine-123 (Rh123) (Molecular Probes, Invitrogen, Carlsbad, CA, USA) that is readily sequestered by active mitochondria in a potential-dependent manner: a loss of ΔΨm is associated with a lack of Rh123 retention and a decrease in fluorescence.

Mitochondrial mass was measured by Acridine Orange 10-Nonyl bromide (NAO) staining. NAO is a fluorescent probe that selectively binds to cardiolipin (CL) of mitochondrial membrane regardless of mitochondrial membrane potential determining mitochondrial mass.

Cells were seeded and incubated for 48 hours, washed with phosphate buffer saline solution (PBS), detached with 0.25% trypsin-0.2% EDTA and centrifuged for 5 min at 1200xrpm. The cell pellet was then resuspended with Rh123 (10 μM) or NAO (25 nM) and incubated for 15 minutes in dark. Fluorescence intensity was analyzed using an Epics XL flow cytometer (Coulter Systems, Fullerton, CA, USA) equipped with a 488 Argon laser. The green emission signal of Rh123 was measured at 525 nm and the orange emission signal of NAO at 580 nm. Necrotic cells were excluded by electronically gating data on the basis of forward versus side scatter profiles; a minimum of 10^4 cells of interest were analyzed further. Mean fluorescence intensity (MFI) values were obtained using the EXPO 32 software (Coulter Systems, Fullerton, CA, USA).

5.2 In live cells confocal microscopy

Cells were grown in 3.5 cm glass-bottom dishes (MatTek coprporation, Ashland, USA) and, after 24 hrs, were loaded with 100 nmol/L Mitotracker Green(MTG; Invitrogen) and 10 nmol/L Tetramethyl Rhodamine Methyl Ester (TMRM; Invitrogen) for 30 minutes. Cells were imaged using a laser scanner microscope (Leica TCS SP5, 60X magnification). A volumetric reconstruction was then obtained using the software Volocity and the MTG volume was used as a reference volume over imposed to the red channel for calculation of the TMRM volume's intensity. A ratio between the two intensities was then provided as a read-out of mitochondrial potential. 10 μmol/L carbonyl cyanide p-trifluoromethoxyphenylhydrazone (FCCP) was used as positive control.

6. Mitochondrial DNA analysis

6.1 qRT-PCR

Total DNA was isolated by Wizard Genomic DNA Purification Kit (Promega, Madison, WI, USA). Evaluation of mitochondrial DNA copy number by quantitative real-time polymerase chain reaction (PCR) was performed as previously described [Mussini et al., 2005]. Briefly, a mitochondrial DNA fragment (nt 4625–4714) and a nuclear DNA fragment (FasL gene) were co-amplified by using TaqMan® probe system and Platinum® Quantitative PCR SuperMix-UDG (Invitrogen, Life Technologies, Carlsbad, CA, USA). With each assay, a standard curve for mitochondrial and nuclear DNA was generated using serial known dilutions of a vector (a kind gift from Dr Andrea Cossarizza) in which the regions used as template for the two amplifications were

cloned tail to tail to have a ratio of 1:1 of the reference molecules. The absolute mitochondrial DNA copy number per cell was obtained by the ratio of mitochondrial to nuclear DNA values multiplied by two (as two copies of the nuclear gene are present in a cell). PCR was carried out in an iCycler Thermal cycler (BioRad, Hercules, CA, USA) and at least three measurements were obtained for each sample.

6.2. Genome sequences

The entire mitochondrial genome was sequenced in a series of overlapping fragments using M13-tagged oligodeoxynucleotide primers to facilitate direct sequencing of the PCR amplified products with BigDye® terminator chemistries on an Applied Biosystem 3100 automated sequencer (Applied Biosystems, Warrington, UK) [Tuppen, 2010]. All sequences were directly compared to the revised Cambridge reference sequence for human mtDNA (GenBank Accession number NC_012920).

7. ^{1}H-NMR spectroscopy

Cells were harvested by trypsinization 0.05% trypsin-0.02% EDTA (CAMBREX), washed in PBS and centrifuged for 3 min at 425xg and washed once with PBS. A cell pellet of about 2 x 10^{7} cells was resuspended in 500 µl of PBS-D_2O in the presence of 0.1% TSP (2,2'-3,3'-tetradeutero-trimethyl-sylilpropionate sodium salt (Sigma), used as an external chemical shift reference at 0.00 ppm. This volume of cells was enough to fill the sensitive volume of the observation coil in the 5-mm probe. ^{1}H-NMR spectra were recorded on a BRUKER AVANCE DMX-600spectrometer operating at the frequency of 600 MHz in the proton dimension, at 298 K. Spectra were acquired with a pulse-and-acquire sequence (90° pulse of 11.2 µs). Intensity of the residual water signal was reduced by the WATERGATE field gradient-based sequence. The total delay between pulses was set to 6 s to allow for full relaxation of the interesting metabolites. Data were acquired over a 8000 Hz sweep width and digitized with 16K data points. Final spectra were the result of the accumulation of 128 scans with a total acquisition time of around 14 min. The whole experiment, cell preparation and NMR spectroscopy, lasted 60–75 min after the addition of PBS to the cell culture flasks before trypsinization. Cell viability, as measured by trypan blue exclusion, was always above 95% after trypsinization and above 80% after NMR spectroscopy.

Spectra were processed using the Bruker Software XWINNMR. The measured FIDs were zero-filled to 32 K and Fourier-transformed without apodization. The spectra were manually phase-corrected and finally a baseline correction was applied. The signals of the 1D NMR spectra were quantified by resonance deconvolution, using the DMFIT5 program. Peaks areas have been

normalised to the peak area of polypeptide CH_3 signal at 0.94 ppm. Homonuclear two-dimensional total correlation spectroscopy (TOCSY) experiments were recorded over a spectral width of 8000 Hz, as a matrix of 1024X256 data points by summing 32 scans for each increment in t_1. A repetition time of 1 s was used. Suppression of water signal was obtained by the WATERGATE sequence. TOCSY experiments were acquired with a spin-lock period of 70 ms achieved with the MLEV17 pulse scheme. The measurement time for the 2D spectra was around 2 hours. Prior to Fourier transformation the data matrices were zero-filled to 2048X1024 points and multiplied for Lorentian-Gaussian and shifted squared sine bell functions in t2 and t1 respectively.

8. Lipid droplet content

Nile red (also known as Nile blue oxazone) is a lipophilic stain produced by boiling a solution of Nile blue with sulfuric acid. It is used to localize and quantitate lipids, particularly neutral lipid droplets within cells. The fluorescence of the dye is heavily dependent on the solvent used: in most polar solvents Nile Red will not fluoresce, however when in a lipid-rich environment can be intensely fluorescent, with varying colours from deep red to strong yellow-gold emission.
For the experiment it was prepared a stock solution of Nile red in acetone (500 µg/mL) and the fluorescence intensity was measured both by cytometry and microscopy. Nile red fluorescence intensity was measured both by cytometry and confocal microscopy.

8.1 Flow cytometer

Multiwells plate were seeded with a constant number of cells and, following overnight incubation, cells were stained with 1 µmol/L Nile red for 15 minutes. After detachment, cells were resuspended in 300 µl of PBS, 2% FBS and 0.02% sodium azide buffer and the fluorescence intensity was analysed by Epics XL flow cytometer (Coulter Systems, Fullerton, CA, USA) at laser excitation of 488 nm. The yellow signal emission from Nile red was measured at >528 nm.

8.2. Confocal microscope

Cells were seeded at approximately 30% confluence on glass cover slips and incubated overnight. After 24h, cells were fixed with 4% formaldehyde (SIGMA St Louis, USA) for 15 min, permeabilized with 0.1% of Triton for 5 min and stained with 1 µmol/L Nile red and 0.33 µM phalloidin in growth medium (SIGMA-ALDRICH) for 1 hrs. After repeated washings, Mowiol 40-88 (Sigma, St Louis, MO) was added at a final concentration of 0.5 µg/ml and the slides were examined by fluorescence

laser scanning microscope (Nikon C1 confocal microscope and Nikon EZ-C1 software (version 2.10), magnification 60X).

9. Immunoblot assay

Cells were plated in 100 mm cell culture dish and allowed to attach overnight. After 24 hrs cells were washed 3 times with PBS and lysed with ice-cold lysis buffer [TRIS 25 mM pH 7,4; NaCl 150 mM; IGEPAL 1%; sodium deoxycholate 1%; SDS 0,1%; EDTA 1 mM] supplemented with the protease inhibitor cocktails (Protease Inhibitor cocktail tablets EDTA-free, Roche Molecular Biochemicals, Mannheim, Germany). Cell lysates were then centrifuged at 14000 g for 15 minutes at 4°C and the supernatant protein content was determined by Lowry procedure (Bio-rad DC Protein Assay) using bovine serum albumin as standard. Laemmli buffer 5X [250 mM Tris-HCl pH=6.8, 50% glycerol, 10% SDS, 500 mM β-mercaptoethanol, 0.004% bromophenol blue, H_2O q.b] was added (1/5 v/v) to protein lysates, and the samples were denatured for 5 min at 100°C. Equal amounts of protein (40 µg) were loaded on a 8% polyacrylamide gel and electrophoretically separated in running buffer [25 Mm TRIS, 250 mM glicina (Applichem), 0.1% SDS, H_2O q.b.], for 1h at a constant current of 200 V (Bio-rad Mini-PROTEAN® Tetra System). A molecular weights marker was used (Full Range Rainbow Molecular Weight Markers, Amersham Biosciences). After electrophoresis, the proteins were blotted onto an Hybond-P PVDF membrane (Amersham Biosciences), previously soaked in methanol, using a transfer buffer [25 mM Tris,192 mM glicina, H_2O q.b.]. A current of 250 mA was applied for 1h and 45min at 4°C. Non specific binding sites were blocked by immersing the membrane in TBS-Tween 20 solution containing 10% non-fat dried milk and shaking for 1h at room temperature. After 3x10 min washes with TBS-Tween 20 [10 mM TRIS, 150 mM NaCl, 0,1% Tween 20 (Sigma-Aldrich), H_2O q.b.] at room temperature, the membrane was exposed to the primary anti-HIF-1α antibody (1:1000; Santa Cruz Biotechnology) overnight at 4°C. After washing, the membrane was incubated with HRP-conjugated anti-mouse secondary antibody (1:10000; Dako), for 2h at room temperature. The signal was visualized with enhanced chemiluminescent kit (Amersham Biosciences) according to the manufacturer's instructions and analyzed by Molecular Imager VersaDoc MP 4000 (Bio-rad). The integrated intensity was normalized to beta-actin (1:5000; AbCam).

10. qRT-PCR analysis

Cells were grown as indicated and total mRNA was isolated as per manufacturer's instructions using QIAshredder and RNEasy kits (Qiagen) and measured with a NanoDrop ND-1000 spectrophotometer (NanoDrop Technologies, Inc. Wilmington, DE, USA). 0,5 µg of total mRNA

was reverse-transcribed to complementary DNA using The High Capacity cDNA Reverse Transcription Kits of Applied biosystem by life technologies [10X RT Buffer, 10X RT random Primers, 25X dNTP Mix (100mM), MultiScribe reverse Transcriptase (50U/µL)]. Relative expression of each gene was determined by quantitative real-time PCR (StepOne™ Systems of Applied biosystem by life technologies) using Power SYBR® Green PCR Master Mix (Applied biosystem by life technologies) and the primers designed as follow: GLUT1: 5': gaccctgcacctcattgg, 3': gatgctcagataggacatccaag; BNIP3: 5' gaatttctgaaagttttccttcca, 3' ttgtcagacgccttccaata; LDHA: 5' cgccctctgctcttgattt, 3' catcacccagagccctacag, MYC: 5' gctgcttagacgctggattt, 3' taacgttgaggggcatcg; HIF-β (ARNT): 5' ctacccgctcaggcttttc, 3' caccaaactgggaagtacgag; PGK1: 5' cagctgctgggtctgtcat, 3' gctggctcggctttaacc; PFKM: 5' gccatcagcctttgacaga, 3' ctccaaaagtgccatcactg. qRT-PCR was performed in quadruple using 1 µl of complementary DNA template in a 20-µl reaction. Linearity and efficiency of PCR amplifications were assessed using standard curves generated by serial dilution of complementary DNA; melt-curve analysis was used to confirm the specificity of amplification and absence of primer dimers. All genes were normalized to β-actin designed as follow: 5': ccaaccgcgagaagatga 3': ccagaggcgtacagggatag. Expression levels of the indicated genes were calculated by the ΔΔCt method using the dedicated StepOne software.

11. Liquid Chromatography-Mass Spectroscopy (LC-MS)

Intracellular metabolites analysis: a predefined number of cells was incubated for 48 hours and then quickly washed with ice cold PBS on an ice bath. Cells were then lysed with a dry ice/methanol solution (-80°C) of 50% methanol/30% acetonitrile in water and quickly scraped. The extracts were mixed at 4°C for 15 minutes and pelleted in a cooled centrifuge (4°C). After that, the supernatant was collected for subsequent LC-MS analysis. The amount of extraction solution was calculated according to the number of cells present in the sample dish, extrapolated using a "counter dish" cultured in the same conditions of the sample dishes. A concentration of 1ml per $1x10^6$ cells was used in the extraction solutions.

Extracellular metabolites analysis: 50 µL of cells growth medium were collected after 24 and 48 hrs of incubation, added to an acetonitrile-water solution and vortexed for 15 minutes. The suspension was then centrifuged for 10 minutes at 16000xg at 4°C and the supernatant was submitted to LC-MS analysis.

LC-MS analysis: Intermediates were separated using a liquid chromatography system. The LC system consisted of Finnigan Surveyor Autosampler Plus (ThermoElectron, Hemel Hempstead UK) and MS Pump Plus (ThermoElectron, Hemel Hempstead UK).

The column was Sequant Zic-Hilic (150mm X 4.6 mm i.d. 5 microns) with a guard column (20 mm X 2.1 mm i.d. 5 microns) from HiChrom, Reading, UK. Mobile phase A: 0.1% formic acid v/v in water. Mobile B: 0.1% formic acid v/v in acetonitrile. The flow rate was at 300 µL/minute and gradient was as follow: 0 minutes 80% of B, 12 minutes 50% of B, 26 minutes 50% of B, 28 minutes 20% of B, 36 minutes 20% of B, 37-46 minutes 80% of B.The autosampler tray temperature was set at 3°C.

The LC system was coupled online to an LTQ Orbitrap mass spectrometer (ThermoElectron, Hemel Hempstead UK) equipped with an electrospray ionization source set at 4.5 KV in the positive ion and negative ion mode. The capillary was set to 35 V. The heated capillary temperature was set to 250 °C. Tube lense was set to 100 V for positive and -95 V for negative ion modes. The machine was calibrated and tuned with calibration solution freshly before each run. The ion current at every mass to charge ratio (m/z) and elution time was measured by the LC-FTMS.

Data acquisition was controlled with Xcalibur 2.0 (ThermoElectron). The mass accuracy was maintained below 1 ppm due to use of a lock mass. The raw chromatograms were then aligned using the software SIEVE™ (ThermoElectron). The integration of the measured ion current over a metabolite's elution time and m/z interval is directly proportional to its absolute abundance in the solution. We manually removed from the SIEVE's output unspecific and misaligned peaks to eliminate the noise.

12. Data analysis and statistics of metabolomic results

To identify the most significant differences between groups, univariate statistical analysis was used. Filtering procedures, such as fold-change analysis, t-test (for paired and unpaired data) and ANOVA were applied, as provided by MetaboAnalyst web-based software [Xia J.et al., (2009); Xia J.and Wishart D.S., (2011)]. Significantly different data at the probability level of $p<0.05$ were used for further procedures of multivariate analysis, to obtain identification of relevant biomarkers. Tentatively, the entire metabolomic data set was submitted to multivariate analysis by means of the procedures provided by MetaboAnalyst [Xia J. et al., (2009); Xia J. and Wishart D.S., (2011)] and meta-P server [Kastenmüller G. et al., (2011)].

Principal Component Analysis (PCA). PCA is an unsupervised method to detect the directions which best explain the variance in a data set, transforming a number of possibly correlated variables into a smaller number of uncorrelated variables defined as principal components, which are linear combinations of the original variables. The first principal component explains as much

of the variability in the data as possible, and each following component accounts for the remaining variability. The data are represented in a dimensional space of n variables, which are reduced into a few principal components; these are descriptive dimensions indicating the maximum variation within the data. After the principal components scores have been obtained, they can be graphically plotted to observe any groupings in the data set. PCA computation was obtained with MetaboAnalyst based on R prcomp package, using singular value decomposition algorithm. The covariance matrix and standardized principal component score were selected. The scores of the first two principal components were graphically plotted to observe any groupings in the data set.

Cluster analysis. Cluster analysis is a multivariate procedure of exploratory data analysis for detecting natural groupings in data. Data classification consists of placing samples into more or less homogeneous groups, in order to reveal any relationship among groups. Ward's method (minimizing the sum of squares of any two clusters), provided by MetaboAnalyst, was used. Distance indices were determined by Pearson's method. Hierarchical clustering was performed with the hclust function provided by R package stat. Results were presented as dendrograms or heat maps.

12.1 Metabolite identification

The putative masses responsible for the metabolic differentiation between the groups were used to make queries in the METLIN (http:// metlin.scripps.edu/), Mass Bank Database (http://www. massbank.jp/en/database.html) and Human Metabolome Database (http://www.hmdb.ca/) online databases in order to obtain corresponding chemical structures.Keggs Database (http://www.genome.jp/kegg/) was used to identify metabolic pathways of interest.

13. Statistical analyses

All data are expressed as mean ± SEM. Standard ANOVA procedures followed by multiple pair-wise comparison adjusted with Bonferroni corrections were performed for cell viability assays. Paired t-tests were used to analyse all the other results. Significance was considered at $P < 0.05$.

RESULTS

Cisplatin is known as one of the more effective chemotherapeutic agent for a wide variety of solid tumour [Vincent, 2001] however, despite a consistent rate of initial responses, the treatment often results in resistance leading to therapeutic failure. In this project cisplatin-sensitive (2008) and cisplatin-resistant (C13) human ovarian cancer cells, whose CDDP IC_{50} are shown in **Table 1**, have been characterized in order to define mechanisms of resistance not jet discovered and possibly useful pharmacological targets.

Table 1: CDDP IC_{50} of cisplatin-sensitive (2008) and cisplatin-resistant (C13) ovarian cancer cells.

	IC_{50} CDDP (μM)
2008	**1.4** 1.31-1.49
C13	**10.36** 9.96-10.75

The ability of certain cancers to rely heavily on glycolytic metabolism, even in the presence of an adequate oxygen supply, has been pioneered by Warburg [Warburg O., 1956]. Recently, besides a number of molecular alterations, a metabolic reprogramming involved in the faster growth and proliferation of cancer cells have been demonstrated. Herein, in order to investigate the hypothesis that after repeated exposure to cisplatin, cancer cells might further reprogram their metabolism, wild type sensitive and cisplatin-resistant ovarian carcinoma cells and their derived transmitochondrial hybrids were phenotyped for metabolic, morphological and molecular aspects.

1. Phenotyping Of Ovarian Carcinoma Cells Sensitive (2008) And Resistant (C13) To Cisplatin

1.1 Oxygen Consumption

To investigate the respiratory chain activity of cancer cells, the different rate of basal oxygen consumption was measured in viable cells using a Clark-type oxygen electrode. **Figure 1** shows a significantly lower oxygen consumption in C13 cells, compared to 2008 cells, indicating a reduction of mitochondrial respiration in chemoresistant cancer cells.

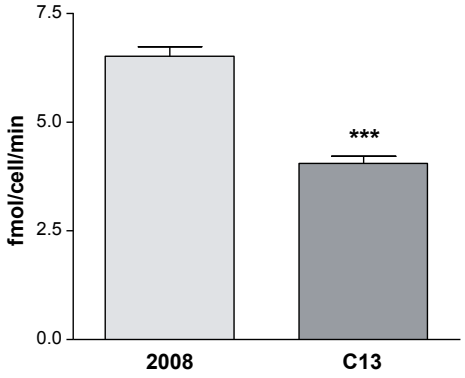

Figure 1: Oxygen consumption [fmol oxygen/cell/min] in 2008 and C13 cells. ***p < 0.001, C13 vs.2008 cells.

1.2 Effect of Galactose and Rotenone on Cell growth and ATP production

To test the mitochondrial functionality of cancer cells and to understand their dependency from glycolysis for the energy production, cell viability and ATP level were measured after exposure to two different experimental tool causing mitochondrial stress. The first experimental strategy was to incubate the cancer cells in a glucose-free/galactose medium. Galactose is very slowly metabolized through the glycolytic pathway, therefore glycolysis dependent cells are not able to survive for a long time unlike those with an efficient oxidative phosphorylation [Reitzer et al., 1979]. **Fig. 2** shows the time course of 2008 and C13 cell proliferation in DMEM or in DMEM glucose-free and added with 5 mM galactose. It is evident that in galactose stressed metabolic condition, the cell proliferation is lower than in DMEM. Further the effect is more significantly pronounced in the cisplatin-resistant cell line. This data suggests a major glucose-dependence of C13 whose oxidative phosporylation is not so efficient to counteract the block of the glycolysis.

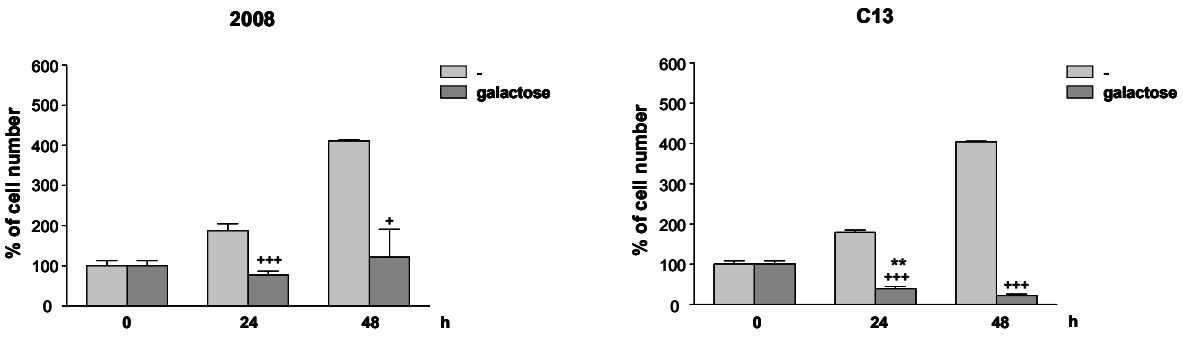

Figure 2: Effect of galactose on cell viability of 2008 and C13 cells incubated for 24 and 48 hours in DMEM or in glucose free/galactose medium. Data are expressed as % of cell number after 24-48 h compared to the t_0. Data are the mean ± SEM of 3 different experiments. ** $p < 0.01$, C13 *vs* 2008; +$p < 0.05$, +++$p < 0.001$, galactose vs control.

The second experimental strategy was to incubate cells with rotenone, an inhibitor of NADH-CoQ oxidoreductase (complex I) in the mitochondrial respiratory chain [Pitkänen S. and Robinson B.H., (1996)]. The results clearly demonstrate that CDDP-resistant cells (C13) are less sensitive than wild-type chemosensitive cells (2008) to the respiratory chain inhibitor (**Fig. 3**), suggesting a possibly lower activity of mitochondria.

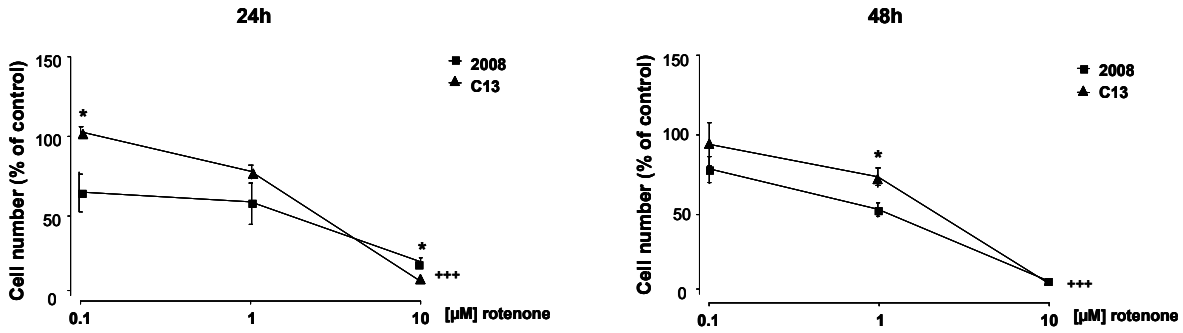

Figure 3: Effect of rotenone (0.1-10 µM) on 2008 and C13 cell viability after 24 and 48 hours of treatment. Data are expressed as % of cell number compared to the respective control. Data are the mean ± SEM of 3 different experiments. *$p < 0.05$, C13 vs 2008; +++ $p. < 0.001$ rotenone vs control.

The effect of galactose and rotenone was further investigated on ATP generation after 24 hours of incubation. As shown in **fig. 4**, the total ATP is lower in CDDP resistant-cells incubated in a glucose-free/galactose medium as compared to basal condition , while is higher after treatment with rotenone.

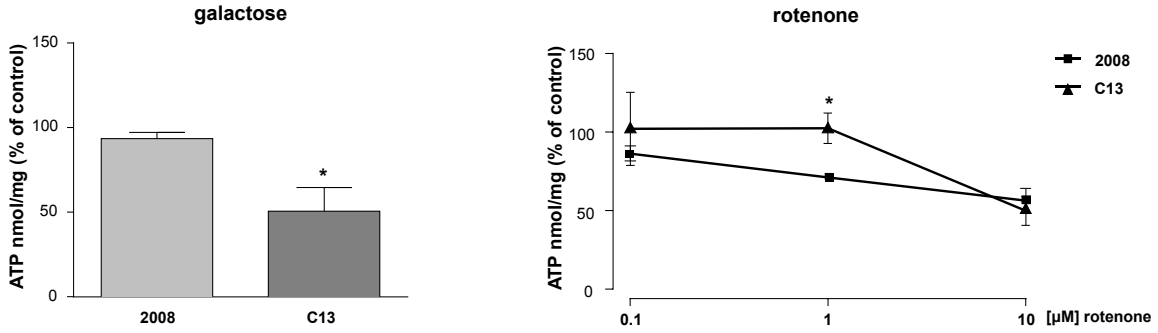

Figure 4: Effect of 5mM galactose and rotenone (0.1-10 μM) on 2008-C13 total ATP production. Data are expressed as % of nmol ATP/mg protein, compared to the respective control. Data are the mean ± SEM of 3 different experiments. *p < 0.05, C13 vs 2008.

1.3 Mitochondrial Mass and Membrane Potential

Mitochondrial mass and mitochondrial membrane potential (ΔΨm), which is generated by the proton gradient across the inner mitochondrial membrane, were both analysed by flow cytometer (**Fig. 5**) and in live confocal microscopy (**Fig. 6**), using specific different fluorescent probes**.** Flow cytometer assay shows that mitochondrial mass is significantly lower in C13 than in 2008 cells, as probed by MFI of 10-Nonyl bromide Acridine Orange (NAO) (**fig. 5a**); similarly the ΔΨm is lower in C13 cells as probed by potential-dependent rhodamine-123 (Rh123) (**fig. 5b**).

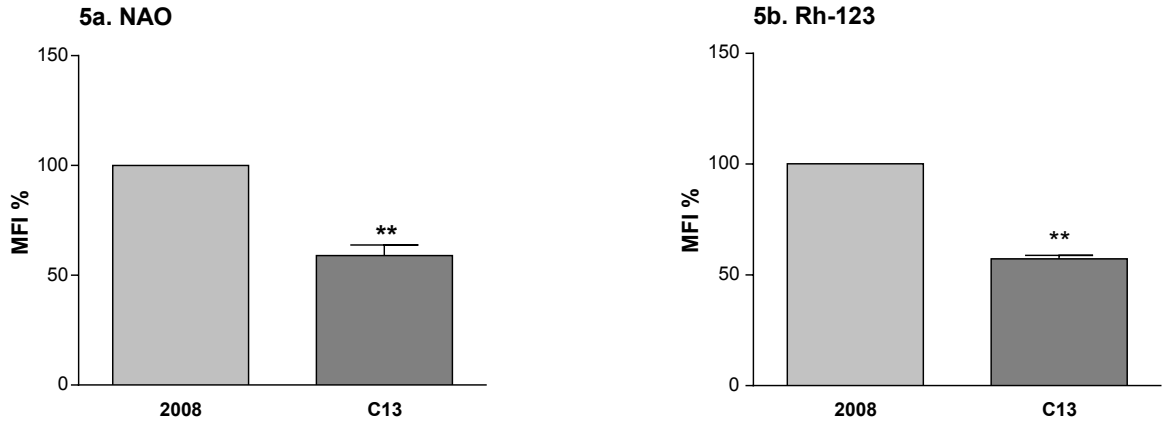

Figure 5: Mitochondrial mass **(a)** and potential **(b)** in 2008 and C13 cells, measured by flow cytometry and expressed as mean fluorescent intensity [MFI] of NAO (25 nM) and Rh123 (10 μM). Each bar represents the mean ± SEM of 5 independent experiments. ***p* < 0.01. C13 *vs* 2008.

These results were confirmed by confocal microscopy (**Fig. 6**). Live cells were incubated with the MitoTracker Green (MTG) to probe mitochondrial mass, and with Tetramethyl-Rhodamine Methyl-esther (TMRM), to probe ΔΨm. Cumulative images of sequential focal sections were acquired and z-stacks of the whole microscopic field were generated in order to measure the volume and intensity of the green and red markers. Representative images show significantly lower fluorescence intensity in the C13 than in 2008 cells. Furthermore in C13 cells the mitochondrial network appear scattered and less structured than in 2008 cells.

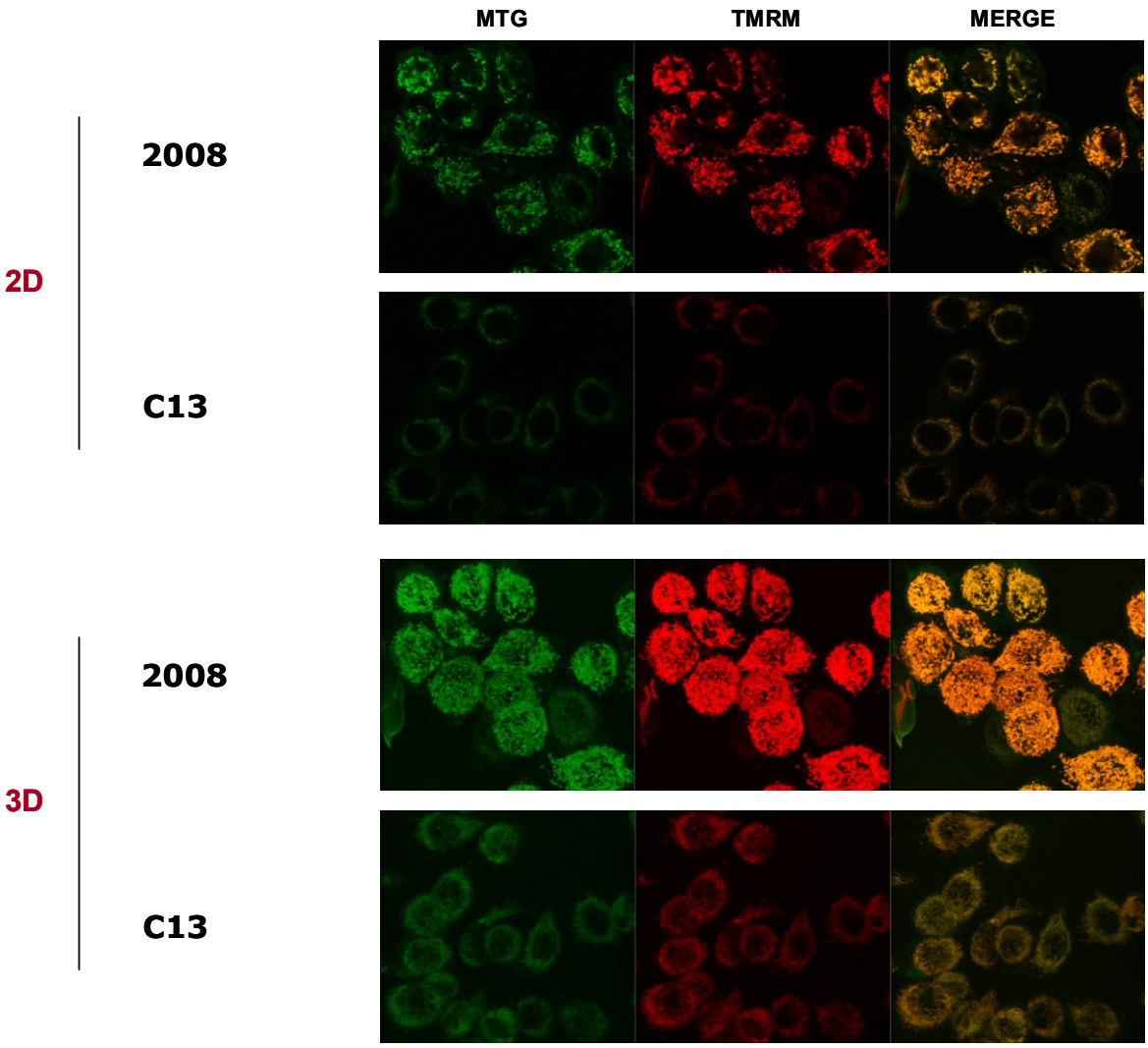

Figure 6: Images of 2008 and C13 cells, acquired with Leica confocal microscope (60X) using MTG (100 nM; λec/em= 490/516) and TMRM (10 nM; λec/em= 544/590).Images acquired in C. Frezza lab (Hutchison/MRC Research Centre, Cambridge).

In order to reduce the possible artefacts of fluorescence emission due to changes in mitochondrial shape and volume, rather than in ΔΨm, the ratiometric (red/green) was calculated (**Table 2**). Results show that the fluorescence intensity of both MTG and TMRM probes is significantly lower in resistant-cells (C13), however the ratio TMRM/MTG values are similar suggesting that the reduced mitochondrial potential of C13 is not due to a loss of mitochondrial functionality, but to a lower mitochondrial mass.

Table 2: Mean Fluorescence intensity (MFI) of MitoTracker Green (MTG)and TetraMethyl-Rhodamine Methyl-esther (TMRM) and their ratio in 2008 and C13

MFI / Cell lines	MTG	TMRM	TMRM/MTG
2008	**98,45** ±26,74	**139,84** ±18,08	**1,49** 1.17-1.81
C13	**25,61** ± 5,34	**39,39** ±5,41	**1,6** 1.14-2.06

1.4 mtDNA content

In order to understand the lower mitochondrial mass of C13 cells, mtDNA content was analyzed in C. Giordano lab (Istituto di Anatomia Patologica, Università "La Sapienza" di Roma). The results revealed significantly lower mtDNA levels in the cisplatin-resistant cell line than in wild type cancer cells (**Fig. 7**).

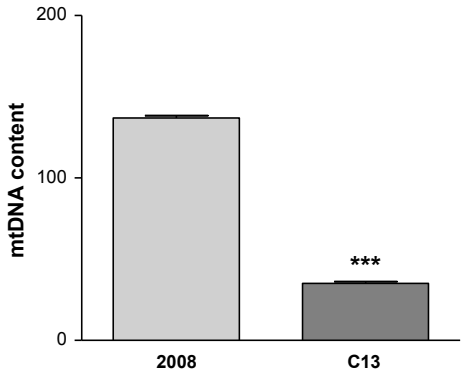

Fig. 7: mtDNA content measured by qRT-PCR in 2008 and C13 cells. ***p < 0.001, C13 vs.2008 cells. .

1.5 Mitochondrial DNA Sequences

To better investigate the previously described mitochondrial differences of 2008 and C13 ovarian cancer cells, mitochondrial DNA of both cell lines was totally sequenced by C. Giordano group (Istituto di Anatomia Patologica, Università "La Sapienza" di Roma) (**Tables 3 a-b**).

Table 3a: mtDNA polymorfism in 2008 cells

POLYMORPHISM	GENE	VARIATION
66delG	*MT-DLOOP*	
309insC	*MT-DLOOP*	
315insC	*MT-DLOOP*	
379 A>T		
709 G>A	*MT-RNR1*	non cod
1438 A>G	*MT-RNR1*	non cod
1888 G>A	*MT-RNR2*	non cod
4769 A>G	*MT-ND2*	syn
6734G>A	*MT-CO1*	syn
8860A>G	*MT-ATP6*	T-A
15287T>C	*MT-CYB*	F-L
15326A>G	*MT-CYB*	T-A
16519T>C	*MT-DLOOP*	

***** 30% of mtDNA polymorfism rate in C13 compared to 2008 cells ;

****** 50% of mtDNA polymorfism rate in C13 compared to 2008 cells.

Table 3b: mtDNA polymorfism in C13 cells

POLYMORPHISM	GENE	VARIATION
66delG	*MT-DLOOP*	
263A>G	*MT-DLOOP*	
315insC	*MT-DLOOP*	
379 A>T		
709 G>A	*MT-RNR1*	non cod
1438 A>G	*MT-RNR1*	non cod
1888 G>A	*MT-RNR2*	non cod
4769 A>G	*MT-ND2*	syn
6734G>A	*MT-CO1*	syn
8156 heteroplasmy G>T *	*MT-CO2*	V-L LD=0,53
8860A>G	*MT-ATP6*	T-A
12018 heteroplasmy C>T **	*MT-ND4*	T-I LD=0,69
13828 heteroplasmy C>T **	*MT-ND5*	L-P LD=0,05
14470T>A	*MT-ND6*	syn
15287T>C	*MT-CYB*	F-L
15326A>G	*MT-CYB*	T-A
16519T>C	*MT-DLOOP*	

The comparison between 2008 and C13 cells was analyzed by an electropherogram and three levels of heteroplasmy were identified in C13 cells: 8156 G>T, 12018 C>T, 13828 C>T. These polymorphisms were further analyzed by the PolyPhen program on the site: http://genetics.bwh.harvard.edu/pph2/, and the polymorphisms 8156 G>T and 13828 C>T resulted with low probability to be pathogenic, while the polymorphism 12018 C>T was borderline, suggesting further genetic study.

1.6 ^{1}H-NMR

Nuclear Magnetic Resonance (NMR) spectroscopy is a non-invasive, accurate technique increasingly applied to define the metabolic phenotype of tissues or cells. Even if NMR detects only a fairly small number of metabolites, it can be used to monitor different metabolic pathways and to delineate the fingerprint of different cell lines. ^{1}H-NMR analysis were performed in Mammi lab by M. Bellanda (Dipartimento di Scienze Chimiche, Università degli Studi di Padova). **Fig. 8a** shows representative ^{1}H-NMR spectra of 2008 and C13 cell samples, and a typical deconvolution pattern is reported in **Fig. 8b**. Two-dimensional and one-dimensional proton spectra were used for signal identification and signal quantification, respectively, as described in the Methods section. For normalization purposes, the peak area were divided by the area of the peak at 0.96 ppm, deriving from polypeptide chains and, because indicative of cell mass, used as an internal reference for one-dimensional spectra [Luciani et al., 2009].

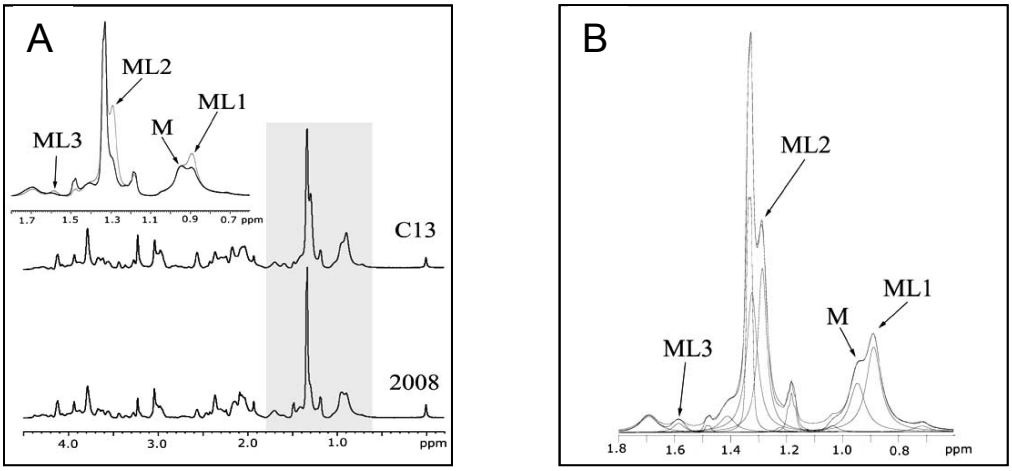

Figure 8: (**A**) Representative 1H NMR spectra of 2008 [bottom] and C13 cells [top]. The regions between 0.6 and 1.8 ppm of the two spectra (highlighted in gray) are expanded and superimposed in the inset. The spectra were normalized with respect of the polypeptide CH3 signal at 0.94 ppm (M). Signals of mobile lipids at 0.90 ppm [CH3-], 1.29 ppm [-(CH2)n-], and 1.59 ppm [-CH2-CH2-CO-] are indicated. (**B**) Example of the deconvolution pattern of the region 0.6-1.8 ppm in the spectrum of C13 cells.

The ^{1}H-NMR spectra of 2008 and C13 cell lines showed similar general features, however, at a more detailed analysis some significant differences were observed as reported in **Tables 4-5.** The levels of glutathione detected was about 1.6 times higher in C13 cells in comparison to sensitive 2008 cells (**Table 4**). Furthermore, most of mobile lipid (ML) signals, that were intense for both cell lines, in agreement with data reported for many cancer cells, were significantly higher in C13 than in 2008 cells: at 0.90 ppm [CH_3-], 1.29 ppm [-$(CH_2)_n$-], at 1.32 ppm [-CH_2- CH_2-CH=], at 1.59 ppm [-CH_2-CH_2-CO-] and at 2.24 ppm [-CH_2- CO] (**Table 5)**.

Table 4: **Peak Area Ratios of the Glutathione signals to the Polypeptide –CH3 resonance at 0.94 ppm, in 2008 and C13 cells.**

NMR signal	δ (ppm)	2008 (n=7)	C13 (n=5)
βCH_2 of Glu	2.16	0.28 ±0.04	0.52 ± 0.07***
γCH_2 of Glu	2.56	0.32 ± 0.09	0.46 ± 0.07*

Data are the Mean ± SD of 7 and 5 measurements. *p<0.05, ***p<0.001, Student's t test, comparison 2008 *vs.* C13 cells.

Table 5: **Peak Area Ratios of Mobile Lipid Signals to the Polypeptide –CH3 resonance at 0.94 ppm, in 2008 and C13 cells.**

NMR signal	δ (ppm)	2008 (n=7)	C13 (n=5)
$-C\underline{H}_3$	0.9	1.35 ± 0.22	1.85 ± 0.22**
$-(C\underline{H}_2)_n-$	1.29	1.07 ± 0.41	2.45 ± 0.72**
$-C\underline{H}_3CH_2CH=$	1.32	0.93 ± 0.21	2.35 ± 0.50***
$-C\underline{H}_2CH_2CO-$	1.59	0.03 ± 0.01	0.26 ± 0.12***
$-C\underline{H}_2CH=$	2.03	0.39 ± 0.17	0.77 ± 0.23*
$-C\underline{H}_2CO$	2.24	0.05 ± 0.02	0.11 ± 0.02***
$=CHC\underline{H}_2CH=$	2.73	0.21 ± 0.21	0.47 ± 0.69

Data are the Mean ± SD of 7 and 5 measurements. *p<0.01, **p<0.005, ***p<0.001, Student's t test, comparison 2008 *vs.* C13 cells.

To better appreciate differences between wild-type and CDDP-resistant cells, a multivariate analysis by means of principal component analysis (PCA) was conducted for glutathione and MLs and peak areas detected by ^{1}H-NMR spectra. As shown by the plot in **Fig. 9**, the PC1 vs PC2 scores indicate that 2008 and C13 are clearly separated cell population.

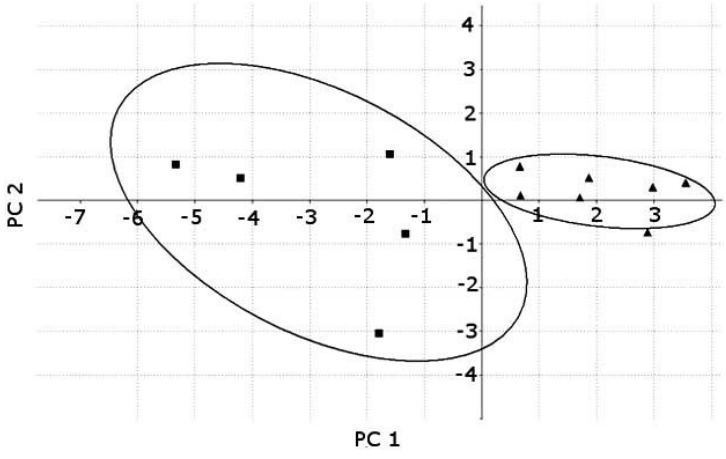

Figure 9: Scores plot of the Principal Component Analysis (PC1 vs PC2) conducted on MLs and GSH peak area in ^{1}H-NMR spectra of 2008 ■ and C13 ▲ cells (see Tables **2** and **3**; data are the mean ± SEM of 5-7 measurements). The two cell lines present well-distinct groupings, suggesting an overall different metabolic pattern. The ellipses indicate the 68% confidence interval for each group.

1.7 Nile Red Neutral Lipid Staining

It has been demonstrated that in many tumours, cells catabolize glucose at a rate that exceeds bio-energetic needs by shifting from oxidative to glycolytic metabolism [Shaw R. J., 2006; Bui T. and Thompson C.B., 2006; Garber K., 2006]. Furthermore, frequently de novo fatty acids synthesis is increased [Kuhajda F.P., 2000].

To confirm the mobile lipids (MLs) results, the intracellular lipid content of 2008 and C13 cells was stained with Nile red neutral lipid dye and the fluorescence was observed by confocal microscopy (**Fig. 10A)**. Results show neutral lipid accumulation mainly into cytoplasmic droplets in both cell lines, but more intensely labelled spots in resistant cells (C13) than in cisplatin sensitive cells (2008). Quantitative determination of Nile red fluorescence was therefore carried out with cytofluorimetry (**Fig. 10B**), demonstrating about two fold more elevated MFI in C13 cells than in 2008 cells.

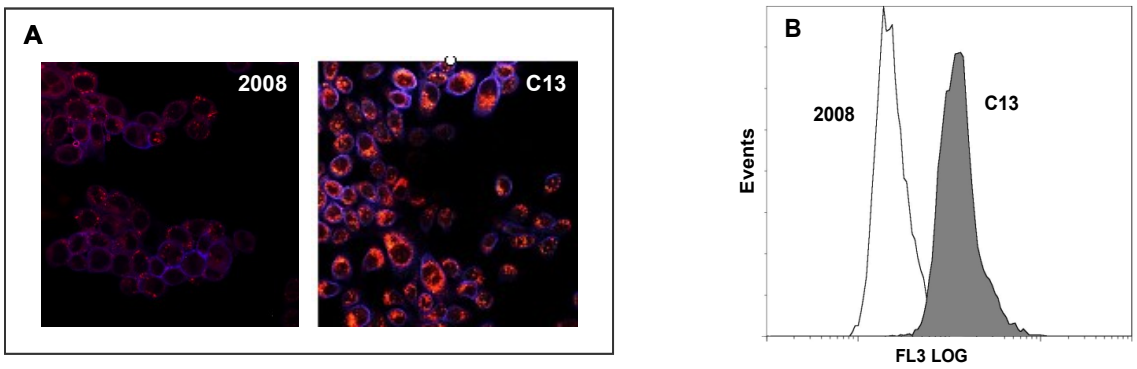

Figure 10: Nile red neutral lipid staining in 2008 and C13 cells. (**A**) Images acquired with a Nikon C1 confocal microscope and Nikon EZ-C1 software (version 2.10), magnification 60X. (**B**) Mean fluorescence intensity [MFI] measured by flow cytometry. All images are exemplificative of at least four different experiments.

2. Phenotyping of Transmitochondrial Hybrids derived from 2008 and C13 Cells

To deeply investigate a possible role of the mitochondria on the metabolic remodelling observed in cisplatin-resistant ovarian cancer cells, the hybrid cell model was used. Transmitochondrial hybrids (H2008 and HC13) were generated by fusion of ovarian carcinoma cells (2008-C13), previously enucleated, with mtDNA depleted osteosarcoma cells (206-ρ°). This cellular model permits to study the influence of mtDNAs on cell function, independently from its own nuclear DNA. Firstly the hybrids generated from ovarian carcinoma cells (H2008 and HC13) were sequenced for their mitochondrial DNA, to confirm their genetic stability. Results showed the same polymorphisms observed in the parental cells (data not shown). Therefore, hybrids were phenotyped for comparison with parent cell lines.

2.1. Cell viability and apoptosis following CDDP treatment

The effect cisplatin (0.1-100 µM). was evaluated on cytoplasmatic hybrids (H2008 and HC13) after 24 hours of exposure. The experiments, performed by MTT test (**Fig. 11a**) and trypan blue exclusion assay (**Fig. 11b**), show a concentration-dependent activity in both cell lines, whose drug sensitivity is practically superimposable.

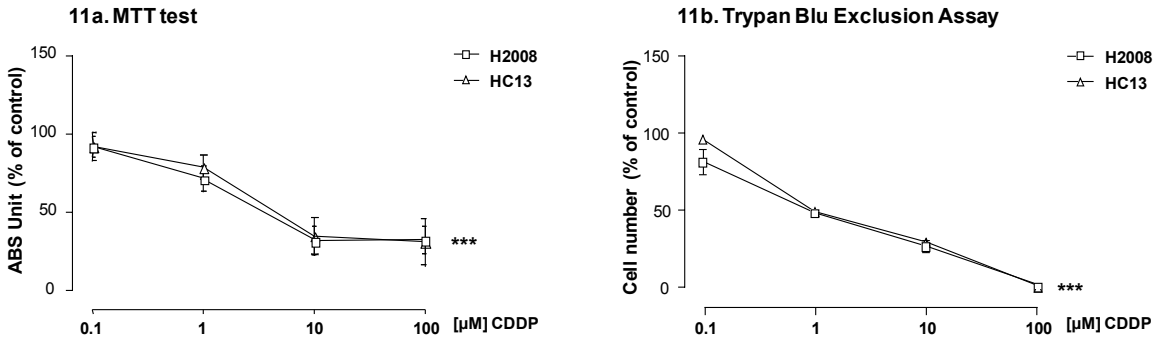

Figure 11: Effect of cisplatin (0.1-100 µM) on cybrids' cell viability measured by MTT **(a)** and trypan blu exclusion assay **(b)**. Data are the mean ± SEM of 4 different experiments in quadruplicate for MTT and in duplicate fo Trypan blu assay. ***p < 0.001, ***p* < 0.01; CDDP vs control.

As shown by flow cytometer assay (**Fig. 12**), also the percentage of apoptotic cells after cisplatin treatment (1-10 µM) is similar between H2008 and HC13, demonstrating that the two cybrid cell lines, having the same nuclear background, lose the different susceptibility to cisplatin observed in 2008 and C13.

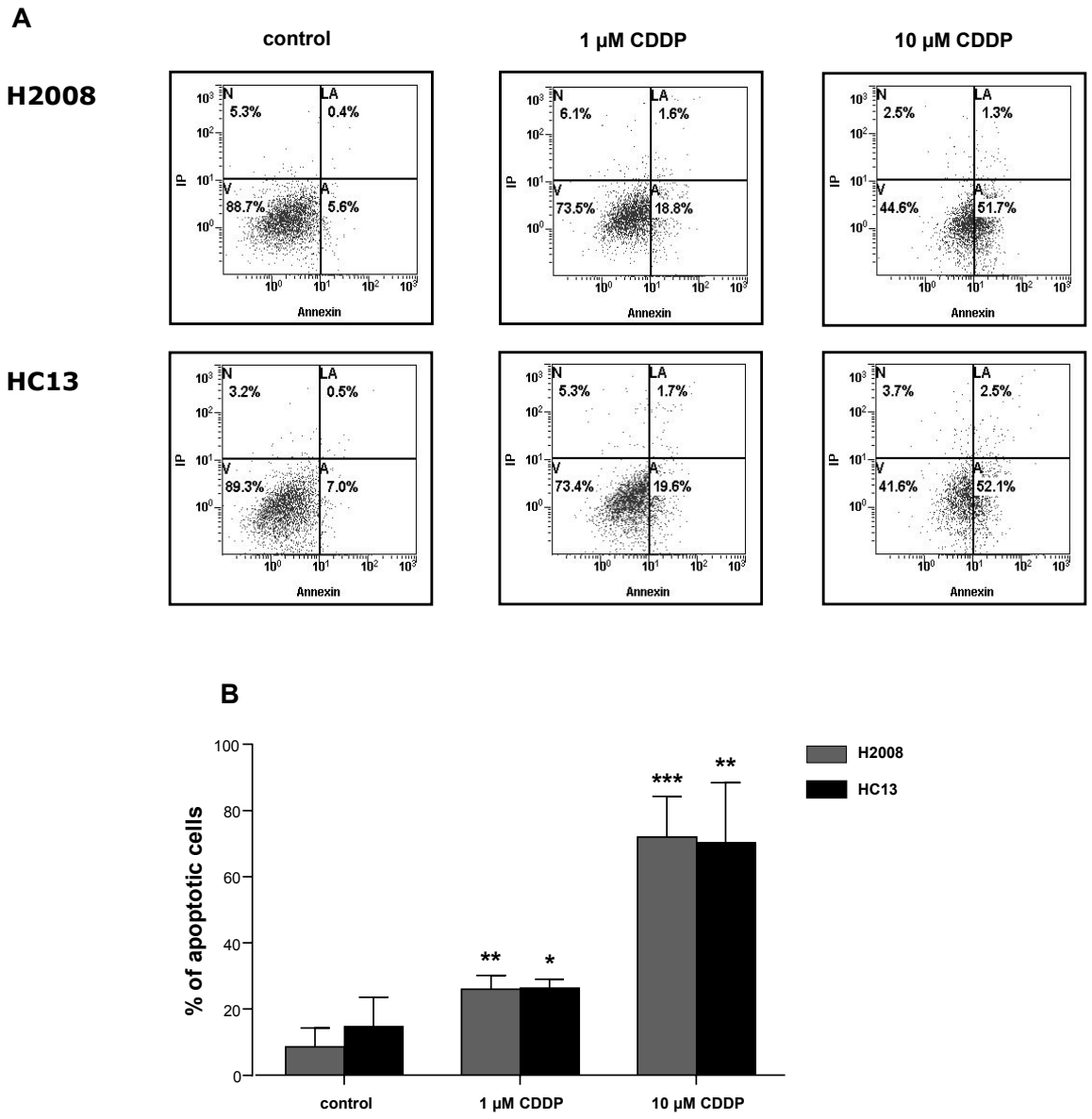

Figure 12: Apoptosis induced by cisplatin (1-10 µM) in H2008 and HC13**.** In **Fig. 12(A)** there are plots obtained by flow cytometer. In **Fig 12(B)** data are expressed as percentage of apoptotic cells under basal condition (control) and after 24h of treatment with CDDP. ***p < 0.001, **p < 0.01, *p < 0.05; CDDP vs control.

2.2 Oxygen consumption

To investigate the role of nuclear genome on the respiratory chain's activity, the oxygen consumption was parallely detected in ovarian cancer cells and in their derived cybrids. The result (**Fig. 13**) is expressed as ratio C13/2008 compared with HC13/H2008 and highlights that, differently to ovarian cancer cells, the hybrids cell lines haven't significant differences in the oxygen consumption.

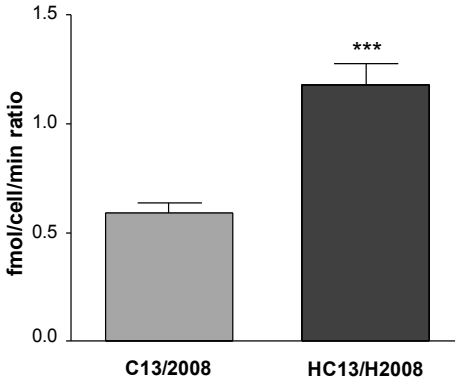

Figure 13: Oxygen consumption [fmol oxygen/cell/min] in ovarian cancer cells (C13/2008) and their derived cybrids (HC13/H2008). ***p < 0.001, cybrids vs tumoral cells.

2.3. Effect of galactose and rotenone on Cell Growth

As depicted in **Figures 14 a-b**, HC13 and H2008 didn't show any difference in cell growth when incubated in glucose free/galactose medium or in the presence of (0.1-10 μM) rotenone. These results evidence a similar sensitivity to mitochondrial stress.

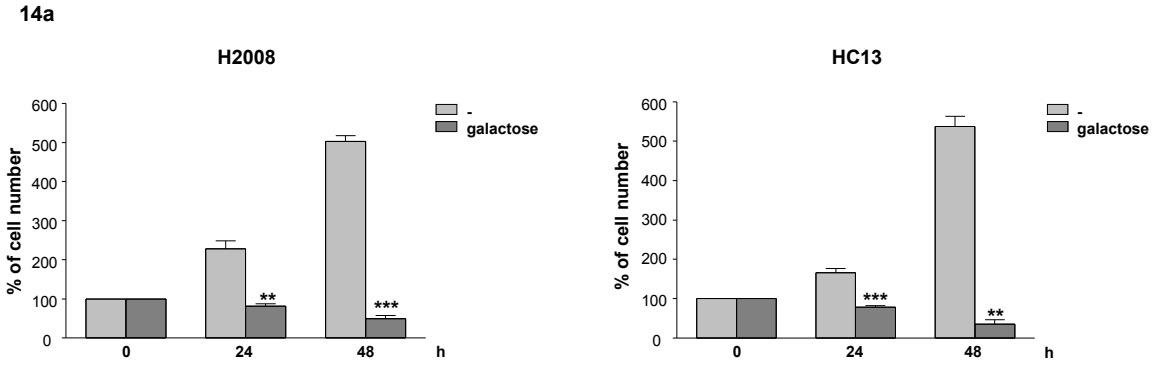

Figure 14a: Effect of 5mM galactose on H2008 and HC13 cell viability after 24 and 48 hours of treatment. Data are expressed as as % of cell number after 24-48 h compared to the $t_{0.}$ Data are the mean ± SEM of 3 different experiment. ***p < 0.001, **p < 0.01; galactose vs control.

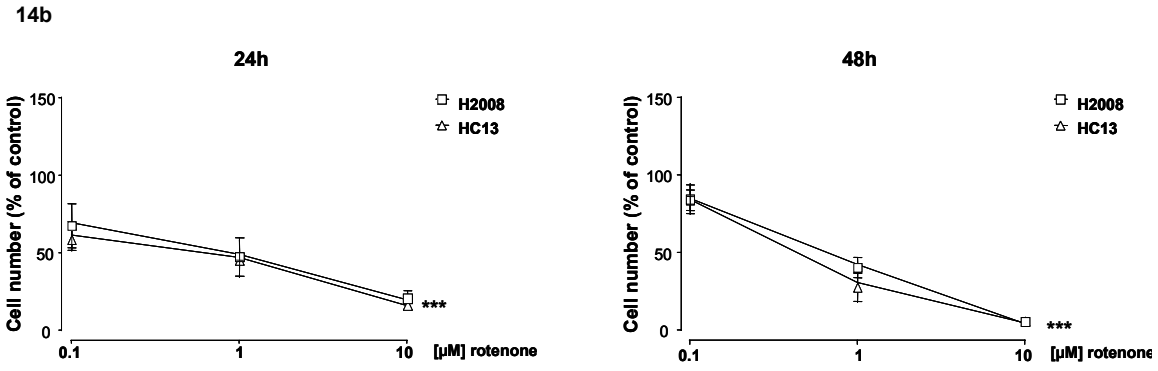

Figure 14b: Effect of rotenone (0.1-10 µM) on H2008 and HC13 cell viability after 24 and 48 hours of treatment. Data are expressed as % of cell number compared to the respective control. Data are the mean ± SDM of 3 different experiment. ***p < 0.001; rotenon vs control.

2.4 Mitochondrial Mass and Membrane Potential

Markers of mitochondrial functionality were assayed in H2008 and HC13 hybrids and the results, expressed as ratio (C13/2008) and (HC13/H2008), were compared with those in 2008 and C13 parent cells.

As previously observed, results confirm that C13 CDDP-resistant cells, as compared to wild type 2008 cells, present a fall of mitochondrial potential (**Fig 15b**), associated with a significantly reduced mitochondrial mass (**Fig. 15a**). By contrast no significant differences exist between HC13 and H2008 hybrids, confirming that there is a nuclear control in the mitochondrial remodelling undergone from the cisplatin-resistant cells.

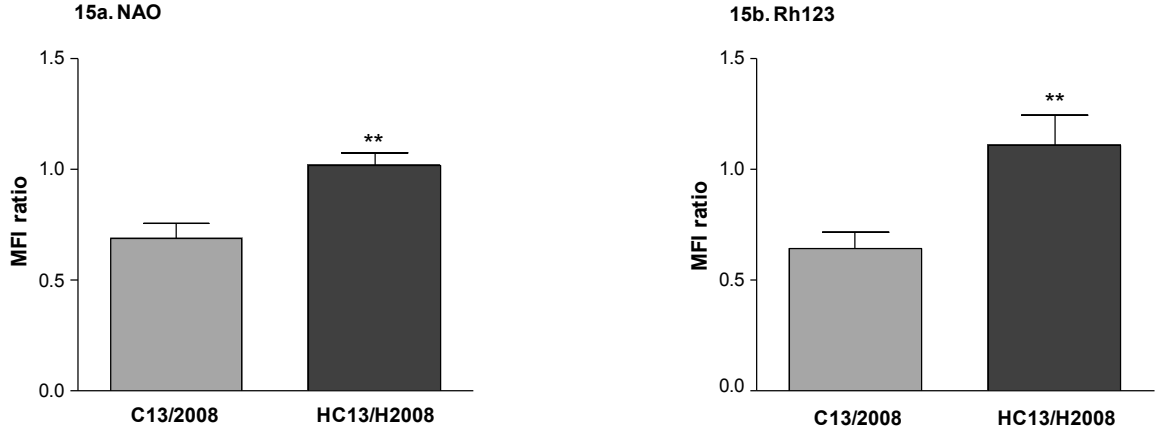

Figure 15: Mitochondrial mass **(a)** and potential **(b)** in ovarian cancer cells and in their derived cybrids, measured by flow cytometry and expressed as mean fluorescent intensity [MFI] of NAO (25 nM) and Rh123 (10 µM). Each bar represents the mean ± SEM of 5 independent experiments. ** $p < 0.01$. cybrids *vs* cancer cells.

The cytofluorimetric data of mitochondrial membrane potential and mitochondrial mass were consolidated with in live microscopy whose images are shown in **fig. 16** and the ratiometric quantification of red signal on green one (TMRM/MTG) of hybrids is reported in **Table 6**.

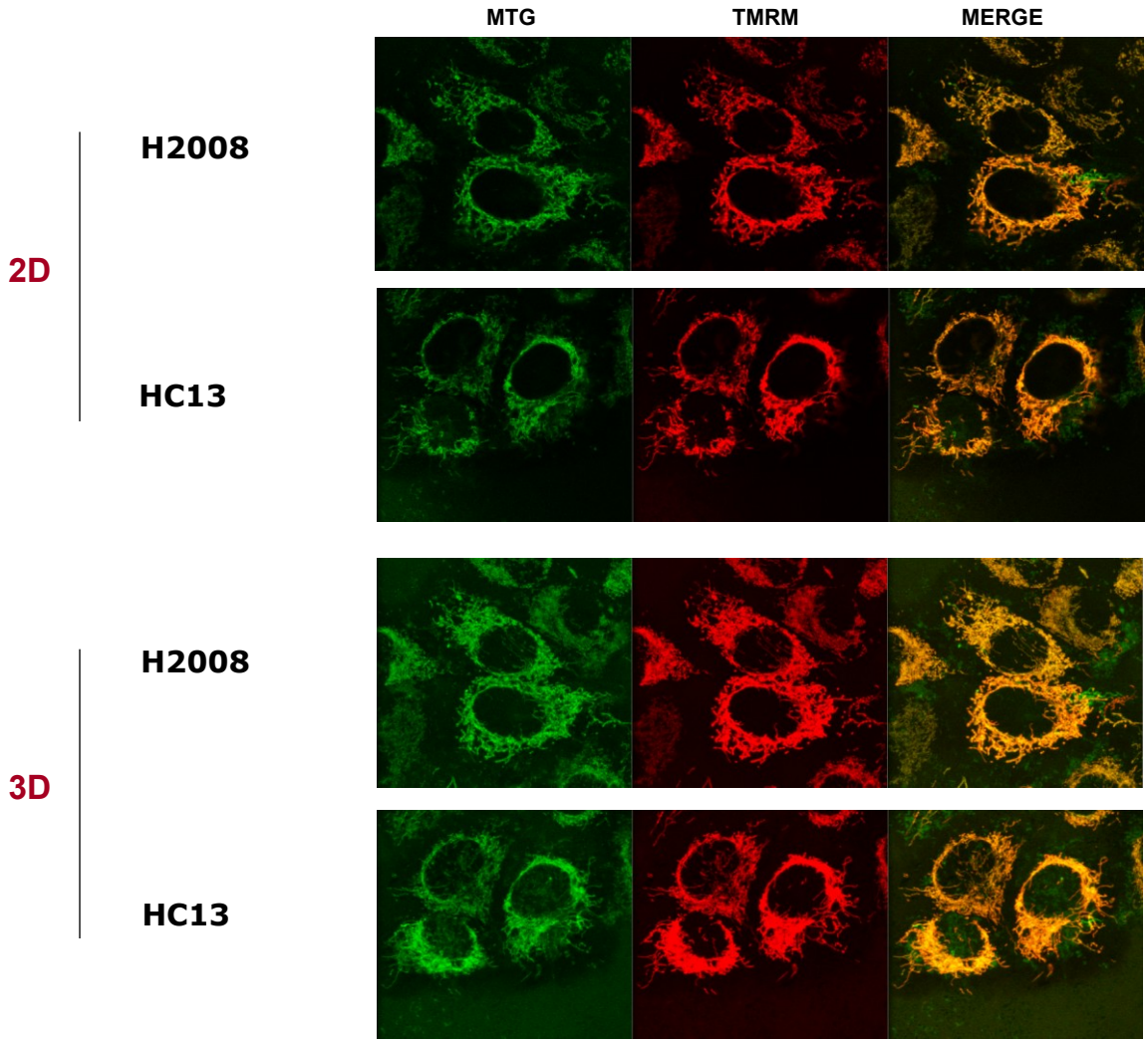

Figure 16: Images of cybrids cells acquired with Leica confocal microscope (60X) using MTG (100 nM; λec/em= 490/516) and TMRM (10 nM; λec/em= 544/590). Images acquired in C. Frezza lab (Hutchison/MRC Research Centre, Cambridge).

Table 6: Mean Fluorescence intensity (MFI) of MitoTracker Green (MTG) and TetraMethyl-Rhodamine Methyl-esther (TMRM) and their ratio in H2008 and HC13

MFI / Cell lines	MTG	TMRM	TMRM/MTG
H2008	**70,92** ±20,29	**105,19** ±32,21	**1,49** 1.09-1.79
HC13	**72,48** ±14,01	**108,69** ±20,24	**1,56** 1.23-1.89

2.5 mtDNA content

The last mitochondrial parameter that was investigated, is the mtDNA content. Results confirm that the levels of mtDNA are significantly lower in the resistant cell line as compared with the sensitive, while no significant differences were observed in cybrid cell lines (**Fig. 17**).

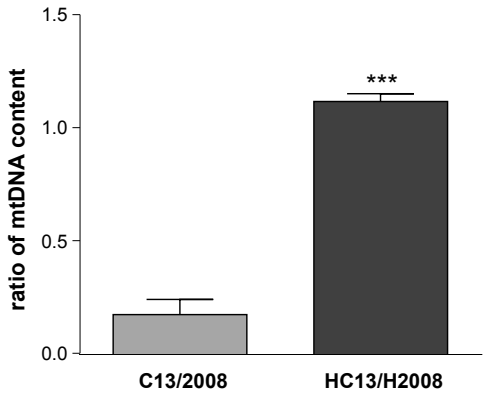

Fig. 17: mtDNA content measured by qRT-PCR in ovarian cancer cells (2008-C13) and their derived cybrids (H2008-HC13). ***p < 0.001, cybrids vs.tumoral cells. .

3. Metabolic reprogramming

3.1 Nuclear transcription factors and target genes

HIF-1 is an heterodimeric complex, consisting of a constitutive subunit HIF-1β and an hypoxia inducible subunit HIF-1α: under normoxia, HIF-1α is rapidly degraded, while during hypoxia is stabilized and translocates into the nucleus, where it dimerizes with HIF-1β, forming the transcriptionally active complex inducing several target genes to favour the metabolic adaptation [Papandreou I. et al., (2006); Wang et al., (1995); Pugh C.W. and Ratcliffe P.J., (2003)].
In this study basal HIF-1α expression was determined in ovarian cancer cells and in their cybrids under basal condition. Interestingly, HIF-1α was measurable in all cell lines, even if mostly in C13 cells (**Figure 18)**.

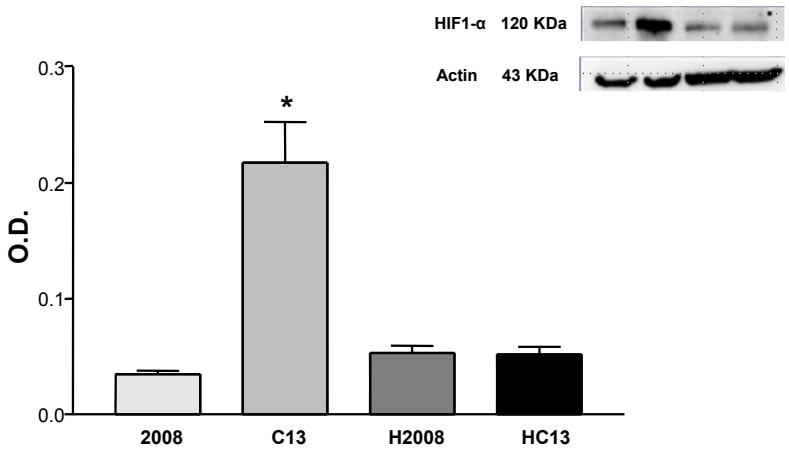

Fig 18: HIF-1α expression in normoxia. Optical density (O.D.) was normalized to that of actin. Data are the mean±SEM of four determinations. *p < 0.05 C13 *vs* 2008 and hybrid lines.

Intriguingly c-Myc is a nuclear transcription factor capable to induce genes involved in glycolysis, but in contrast to HIF-1, promoting mitochondrial biogenesis under non hypoxic conditions [Kim J. W. et al., (2004); Li F. Y. et al., (2005); Zhang H. et al. (2007)]. In this study the crosstalk between HIF-1 and cMYC transcription factors was investigated in ovarian cancer cells and in cybrid cell lines, by measuring the mRNA levels of c-Myc and of several genes involved in the regulation of the glycolytic flux (**Fig 19)**. In particular some genes controlled both by HIF-1α and c-MYC (GLUT1-LDHA-PFKM-PGK1), and BNIP3, gene induced only by HIF-1α, were analysed in C. Frezza lab (Hutchison/MRC Research Centre, Cambridge).

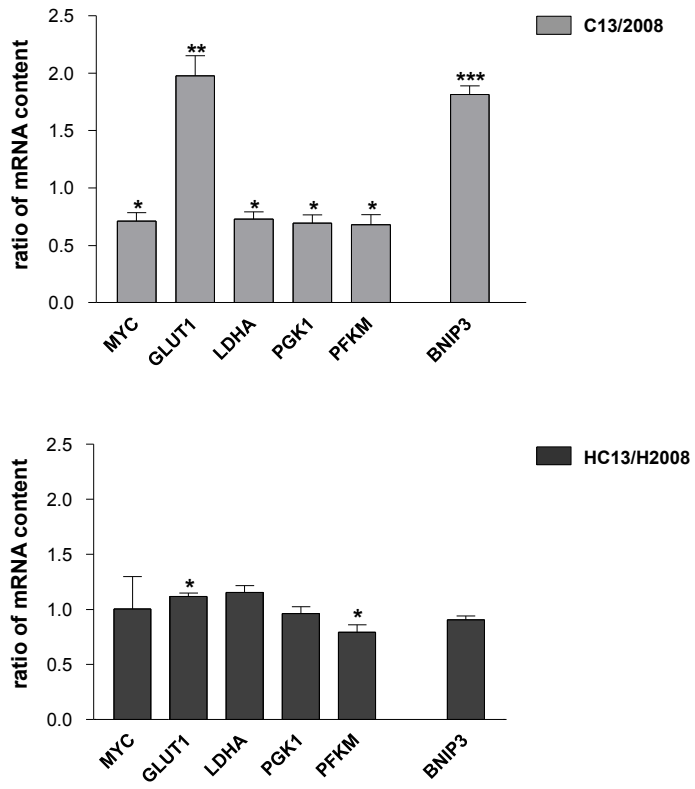

Fig 19: mRNA content of c-Myc and of target genes (of HIF-1α and c-Myc) under normoxia. mRNA measured by qRT-PCR and normalized with the actin levels. Data are expressed as ratio of C13/2008 mRNA content. Mean±SEM of four determinations. ***p < 0.001, **p < 0.01, *p < 0.05, C13 vs.2008; HC13 *vs* H2008.

As expected significant differences were observed between 2008 and C13 wild type cells, being GLUT1 and BNIP3 mRNA level more elevated and LDHA-PFKM-PGK1 lower in cisplatin-resistant than sensitive cells. Interestingly also c-MYC was down-regulated in cisplatin-resistant cells. By contrast only marginal differences were observed between the two hybrid cell lines, having similar nuclear background.

3.2 LC-MS

To further investigate the difference between metabolic signature of sensitive and resistant ovarian cancer cells, an unsupervised endo-metabolomic analysis was performed in C. Frezza lab (Hutchison/MRC Research Centre, Cambridge), using LC-MS. The total ion current of the different samples was used as a confirmation for normalized input. The early unsupervised multivariate analysis conducted by E. Ragazzi (Dipartimento di Scienze del Farmaco, Università degli Studi di Padova) for all peak intensities detected from spectra of cell extracts, is shown in **Figures 20 a-b**.

Both hierarchical clustering and the principal component analysis show a clear separation of 2008 and C13 cells, confirming ^{1}H-NMR results obtained in live cells analysis.

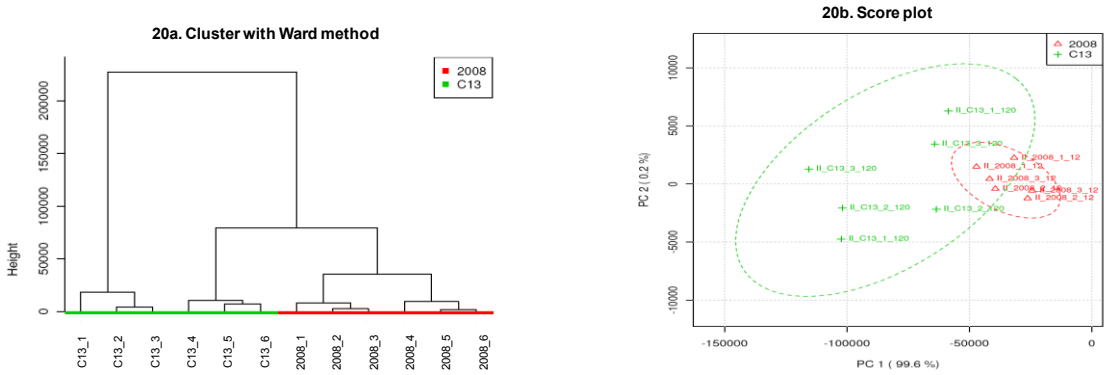

Fig 20: Unsupervised multivariate analysis of LC-MS of ovarian cancer cisplatin intracellular extracts: **a**) hierarchical clustering and **b)** principal component analysis (PCA) of peak signals.

A detailed identification of the most relevant peaks and the relative signal quantitative intensity analysis, revealed significant differences in the metabolic profile of cisplatin-sensitive and resistant-cells, reported as the ratio C13/2008 in **Figure 21**.

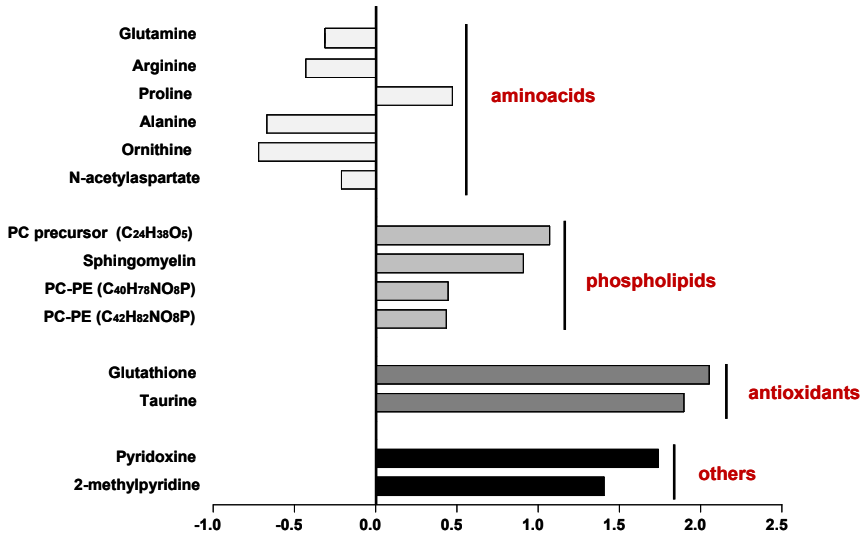

Fig 21: C13 / 2008 ratio of peak intensity signals of selected metabolites revealed by LC-MS analysis.

The results show a significant lower aminoacid content in the cisplatin-resistant cells compared to the sensitive cell line. By contrast there are higher levels of antioxidant glutathione and taurine, as well as of several membrane phospholipids (phosphacholines, phosphaethanolamines, sphingomyelines) in C13 cells than in 2008 ones.

The intensity of peak signals for each metabolite, measured by LC-MS in 2008 and C13 cells as well the mean variation of the amount between the two lines, calculated from 3 different spectra in duplicate is reported in **Figs. 22 a-d**.

Fig 22a. Aminoacid content in 2008 and C13 cells. Box plots of data indicate median (horizontal live), 25th and 75th percentile (box margins), maximum value (wiskers's end).

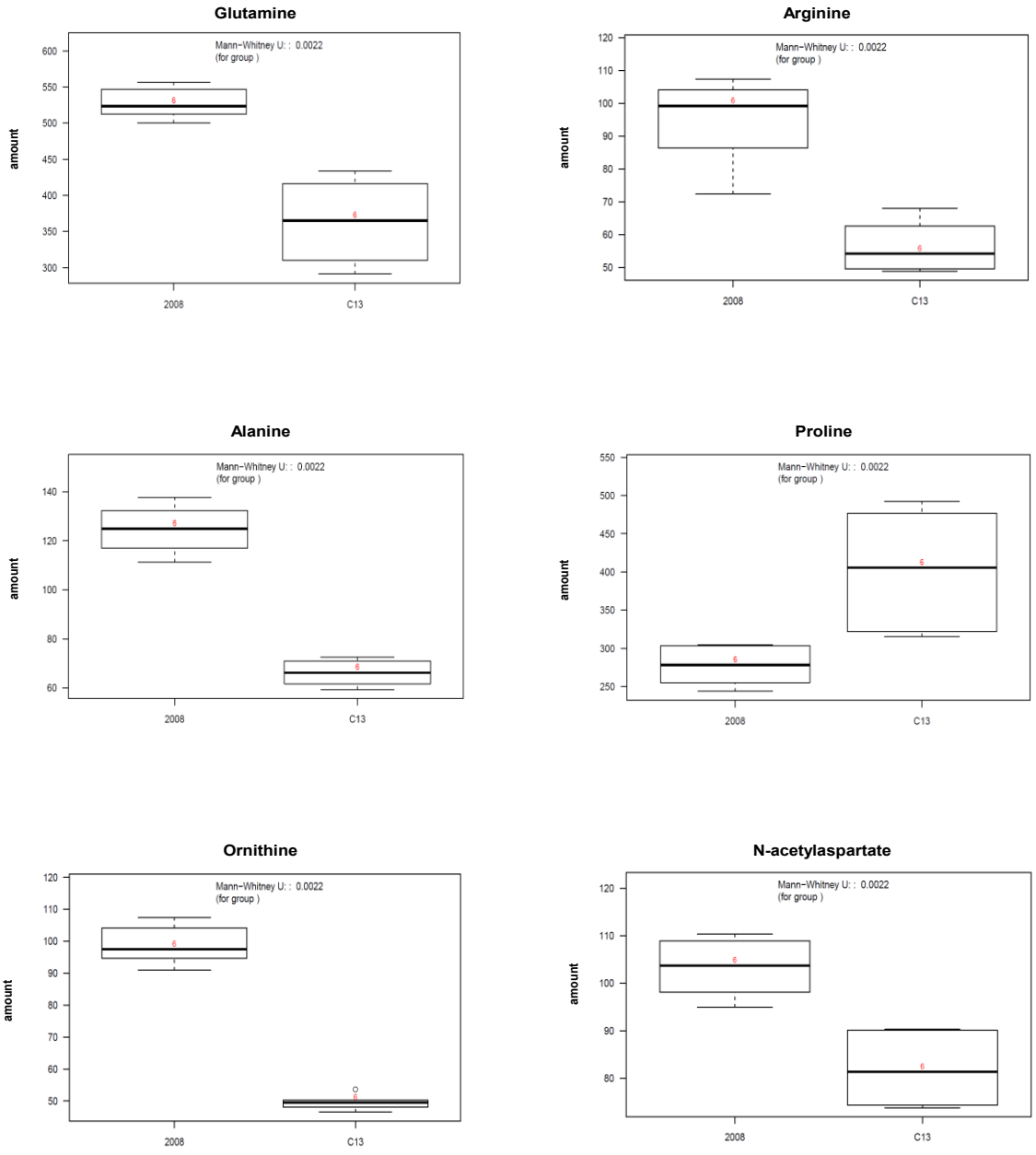

Fig 22b. Phospholipid content in ovarian cancer cells.

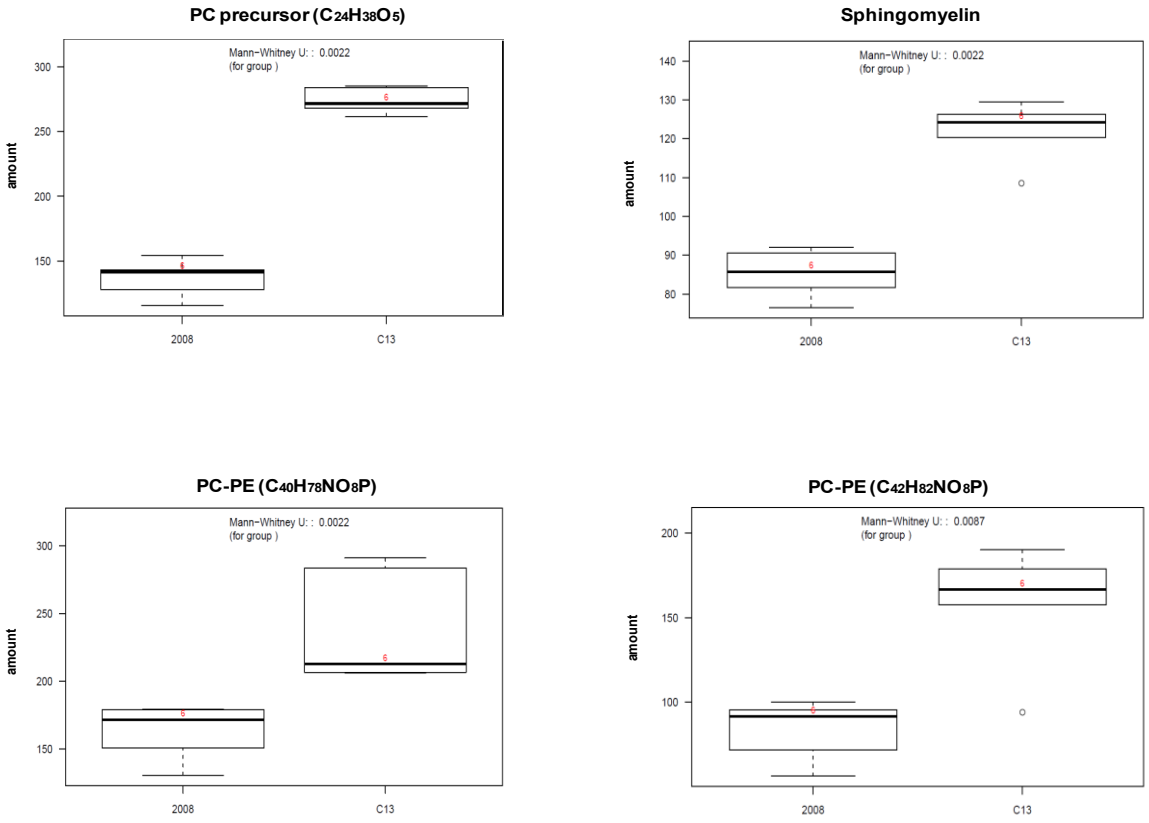

Fig. 22c. GSH and taurine levels in ovarian cancer cells.

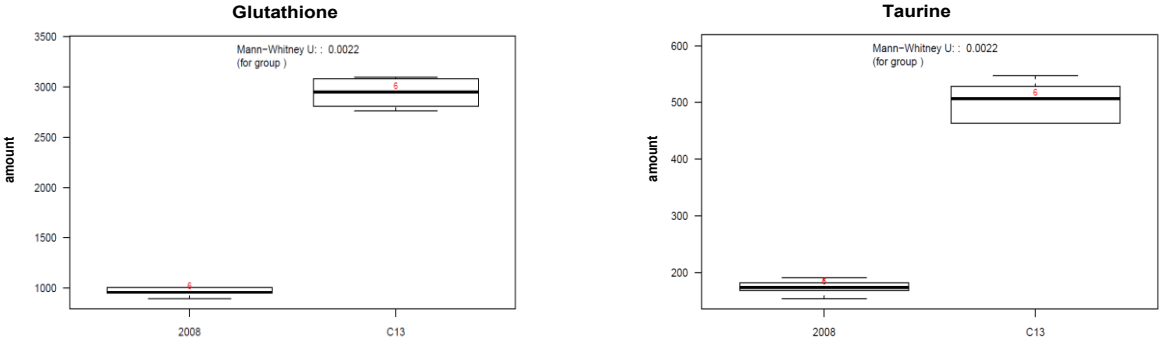

Fig. 22d. Pyridoxine (Vit. B6) and 2-methylpiridine in ovarian cancer cells.

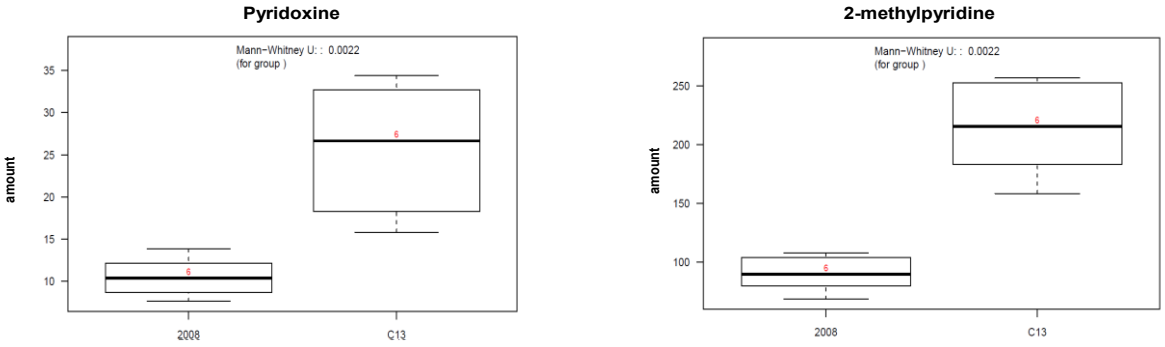

These results suggest that C13 cells might increase their intracellular defence system as well as the aminoacidic consumption for macromolecules synthesis, thus counteracting the cytotoxicity of cisplatin.

3.3. Effect of glutamine deprivation on cell viability

Glutamine, whose carbons can enter into the tricarboxylic acid (TCA) cycle, has been revised as an essential bioenergetic and anabolic substrate for many cancer cell types. Since LC-MS showed a lower glutamine level in cisplatin-resistant C13 cells than in 2008 sensitive cells, cell proliferation of the two cell lines were studied in medium with or without glutamine **(Fig. 23)**.

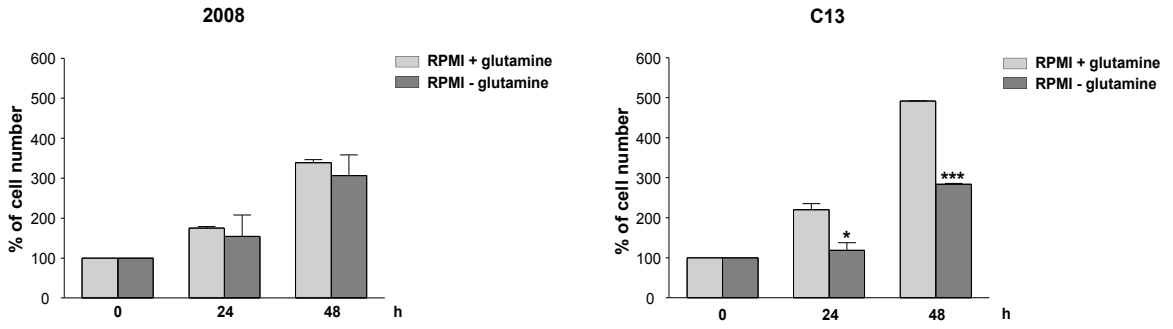

Fig 23: Effect of glutamine deprivation on 2008 and C13 cell viability (24 and 48 hours of treatment). Cell viability was measured by the blue dye exclusion assay. Data are expressed as percentage of the cell number compared to the t_0. Data are the mean ± SEM of 3 different experiments. ***$p < 0.001$, *$p < 0.05$ treatment vs control.

Results clearly showed that the C13 cell growth is significantly reduced when coltured in deprivation of glutamine, while no statistical differences were detected for 2008 cells. Data suggest that C13 cells have a major dependence from glutamine aminoacidic substrate as well as from glucose, as previously shown (see **fig. 2** of cell viability in galactose).

DISCUSSION

In this study the shift of cisplatin-resistant ovarian cancer cells from OXPHOS to a glycolytic metabolism with characteristics of a lipogenic phenotype is shown. By using trans-mitochondrial cell model, it was possible to study the mitochondrial DNA and verify the nucleus involvement in the mitochondrial and metabolic remodelling observed in cisplatin-resistant cells. Cisplatin is one of the most potent chemotherapeutic agents used in the treatment of several types of tumours, including ovarian carcinoma [Galansky M., (2006)]. Even if the benefits of cisplatin are largely recognized, the therapeutic effectiveness of the drug is limited by the onset of cisplatin resistance [Koberle B. et al., (2010)], whose mechanisms are still not clearly understood. Indeed the resistance to cisplatin is a multifactorial phenomenon including, among others, changes in drug transport and accumulation, increased DNA repair and detoxification systems, and evasion from apoptotic cell death [Rabik C.A. and Dolan M.E., (2007); Boulikas T. et al., (2007)]. Recent studies have shown that also the density of mitochondria might affect the chemoresistance suggesting that mitochondria are a potential target for cisplatin. In this study, these issues have been investigated by different experimental approaches. Results from early research in our laboratory demonstrated that in cisplatin-resistant cells (C13) the respiratory chain activity is lower and the dependency on glucose is higher than in cisplatin-sensitive cells 2008 [Montopoli M. et al., (2011)]. It was also observed that cisplatin is equipotent in both mtDNA-deprived 2008-ρ^0 and C13-ρ^0 cells, demonstrating that mtDNA lack decreases drug sensitivity. In the present study, oxygen consumption, ATP generation, cell viability in metabolic stress condition, mitochondrial potential/mass and mtDNA content were measured in 2008 and C13 cells; the results showed a significant reduction of all mitochondrial parameters in cisplatin resistant cells. Since mitochondrial DNA mutations and mitochondrial deficits have been reported for a wide variety of cancers [Wallace D.C., (2011)], mitochondrial DNA of 2008 and C13 cells was completely sequenced. Results showed the same polymorfisms between the two cell lines; however, only in C13 cells heteroplasmic mutations were identified: two classified at low probability of pathogenicity (m.13828 C> T, m.8156 G> T) and one borderline to be pathogenic (m.12018 C> T).

In order to investigate if mtDNA might be responsible of the altered mitochondrial function of C13 cells, we have taken advantage of an innovative experimental model such as the trans-mitochondrial hybrids (cybrids). Cybrids are cytoplasmatic hybrid cells derived from the fusion of enucleated cells (cytoplasts or mitochondria donor) with mtDNA-depleted cells (ρ^0 or nucleus donor). This procedure was chosen to study the influence of mtDNA independently from the original nDNA, because in an identical nuclear background. This experimental model has been

recently used in *in vitro* studies of different mitochondrial diseases [Giordano C. et al., (2012); Perli E. et al., (2012)].

In this study cybrids (H2008 and HC13 cells) were generated from 2008 and C13 cells and phenotyped. mtDNA sequences were identical to those in parent cells. However the two hybrid clones showed similar sensitivity to cisplatin cytotoxicity as well as similar mitochondrial parameters that are amenable to those of 2008. These results indicated that the heteroplasmic mtDNA mutations themselves were not causative factors of the reduced mitochondrial activity of C13 resistant cells that is thus probably associated to nuclear factors. It is indeed known that the coordination between nuclear and mitochondrial genomes is required in all cellular types. In the last years, increasing evidences have suggested that growth signalling pathways directly control cell metabolism, growth and proliferation through the regulation of metabolic enzymes [Cairns R.A. et al. (2011), Ward P.S. et Thompson C.B. (2012)]. It is known that many cancer cells are characterized by alteration of several oncogenes and tumour suppressor genes that can lead to changes of important energy metabolism pathways such as glucose transport, tricarboxylic acid (TCA) cycle, glutaminolysis, oxidative phosphorylation of the mitochondrial respiratory chain and pentose phosphate pathway (PPP) [Chen J.Q. and Russo J., (2012)]. The hypoxia-inducible factors (HIFs) and c-MYC are critical factors for tumorigenesis in a large number of human cancers. Acting alone, HIF and c-Myc partially regulate the adaptation mechanisms that cancer cells undergo in a low O_2 microenvironment. However, acting in concert, these transcription factors reprogram metabolism, protein synthesis, and cell cycle progression to support bioenergetics and cell survival [Gordan J.D. et al., (2007)]. It is also known that HIF and c-Myc can directly act on mitochondria with opposite effects: whereas c-Myc may positively regulate mitochondrial mass promoting mitochondrial biogenesis [Kim J. W. et al., (2004); Li F. Y. et al., (2005); Zhang H. et al. (2007)], HIF is able to reduce mitochondrial mass, inducing mitophagy or inhibiting c-Myc [Zhang H. et al., 2007]. These data prompted us to explore these important transcription factors and some of their target genes involved in glycolytic flux and mitophagic processes. Results showed no differences between hybrid cell lines, while cisplatin-resistant cells (C13), as compared to 2008 cells, present higher levels of HIF and BNIP3, the latter being a gene (protein-coding) triggering mitochondrial-selective autophagy. [Zhang et al. 2008; Bellot et al. 2009]. By contrast, qRT-PCR showed lower levels of c-Myc well correlated with the reduced mitochondrial potential/mass and the lower mtDNA content measured in C13 cells. Molecular findings also showed differences in GLUT1, LDHA, PFKM and PGK1 levels and, in order to better understand the C13 profile, metabolomic studies were undertaken.

Although metabolic reprogramming is thought to be essential for rapid cancer cell proliferation, a systematic characterization of the metabolic pathways in transformed cells is lacking, and the contribution of these pathways remains unclear [Hsu P.P. and Sabatini D.M., (2008)]. Studies of cancer metabolism have examined relatively few cell lines, and have largely focused on the intracellular metabolite pools [Sreekumar A. et al., (2009)], or have relied on isotope tracing to estimate metabolic flux through a limited number of reactions [DeBerardinis R.J. et al., (2007)]. ^{1}H-NMR spectroscopy and liquid chromatography combined with orbitrap-based mass spectroscopy (LC-MS) have recently emerged as invaluable analytical tools, crucial to uncover the determinants of the metabolic transformation of cancer cells but also to discover potential tumour targets. Data obtained by ^{1}H-NMR spectra (*in vivo* cell samples) and LC-MS spectra (cell extracts), showed different fingerprints highlighted from hierarchical clustering methods. In particular C13 cells, compared to 2008 cells, present a significant increase of glutathione, taurine, mobile lipids and phospholipids (phosphacholines, phosphoethanolamine, sphingomyelin), pyridoxine, 2-methylpyridine, but a lower aminoacid content.

Glutathione was expected to be higher in C13 than in 2008 cells since it is one of the well known mechanisms of resistance to cisplatin, whereas the unexpected increase of taurine as molecule with antioxidant activity was an interesting result to better investigate.

Most of the carbon for fatty acid synthesis is derived from glucose, but also glutamine uptake appears to be critical for lipid synthesis in that it supplies carbon in the form of mitochondrial oxaloacetate to maintain citrate production in the first step of the TCA cycle [Wise D.R. et al., (2011); Metallo C.M. et al., (2012); Mullen A.R. et al. (2012)]. In this regard glutamine has been re-discovered as an essential bioenergetic and anabolic substrate for many cancer cell types. In C13 cells the level of TCA intermediates were not different from 2008 cells, therefore it might be assumed that in C13 cells, compared with 2008, there is a higher consumption of glutamine as well as the other aminoacids for a faster substrates synthesis and cell duplication, as confirmed by the low C13 proliferation in glutamine-free medium.

The fundamental role of phospholipid in cellular structure is well known. Recent work shows that intact PLs act as signaling molecules by modulating the activity of nuclear hormone transcription factors responsible for tuning genes involved in metabolism, lipid flux, steroid synthesis and inflammation [Musille P.M. and Kohn J.A.; (2013)]. The reorientation of signaling pathways leads to the expression and/or activation of various enzymes which participate in aerobic glycolysis allowing cancer cells to produce energy (ATP) but also the nucleotides, aminoacids, and lipids required for proliferation. Cancer cells are highly dependent on *de novo* lipid synthesis. In this scenario, resistant ovarian tumour cells (C13) might redirect glycolytic intermediates toward *de novo* fatty acid synthesis, to maintain a constant supply of lipids to fuel membrane production in a

highly-proliferating cell population. Furthermore, ^{1}H-NMR and Nile red staining, showed us that the altered lipid metabolism of C13 cells, culminates in the accumulation of newly formed lipids in cytoplasmic lipid droplets.

Overall, all the results of this study depict a scenario in which C13 resistant cells can be defined as pseudohypoxic phenotype, since they have reformulated their energetic metabolism, presumably bypassing mitochondria that are an important target of cisplatin. Following this hypothesis, HIF-1α overexpression might be crucial to direct substrates toward glutaminolysis and lipid synthesis. In conclusion, cisplatin-resistant ovarian cancer cells adopt a metabolism designed to favor their development and to adapt themselves to the microenvironment. A 'lipogenic categorization' of cisplatin-resistant ovarian cancer cells may also innovate the molecular rationale to identify and develop a new generation of therapeutic agents, interfering with both the initiation of primary carcinomas and the invasive progression of cancer cells. Although further understanding of the the metabolomic fingerprints of cisplatin-resistant cells remains to be elucidated, anti-metabolic strategies associated with the current platinum chemotherapie, could sap the mechanisms of cisplatin chemoresistance and improve their efficacy.

REFERENCES

Andersen M.R., Goff B.A., Lowe K.A., Scholler N., Bergan L., Dresher C.W., Paley P. and Urban N.; (2008). Combining a symptoms index with CA 125 to improve detection of ovarian cancer. *Cancer*: 113(3):484-9.

Andrews P.A., Murphy M.P., Howell S.B.; (1988). cis-Diamminedichloroplatinum(II) accumulation in sensitive and resistant human ovarian carcinoma cells. *Cancer Res.* 48(1):68–73.

Arner ES.J., Nakamura H., Sasada T., Yodoi J., HOmgren A., Spyrou G.; (2001). Analysis of the inhibition of mammalian thioredoxin, thioredoxin reductase; glutaredoxin by cis-diamminidischloroplatinum (II) and its major metabolite, the glutathione-platinum complex. *Free Radic. Biol. Med.* 2001;31:1170–1178.

Arnesano F. and Natile G.; (2008). "Platinum on the road": interactions of antitumoral cisplatin with proteins. *Pure and Applied Chemistry*: 80(12):2715–2725.

Aylon Y., Oren M.; (2007). Living with p53, dying of p53. *Cell*: 130(4):597-600.

Baracca A., Chiaradonna F., Sgarbi G., et al.; (2010). Mitochondrial Complex I decrease is responsible for bioenergetic dysfunction in K-ras transformed cells. *Biochim Biophys Acta*: 1797(2):314-323.

Bauer D.E. et al.; (2005). ATP citrate lyase is an important component of cell growth and transformation. *Oncogene:* 24:6314-6322.

Bensaad K., Tsuruta A., Selak M.A., et al.; (2006). TIGAR, a p53 inducible regulator of glycolysis and apoptosis. *Cell*: 126(1):107-120.

Berardi M.J., Fantin V.R.; (2011). Survival of the fittest: metabolic adaptations in cancer. *Curr Opin Genet Dev.* 21 (1): 59-66.;

Berg J.M., Tymoczko J.L., Stryer L.; (2002). *Biochemistry*. W.H. Freeman and Company, New York.

Bidoli E., La Vecchia C., Montella Dal Maso L., Conti E., Negri E., Scarabeli C., Carbone A., Decarli A., Franceschi S.; (2002). Nutrient intake and ovarian cancer: an Italian case-control study. *Cancer Cause and Control;* 13: 255-261.

Bignami M., Casorelli I., Karran P.; (2003). Mismatch repair and response to DNA-damaging antitumour therapies. *EurJ Cancer*: 39:2142-9.

Binks S.P. and Dobrota M.; (1990). Kinetics and mechanism of uptake of platinum-based pharmaceuticals by the rat small intestine. *Biochem. Pharmacol.* 40, 1329.

Bos J.L.; (2005). ras oncogenes in human cancer: a review [J]. Cancer Res, 1989,49(17):4682-4689.

Bosl G.J. and Motzer R.J., (1997). Testicular germ-cell cancer. *N Engl JMed.* 337:242-54.

Bookman M.; (2005). Standard treatment in advanced ovarian cancer in 2005: the state of the art. *International Journal of Gynecological Cancer:* 15:212–220.

Boulikas T. and Vougiouka M.; (2003). Cisplatin and platinum drugs at the molecular level. (Review). *Oncol Rep.* 10(6):1663-82.

Brunelle J.K., Bell E.L., Quesada N.M., et al.; (2005) Oxygen sensing requires mitochondrial ROS but not oxidative phosphorylation. *Cell Metab*. 1(6):409-414.

Bui T. and Thompson C.B.; 2006. Cancer's sweet tooth. *Cancer Cell*: 9, 419-420.

Buller R.E.; (2003). Mismatch repair gene expression defects contribute to microsatellite instability in ovarian carcinoma. *Cancer*: 98: 2199-206.

Byun S.S., Kim S.W., Choi H., Lee C., Lee E.; (2005). Augmentation of cisplatin sensitivity in cisplatin-resistant human bladder cancer cells by modulating glutathione concentrations and glutathione-related enzyme activities. *BJU Int.* 95(7):1086–90.

Carling D., Sanders M.J., Woods A.; (2008). The regulation of AMP-activated protein kinase by upstream kinases. *Int J Obes*: 32:55-59.

Cepeda V., Fuertes M.A., Castilla J., Alonso C., Quevedo C., Pérez J.M.; (2007). Biochemical mechanisms of cisplatin cytotoxicity. *Anti-Cancer Agents in Medicinal Chemistry*: 7(1):3–18.

Chaney S.G. and Sancar A. J.; (1996). Proceedings: Actions of some drugs on enzymes involved in DNA repair and semi-conservative DNA synthesis. *Natl Cancer Inst.* 88, 1346.

Chapuis N., Tamburini J., Green A.S., et al.; (2010). Perspectives on inhibiting mTOR as a future treatment strategy for hematological malignancies. *Leukemia:* 24 (10):1686 -1699.

Chesney J., Mitchell R., Benigni F., et al.; (1999). An inducible geneproduct for 6-phosphofructo-2- kinase with an AU-rich instability element: role in tumor cell glycolysis and the Warburg effect. *Proc Natl Acad Sci U S A:* 96(6):3047-3052.

Chiaradonna F., Gaglio D., Vanoni M., et al.; (2006). Expression of transforming K-Ras oncogene affects mitochondrial function and morphology in mouse fibroblasts. *Biochim BiophysActa*: 1757(9-10):1338-1356.

Cho K.R. and Shi I.M.; (2009). Ovarian Cancer. *Annual Rev Pathol.* 4:287-313.

Chun S.Y., Johnson C., Washburn J.G., et al.; (2010). Oncogenic KRAS modulates mitochondrial metabolism in human colon cancer cells by inducing HIF-1alpha and HIF-2alpha target genes. *Mol Cancer*: 9:293.

Cobo M., Isla D., Massuti B., Montes A., Sanchez J.M., Provencio M., Viñolas N., Paz-Ares L., Lopez-Vivanco G., Muñoz M.A., Felip E., Alberola V., Camps C., Domine M., Sanchez J.J., Sanchez-Ronco M., Danenberg K., Taron M., Gandara D., Rosell R.; (2007). Customizing cisplatin based on quantitative excision repair crosscomplementing 1 mRNA expression: a phase III trial in non-small-cell lung cancer. *J Clin Oncol.* 25: 2747-54.)

Crino P.B., Nathanson K.L., Henske E.P.; (2006). The tuberous sclerosis complex. *N Engl J Med*. 355(13):1345-1356.

Cullen K. J., Yang Z., Schumaker L. and Guo Z.; (2007) Mitochondria as a critical target of the therapeutic agent cisplatin in head and neck cancer. *J. Bioenerg. Biomembr.* 39, 43–50

Dang C.V., Le A., Gao P.; (2009). MYC induced cancer cell energy metabolism and therapeutic opportunities. *Clin Cancer Res*15(21):6479-6483.

Dan H.C., Sun M., Kaneko S., et al.; (2004). Akt phosphorylation and stabilization of X-linked inhibitor of apoptosis protein (XIAP) *The Journal of Biological Chemistry*: 279(7):5405–5412.

Datta S.R., Brunet A., Greenberg M.E.; (1999). Cellular survival: a play in three akts. *Genes and Development*: 13(22):2905–2927.

DeBerardinis R.J., Mancuso A., Daikhin E., Nissim I., Yudkoff M., Wehrli S., Thompson C.B.; (2007). Beyond aerobic glycolysis: transformed cells can engage in glutamine metabolism that exceeds the requirement for protein and nucleotide synthesis. *Proc Natl Acad Sci U S A*: 104(49):19345-50.

DeBerardinis R.J., Lum J.J., Hatzivassiliou G., et al.; (2008). The biology of cancer: metabolic reprogramming fuels cell growth and proliferation. *Cell Metab.* 7(1):11-20.

DePriest P.D., Banks E.R., Powell D.E., et al.; (1992). Endometrioid carcinoma of the ovary and endometriosis: the association in postmenopausal women. *Gynecol Oncol.* 47(1): 71-5.

Desouki M.M., Kulawiec M., Bansal S., Das G.M., Singh K.K.; (2005). Cross talk between mitochondria and superoxide generating NADPH oxidase in breast and ovarian tumors. *Cancer Biol Ther*. 4:1367-73.

Devarajan P., Savoca M., Castaneda M.P., Park M.S., Esteban-Cruciani N., Kalinec G., Kalinec F.; (2002). Cisplatin-induced apoptosis in auditory cells: role of death receptor and mitochondrial pathways. *Hear Res.* 174:45.

Dornish JM, Pettersen EO.; (1985). Protection from cis-dichlorodiammineplatinum-induced cell inactivation by aldehydes involves cell membrane amino groups. *Cancer Lett.* 29(3):235–43.

Dornish JM, Melvik JE, Pettersen EO.; (1986). Reduced cellular uptake of cis-dichlorodiammine-platinum by benzaldehyde. *Anticancer Res.* 6(4):583–8.]

Dornish JM, Pettersen EO.; (1989). Modulation of cis-dichlorodiammineplatinum(II)-induced cytotoxicity by benzaldehyde derivatives. *Cancer Lett.* 46(1):63–8.

Dunn J.E. Cancer epidemiology in populations of the United States--with emphasis on Hawaii and California and Japan. *Cancer Res*. 35(11 Pt. 2): 3240-5.

Duvel K., Yecies J.L., Menon S., et al.; (2010). Activation of a metabolic gene regulatory network downstream of mTOR complex 1. *Mol Cell*: 39(2):171-183.

Eastman A.; (1999). The mechanism of action of cisplatin: from adducts to apoptosis. In Cisplatin: Chemistry and Biochemistry of a Leading Anticancer Drug. *(Lippert, B., Ed.). Weinheim, Wiley-VCH, Zurich:* 111–134.

Elstrom R.L., Bauer D.E., Buzzai M., et al.; (2004). Akt stimulates aerobic glycolysis in cancer cells. *Cancer Res:* 64(11):3892 -3899.

Espineda C.E., Chang J.H., Twiss J., Rajasekaran S.A., Rajasekaran A.K.; (2004). Repression of Na,KATPase beta1-subunit by the transcription factor snail in carcinoma. *Mol Biol Cell*: 15:1364-73.

Esteller M.; (2000). Epigenetic lesions causing genetic lesions in human cancer: promoter hypermethylation of DNA repair genes. *Eur J Cancer*: 36: 2294-300.

Feng Z., Levine A.J.; (2010). The regulation of energy metabolism and the IGF-1/-mTOR pathways by the p53 protein. *Trends CellBiol*. 20(7):427-434.

Fernandez-Silva P., Enriquez J. A. and Montoya J.; (2003) Replication and transcription of mammalian mitochondrial DNA. *Exp. Physiol.* 88: 41–56.

Ferry K.V., HamiltonT.C., Johnson S.W.; (2000). Increased nucleotide excision repair in cisplatin-resistant ovarian cancer cells: Role of ercc1-xpf. *Biochem Pharmacol.* 60:1305^13.

Fishel R.; (2001). The Selection for Mismatch Repair Defects in Hereditary Hypothesis Nonpolyposis Colorectal Cancer : Revising the Mutator. *Cancer Res.* 61, 7369.

Fraser M., Leung B.M., Yan X., Dan H.C., Cheng J.Q., Tsang B.K.; (2003). p53 is a determinant of X-linked inhibitor of apoptosis protein/Akt-mediated chemoresistance in human ovarian cancer cells. *Cancer Research*: 63(21):7081–7088.

Frezza C. and Gottlieb E.; (2009). Mitochondria in cancer: not just innocent bystanders. *Semin. Cancer Biol.* 19:4–11.

Fuertes M.A., Castilla J., Alonso C., Perez J.M.; (2003). Cisplatin biochemical mechanism of action: from cytotoxicity to induction of cell death through interconnections between apoptotic and necrotic pathways. *Curr Med Chem.* 10:257–266.

Fuertes M.A., Alonso C., Perez J.M.; (2003). Biochemical modulation of Cisplatin mechanisms of action: enhancement of antitumor activity and circumvention of drug resistance. *Chem Rev.* 103(3):645–62.

Fung-Kee M., Oliver T., Elit L., Oza A., Hirte H., Bryson P.; (2007). Optimal chemotherapy treatment for women with recurrent ovarian cancer. *Current Oncology:* 14(5):195.

Galanski M.; (2006). Recent developments in the field of anticancer platinum complexes. *Recent Pat Anticancer Drug Discov.* 1:285–95.

Garber K.; 2006. Energy deregulation: licensing tumor to grow. *Science*: 312, 1158-1159.

Gately D. P. and Howell S. B.; (1993). Cellular accumulation of the anticancer agent cisplatin: a review. *Br. J. Cancer:* 67:1171–1176.

Gatenby R.A. and Gillies R.J.; (2004). Why do cancers have high aerobic glycolysis? *Nat Rev Cancer.* 4(11):891-9. **Geisler J.P., Goodheart M.J., Sood A.K., Holmes R.J., Hatterman-Zogg M.A.,**

Godwin A.K., Meistert A., O'Dwyer P.J., Huangt C.S., Hamilton T.C., Anderson M.E.; (1992). High resistance to cisplatin in human ovarian cancer cell lines is associated with marked increase of glutathione synthesis. *Proc Natl Acad Sci U S A*: 89(7):3070–4.

Goldring E.S., et al.; (1970). The petite mutation in yeast. Loss of mitochondrial deoxyribonucleic acid during induction of petites with ethidium bromide. *J Mol Biol*. 52(2):323-35.

Gonzalez V.M., Fuertes M.A.,Alonso C., Perez J.M.; (2001). Is cisplatin induced cell-death always produced by apoptosis? *Mol Pharmacol*. 59:657–663

Gottlieb E., Tomlinson I.P.; (2005). Mitochondrial tumour suppressors: a genetic and biochemical update. *Nat Rev Cancer*: 5 (11):857-866.

Green A.S., Chapuis N., Lacombe C., et al.; (2011). LKB1/AMPK/m-TOR signaling pathway in hematological malignancies: from metabolism to cancer cell biology. *Cell Cycle*: 10(13).

Green A. E. and Garcia A. A.; (2012). Ovarian Cancer. *Medscape Reference*.

Guppy M., Greiner E., Brand K.; (1993). The role of the Crabtree effect and an endogenous fuel in the energy metabolism of resting and proliferating thymocytes. *Eur J Biochem*. 212(1): 95-99

Harper. M. E., Antoniou A., Villalobos-Menuey E., Russo A., Trauger R., Vendemelio M., George A., Bartholomew R., Carlo D., Shaikh. et al.; (2002). Characterization of a novel metabolic strategy used by drug-resistant tumor cells. *FASEB J.* 16: 1550–1557.

Hanahan D. and Weinberg R.A.; (2011). Hallmarks of Cancer: The Next Generation. *Cell:* 144: 646-674

Hatzivassiliou G. et al.; (2005). ATP citrate lyase inhibition can suppress tumor cell growth. *Cancer Cell:* 8:311-321

Hay N.; (2005). The Akt-mTOR tango and its relevance to cancer. *Cancer Cell:* 8(3):179-183.

Heintz A.P., Odicino F., Maisonneuve P., et al.; (2001). Carcinoma of the ovary. *J Epidemiol Biostat*: 6(1): 107-38.

Himeno S., Imura N.; (2000). HeLa cell transformants overproducing mouse metallothionein show in vivo resistant to cis-platinum in nude mice. *Jpn J Cancer Res.* 91:91–98.

Hishikawa Y., Koji T., Dhar D.K., Kinugasa S., Yamaguchi M., Nagasue N.; (1999). Metallothionein expression correlates with metastatic and proliferativ epotential in squamous cell carcinoma of the esophagus. *Br J Cancer:* 81:712–720.

Holzer A.K., Katano K., Klomp L.W., Howell S.B.; (2004). Cisplatin rapidly down-regulates its own influx transporter hCTR1 in cultured human ovarian carcinoma cells. *Clin Cancer Res.* 2004;10(19):6744–9.

Hsu P.P. and Sabatini D.M.; (2008). Cancer Cell Metabolism: Warburg and Beyond. *Cell:* 134: 703-707.

Huncharek M., Kupelnick B.; (2001). Dietary fat intake and risk of epithelial ovarian cancer: a meta-analysis of 6,689 subjects from 8 observational studies. *Nutr Cancer*: 40: 87-91.

Inoki K., Li Y., Zhu T., et al., (2002). TSC2 is phosphorylated and inhibited by Akt and suppresses m-TOR signalling. *Nat Cell Biol*. 4(9):648-657.

International Federation of Gynecology and Obstetrics (1989). Annual report on the results of treatment in gynecological cancer. *Int J Gynecol Obstet.* 28:189-190.

Ishida S., Lee J, Thiele D.J. and Ira Herskowitz I.; (2002). Uptake of the anticancer drug cisplatin mediated by the copper transporter Ctr1 in yeast and mammals. *PNAS*: 99.

Ishikawa T. and Ali-Osman F.; (1996). Coordinated induction of MRP/GS-X pump and gamma-glutamylcysteine synthetase by heavy metals in human leukemia cells. *J Biol Chem.* 271(25):14981–8.

Isidoro A., Martinez M., Fernandez P.L., Ortega A.D., Santamaria G., Chamorro M., et al.; (2004). Alteration of the bioenergetic phenotype of mitochondria is a hallmark of breast, gastric, lung and oesophageal cancer. *Biochem J*. 378:17-20.

Jascur T. and Boland C.R.; (2006). Structure and function of the components of the human DNA mismatch repair system. Int J *Cancer*: 119:2030-5.

Jemal A., Siegel R., Ward E., Murray T., Xu J., et al.; (2007). Cancer statistics, 2007. *CA Cancer J Clin:* 57: 43–66.

Joerger M., Huitema A. et al.; (2007). Population pharmacokinetics and pharmacodynamics of paclitaxel and carboplatin in ovarian cancer patients: a study by the European organization for research and treatment of cancer-pharmacology and molecular mechanisms group and new drug development group. *Clinical Cancer Research*: 13(21):6410.

Jordan P. and Carmo-Fonseca M.; (2000). *Molecular* mechanisms involved in cisplatin cytotoxicity. *Cell. Mol. Life Sci.* 57, 1229

Judson I. and Kelland L.R.; (2000). New Development and approaches in the platinum Arena. *Drugs*: 59:29-36.

Kartalou M. and Essigmann J. M.; (2001). Mechanisms of resistance to cisplatin. *Mutation Res.* 478: 23 – 43.

Kastenmüller G., Römisch-Margl W., Wägele B., Altmaier E., Suhre K.; (2011). metaP-Server: A Web-Based Metabolomics Data Analysis Tool. *J Biomed Biotechnol.* pii: 839862.

Katano K., Kondo A., Safaei R., Holzer A., Samimi G., Mishima M., Kuo Y.M., Rochdi M. and Howell S.B.; (2002). Acquisition of resistance to cisplatin is accompanied by changes in the cellular pharmacology of copper. *Cancer Res.* 62(22):6559–65.

Kelland L.R.; (2000). Preclinical perspectives on platinum resistance.*Drugs*: 59, 1.

Kennedy A.W., Biscotti C.V., Hart W.R., Webster K.D.; (1989). Ovarian clear cell adenocarcinoma. *Gynecol Oncol.* 32(3): 342-9.

Kim D.H., Sarbassov D.D., Ali S.M., et al.; (2002). mTOR interacts with raptor to form a nutrient-sensitive complex that signals to the cell growth machinery. *Cell*: 110(2):163-175.

King, M.P. and G. Attardi (1989) Human cells lacking mtDNA: repopulation with exogenous mitochondria by complementation. *Science 246(4929)*: p. 500-3.

Kinlaw W.B., Quinn J.L., Wells W.A., Roser-Jones C., Moncur J.T.; (2006). Spot 14: a marker of aggressive breast cancer and a potential therapeutic target. *Endocrinology:* 147:4048–55.

Koberle B,MastersJRW, HartleyJA,Wood RD.; (1999). Defective repair of cisplatin-induced DNA damage caused by reduced XPA protein in testicular germ cell tumours. *Curr Biol.* 9:2738.

Koberle B., Tomicic M.T., Usanova S., Kaina B.; (2010). Cisplatin resistance: preclinical findings and clinical implications. *Biochim Biophys Acta.* 1806:172–82.

Komatsu M., **Sumizawa T., Mutoh M., Chen Z.S., Terada K., Furukawa T., Yang X.L., Gao H., Konishi I., Kuroda H., Mandai M.;** (1999). Review: gonadotropins and development of ovarian cancer. *Oncology*: 57 Suppl 2: 45-8.

Kolasa I.K., Rembiszewska A., Janiec-Jankowska A., Dansonka-Mieszkowska A., Lewandowska A.M., Konopka B. and Kupryjanczyk J.; (2006). PTEN mutation, expression and LOH at its locus in ovarian carcinomas. Relation to TP53, K-RAS and BRCA1 mutations. *Gynecol Oncol.* 103(2): 692–697.

Krishnamachary B., Berg-Dixon S., Kelly B., Agani F., Feldser D. Ferreira G., Iyer N., LaRusch J., Pak B., Taghavi P., Semenza G.L.; (2003). Regulation of colon carcinoma cell invasion by hypoxia-inducible factor1. *Cancer Res.* 63:1138–1143.;

Kroemer G. and Pouyssegur J.; (2008). Tumor cell metabolism: cancer's Achilles' heel. Cancer Cell. 13(6):472-82.

Kuhajda F.P; (2000): Fatty acids synthase and human cancer: new perspective on its role in tumor biology. *Nutrition:* 16: 202-208.

Kuhajda F.P; (2006). Fatty acids synthtase and human cancer: new application of an old pathway. *Cancer Res.* 66:5977-5980.

Kulawiec M., Safina A., Desouki M.M., Still I., Matsui S.I., Bakin A. et al.; (2008). Tumorigenic transformation of human breast epithelial cells induced by mitochondrial DNA depletion. *Cancer Biol Ther.* 7:1732-43.

Kunkel T.A. and Erie D.A.; (2005). DNA mismatch repair. *Annu Rev Biochem*. 74:681-710.;

Kurman R.J., Shih I. M.; (2010). The origin and pathogenesis of epithelial ovarian cancer: a proposed unifying theory. *Am J Surg Pathol.* 34:433–443.

Lautier D., Canitrot Y., Deeley R.G., Cole S.P.; (1996). Multidrug resistance mediated by the multidrug resistance protein (MRP) gene. *Biochem Pharmacol.* 52(7):967–77.

Lee H.C., Yin P.H., Lin J.C., Wu C.C., Chen C.Y., Wu C.W., et al.; (2005). Mitochondrial genome instability and mtDNA depletion in human cancers. *Ann N Y Acad Sci.* 1042:109-22.

Lehninger A.L., Nelson D.L., Cox M.M.; (1993). *Principles of Biochemistry* (II Edition). Worth; New York: 1993

Liedert B., Materna V., Schadendorf D., Thomale J.**, Lage H.;** (2003). Overexpression of cMOAT (MRP2/ABCC2) is associated with decreased formation of platinum-DNA adducts and decreased G2-arrest in melanoma cells resistant to cisplatin. *J Invest Dermatol.* 121(1):172–6.

Lim M.C., Lee D.O., Kang S. et al., (2009). Clinical manifestations in patients with ovarian clear cell carcinoma with or without co-existing endometriosis. *Gynecol Endocrinol*: 25:435-40.

Lim M.C., Chun K.C., Shin S.J., et al.; (2010). Clinical presentation of endometrioid epithelial ovarian cancer with concurrent endometriosis: a multicenter retrospective study. *Cancer Epidemiol Biomarkers Prev.* 19:398-404.

Li X. M., Ganmaa D., Sato A.; (2003). The experience of Japan as a clue to the etiology of breast and ovarian cancers: relationship between death from both malignancies and dietary practices. *Medical Hypotheses*; 60 (2): 268-275.

Luciani A. M., Grande S., Palma A., Rosi A., Giovannini C., Sapora O., Viti V., Guidoni L. ; (2009). Characterization of ^{1}H NMR detectable mobile lipids in cells from human adenocarcinomas. *FEBS J.* 27, 333-346.

Lum J.J., Bui T., Gruber M., et al.; (2007). The transcription factor HIF-1alpha plays a critical role in the growth factor-dependent regulation of both aerobic and anaerobic glycolysis. *Genes Dev*. 21(9):1037-1049.

Luo Z., Zang M., Guo W.; (2010). AMPK as a metabolic tumor suppressor: control of metabolism and cell growth. *Future Oncol*. 6(3):457-470.

Macheda M.L, Rogers S., Best J.D.; (2005). Molecular and cellular regulation of glucose transporter (GLUT) proteins in cancer. *J Cell Physiol*. 202(3):654-662.

Mambo E., Chatterjee A., Xing M., Tallini G., Haugen B.R., Yeung S.C., et al.; (2005). Tumor-specific changes in mtDNA content in human cancer. *Int J Cancer:* 116:920-4.

Mansfield K.D., Guzy R.D., Pan Y., et al.; (2005). Mitochondrial dysfunction resulting from loss of cytochrome c impairs cellular oxygen sensing and hypoxic HIF-alpha activation. *Cell Metab*. 1(6):393-399.

Matoba S., Kang J.G., Patino W.D., et al.; (2006). p53 regulates mitochondrial respiration. *Science:* 312 (5780):1650-1653.

Meijer C., TImmer A., DeVries E.G., Groten J.P, Knol A., Zwart N., Sleijefer D.T., Mulder N.H.; (2000). Role of metallothionein in cisplatin sensitivity of germ-cell tumors. *Int J Cancer* :85(6):777–781.

Menendez J.M. and Lupu R.; (2007). Fatty acid synthase and the lipogenic phenotype in cancer pathogenesis. *Nat Rev Cancer* 7: 10. 763-777.

Menedez J.M.; (2010). Fine-tuning the lipogenic/lipolytic balance to optimize the metabolic requirements of cancer cell growth: molecular mechanisms and therapeutic perspectives. *Biochemica an Biophysica Acta:* 1801:381-391.

Metallo C.M., Gameiro P.A., Bell E.L., Mattaini K.R., Yang J., Hiller K., Jewell C.M., Johnson Z.R., Irvine D.J., Guarente L., et al.; (2012). Reductive glutamine metabolism by IDH1 mediates lipogenesis under hypoxia. *Nature:* 481: 380–384.

Milgraum L.Z. et al.; (1997). Enzymes of the fatty acid synthase pathway are highly expressed in *in situ* breast carcinoma. *Clin. Cancer Res.* 3:2115-2120.

Mitchell P.; (1961). Coupling of phosphorylation to electron and hydrogen transfer by a chemi-osmotic type of mechanism. *Nature*: 191: 144-8.

Miura N., Sugiyama T. and Akiyama S.I.; (2000). Copper-transporting P-type adenosine triphosphatase (ATP7B) is associated with cisplatin resistance. *Cancer Res.* 60(5):1312–6.

Mizumachi T., Muskhelishvili L., Naito A., Furusawa J., Fan C.Y., Siegel E.R., et al.; (2008). Increased distributional variance of mitochondrial DNA content associated with prostate cancer cells as compared with normal prostate cells. *Prostate*: 68:408-17.

Moggs J.G., Szymkowski D.E., Yamada M., et al.; (1997) Differential human nucleotide excision repair of paired and mispaired cisplatin-DNA adducts. *Nucleic Acids Res.* 25(3):480–91.

Montopoli M., Bellanda M., Lonardoni F., Ragazzi E., Dorigo P., Froldi G., Mammi S., Caparrotta L.; (2009). "Metabolic reprogramming" in ovarian cancer cells resistant to cisplatin. *Curr Cancer Drug Targets*: 11(2):226-35.

Morch L.S., Lokkegaard E., Andreasen A.H., Kruger-Kjaer S. and Lidegaard O.; (2009). Ormon Therapy and ovarian cancer. *Jama:* 302(3): 298-305.

Mullen A.R., Wheaton W.W., Jin E.S., Chen P.H., Sullivan L.B., Cheng T., Yang Y., Linehan W.M., Chandel N.S., DeBerardinis R.J.; (2012). Reductive carboxylation supports growth in tumour cells with defective mitochondria. *Nature*: 481: 385–388

Muramatsu Y., Yasegawa Y., Fukano H., Ogawa T., Namuba M., Mour S., Fujimoto Y., Matsuura H., Takai Y., Mori M.; (2000). Metallothionein immunoreactivitiy in head and neck carcinomas - special reference to clinical behaviors and chemotherapy responses. *Anticancer Res.* 20:257

Murdoch W.J.; (2003). Metaplastic potential of p53 down-regulation in ovarian surface epithelial cells affected by ovulation. *Cancer Lett.* 191(1): 75-81.

Musille P. M. and Kohn J. A.; (2013). Phospholipid – Driven gene regulation. *FEBS Lett.*

Mussini C., Pinti M., Bugarini R., Borghi V., Nasi M., Nemes E., et al.; (2005). Effect of CD4-monitored treatment interruption on mitochondrial DNA content in HIV-infected patients: a prospective study. *AIDS*: 19:1627–33.

Mutlu G.M., Scott Budinger G.R., Chandel N.S.; (2010). Mitochondrial metabolism and ROS generation are essential for Kras-mediated tumorigenicity. *Proc. Natl Acad. Sci. USA* 107:8788–8793.

Nagley P. and Linnane A.W.; (1970). Mitochondrial DNA deficient petite mutants of yeast. *Biochem Biophys Res Commun*. 39(5): p. 989-96.

Nakayama K., **Miyazaki K., Kanzaki A., Fukumoto M., Takebayashi Y.;** (2001). Expression and cisplatin sensitivity of copper-transporting P-type adenosine triphosphatase (ATP7B) in human solid carcinoma cell lines. *Oncol Rep.* 8(6):1285–7.

Nakayama K., **Kanzaki A., Ogawa K., Miyazaki K., Neamati N., Takebayashi Y.;** (2002). Copper-transporting P-type adenosine triphosphatase (ATP7B) as a cisplatin based chemoresistance marker in ovarian carcinoma: comparative analysis with expression of MDR1, MRP1, MRP2, LRP and BCRP. *Int J Cancer*: 101(5):488–95.

Neeraj L., Srinivasa R. P., Raghunandan V., Alampady K. S., Phyllis C. H., Najla F.; (2011) Histologic, Molecular, and Cytogenetic Features of Ovarian Cancers: Implications for Diagnosis and Treatment1. *RadioGraphics:* 31:625-646

NelsonD.L and Cox M.M; (2002). *I Principi di Biochimica di Lehninger, 3^{a} ed., Bologna,* Zanichelli.

Ookhtens M., Kannan R., Lyon I., Baker N.; (1984). Liver and adipose tissue contributions to newly formed fatty acids in an ascites tumor. *Am J.Physiol.* 247:146-153.;

Ohta S.; (2006). Contribution of somatic mutations in the mitochondrial genome to the development of cancer and tolerance against anticancer drugs. *Oncogene*: 25:4768–4776

Papandreou I., Cairns R.A., Fontana L., et al.; (2006). HIF-1 mediates adaptation to hypoxia by actively downregulating mitochondrial oxygen consumption. *Cell Metab*. 3(3):187-197.

Pastorino J.G., Hoek J.B., Shulga N.; (2005). Activation of glycogen synthase kinase 3beta disrupts the binding of hexokinase II tomitochondria by phosphorylating voltage-dependent anion channel and potentiates chemotherapy-induced cytotoxicity. *Cancer Res*. 65(22):10545-10554.

Park S.Y., Chang I., Kim J.Y., Kang S.W., Park S.H., Singh K. et al.; (2004). Resistance of mitochondrial DNA-depleted cells against cell death: role of mitochondrial superoxide dismutase. *J Biol Chem.* 279:7512–7520.

Park M.S., De Leon M., Devarajan P.; (2002). Cisplatin induces apoptosis in LLC-PK1 cells via activation of mitochondrial pathways. *J Am Soc Nephrol* .13:858– 865;

Pasetto L.M., D'Andrea M.R., Brandes A.A., Rossi E., Monfardini S.; (2006). The development of platinum compounds and their possible combination. *Crit Rev Oncol Hematol:* 60 :59–75.

Patiar S. and Harris L.; (2006). Role of hypoxia-inducible factor-1alpha as a cancer therapy target. *Endocr Relat Cancer*: 13 :61-75.

Payet D.G., Sip F., Leng M.; (1993). Instability of the monofunctional adducts in cis-[Pt(NH3)2(N7-N-methyl-2-diazapyrenium)Cl](2+)-modified DNA: rates of cross-linking reactions in cis-platinum-modified DNA. *Nucl. Acids Res.* 21, 5846.

Peleg-Shulman T. and Gibson D. J.; (2001). Cisplatin-protein adducts are efficiently removed by glutathione but not by 5′-guanosine monophosphate. *Am.Chem. Soc.* 123, 3171.

Pettersen E.O., Schwarze P.E., Dornish J.M., Nesland J.M.; (1986). Antitumour effect of benzylidene-glucose (BG) in rats with chemically induced hepatocellular carcinoma. *Anticancer Res.* 6(2):147–52.

Peltomaki P.; (2003). Role of DNA mismatch repair defects in the pathogenesis of human cancer. *JClinOncol*. 21:1174-9.

Peyrone M.; (1845). *Ann. Chem. Pharm*. *51*, 1.

Pitkänen S. and Robinson B.H.; (1996)Mitochondrial complex I deficiency leads to increased production of superoxide radicals and induction of superoxide dismutase. *J Clin Invest.* 98*:* 345*–351,.*

Pizer E.S., Jackisch C., Wood F.D., Pasternack G.R., Davidson N.E., Kuhajda F.P.; (1996). Inhibition of fatty acid synthesis induces programmed cell death in human breast cancer cells. *Cancer Res.* 56:2745–7.

Pouyssegur J., Dayan F., Mazure N.M.; (2006). Hypoxia signalling in cancer and approaches to enforce tumour regression. *Nature*: 441(7092):437-443.

Preston TJ, Abadi A, Wilson L, Singh G.; (2001). Mitochondrial contribution to cancer cell physiology: potential for drug development. *Adv Drug Deliv Rev.* 49:45–61.

Quirk J.T. and Natarajan N.; (2005). Ovarian cancer incidence in the United States, 1992-1999. *Gynecol Oncol.* 97(2): 519-23.

Rabik. C. A. and Dolan M. E.; (2007). Molecular mechanisms of resistance and toxicity associated with platinating agents. *Cancer Treatment Rev.* 33: 9 – 23.

Rashid A., Pizer E.S., Moga M., Milgraum L.Z., Zahurak M., Pasternack G.R., Kuhajda F.P., Hamilton S.R.; (1997). Elevated expression of fatty acid synthase and fatty acid synthetic activity in colonrectal neoplasia. *Am J.Physiol.* 150:201-208

Rebbeck T.R., Kauff N.D., Domchek S.M.; (2009). Meta-analysis of risk reduc tion estimates associated with risk-reducing salpingo-ophorectomy in BRCA1 or BRCA2 mutation carriers. *J Natl Cancer Inst*: 101(2): 80–7

Reitzer L. J., Wice B. M., Scheffler I. C.; (1979).Evidence that glutamine, not sugar, is the major energy source for cultured HeLa cells*. J. Biol. Chem.* 254, 2669-2676.

Rosenberg B., VanCamp L., Krigas T.; (1965). *Nature: 205*, 698.

Rossing M.A, Tang M.T, Flagg E.W., Weiss L.K. and Wicklund K.G.; (2004). A case-control study of ovarian cancer in relation to infertility and the use of ovulation-inducing drugs. *Am J. Epidemiol.* 160(11): 1070-8.

Rudin C.M., Yang Z., Schumaker L.M., VanderWeele D.J., Newkirk K., Egorin M.J., Zuhowski E.G., Cullen K.J.; (2003). Inhibition of glutathione synthesis reverses Bcl-2-mediated cisplatin resistance. *Cancer Res.* 63(2):312–8.

Saiati L.M. and Amir-Ahmady B.; (2001). Dietary regulation of expression of glucose-6-phosphate dehydrogenase. *Annu Rev Nutr.* 21:121–40.

Salani R., Kurman R.J., Giuntoli R., Gardner G., Bristow R., Wang T.L. and Shih I.M.; (2008). Assessment of TP53 mutation using purified tissue samples of ovarian serous carcinomas reveals a higher mutation rate than previously reported and does not correlate with drug resistance. *Int J Gynecol Cancer*:18(3): 487–491.

Samimi G., Safaei R., Katano K., Holzer A.K., Rochdi M., Tomioka M., Goodman M., Howell S.B.; (2004). Increased expression of the copper efflux transporter ATP7A mediates resistance to cisplatin, carboplatin, and oxaliplatin in ovarian cancer cells. *Clin Cancer Res.* 10(14):4661–9.

Scholl C., Gilliland D.G., Frohling S.; (2008). Deregulation of signaling pathways in acute myeloid leukemia. *Semin Oncol*. 35 (4):336-345.

Selvanayagam P. and Rajaraman S.; (1996). Detection of mitochondrial genome depletion by a novel cDNA in renal cell carcinoma. *Lab Invest*. 74:592-9.

Selvakumaran M., Pisarcik D.A., Bao R., Yeung A.T., Hamilton T.C.; (2003). Enhanced cisplatin cytotoxicity by disturbing the nucleotide excision repair pathway in ovarian cancer cell lines. *Cancer Res.* 63:1311-6.

Semenza G.L.; (2007). Hypoxia-inducible factor 1 (HIF-1) pathway. *Sci STKE, 2007*: (407):cm8.

Semenza G.L.; (2003). Targeting HIF-1 for cancer therapy. *Nat Rev Cancer:* 3(10):721-732.

Shackelford D.B. and Shaw R.J.; (2009). The LKB1-AMPK pathway: metabolism and growth control in tumour suppression. *Nat Rev Cancer*: 9(8):563-575.

Shaul Y.; (2000). c-Abl: activation and nuclear targets. *Cell Death and Differentiation*: 7(1):10–16.

Shaw R.J; (2006). Glucose metabolism and cancer. *Curr Opin Cell Biol.* 18(6):598-608; Bui T. and

Schrenk D., Baus P.R., Ermel N., Klein C., Vorderstemann B., Kauffmann H.M.; (2001). Up-regulation of transporters of the MRP family by drugs and toxins. *Toxicol Lett.* 120(13):51–7.

Siddik Z.H.; (2003). Cisplatin: mode of cytotoxic action and molecular basis of resistance. *Oncogene:* 22(47):7265–79.

Siegsmund M.J., Marx C, Seeman O, Schummer B, Steidler A, Toktomambetova L, Kohrmann K-U, Rassweiler J, Alken P.; (1999). Cisplatin-resistant bladder carcinoma cells: enhanced expression of metallotioneins. *Urol Res.* 27:157–163. [

Singer G., Oldt R., Cohen Y., Wang B.G., Sidransky D., Kurman R.J. and Shih I.; (2003). Mutations in BRAF and KRAS characterize the development of low-grade ovarian serous carcinoma. *J Natl Cancer Inst.* 95(6): 484–486.

Soslow R.A.; (2008). Histologic subtypes of ovarian carcinoma: an overview. *Int J Gynecol Pathol*. 27(2):161-74.

Soti C., Racz A., Csermely P. J.; (2002). Heat shock proteins as emerging therapeutic targets. *Biol.Chem.* 277, 7066.

Speelmans G., Staffhorst R.W., Versluis K., Reedijk J., de Kruijff B.; (1997). Cisplatin complexes with phosphatidylserine in membranes. *Biochemistry*: 36, 10545.

Sreekumar A., Poisson L.M., Rajendiran T.M., Khan A.P., Cao Q., Yu J., Laxman B., Mehra R., Lonigro R.J., Li Y., Nyati M.K., Ahsan A., Kalyana-Sundaram S., Han B., Cao X., Byun J., Omenn G.S., Ghosh D., Pennathur S., Alexander D.C., Berger A., Shuster J.R., Wei J.T., Varambally S., Beecher C., Chinnaiyan A.M.; (2009). Metabolomic profiles delineate potential role for sarcosine in prostate cancer progression. *Nature:* 457(7231):910-4.

Stojic L., Brun R., Jiricny J.; (2004). Mismatch repair and DNA damage signalling. *DNA Repair (Amst):* 3(89):1091–101.

Suzuki H., Itoh F.,Toyota M., et al.; (1999). Distinctmethylation pattern andmicrosatellite instability in sporadic gastric cancer. *Int J Cancer:* 83:309-13.

Swinnen J.V., Brusselmans K., Verhoeven G.; (2006). Increased lipogenesis in cancer cells. New players, novel targets. *Curr. Opin. Clin.Nutr. Metab. Care*: 9:358-365.

Taanman J.W.; (1999). The mitochondrial genome: structure, transcription, translation and replication. *Biochim Biophys Acta:* 1410:103-23.

Tacka K. A., Dabrowiak J. C., Goodisman J., **Penefsky H. S. and Souid A. K.;** (2004). Effects of cisplatin on mitochondrial function in Jurkat cells. *Chem. Res. Toxicol.* 17: 1102–1111.

Thompson C.B.; (2006). Cancer's sweeth tooth. *Cancer Cells*: 9:419-420.; Garber K.; (2006). Energy deregulation licensing tumors to grow. *Science*: 312:1158-1159.

Tong L. (2005). Acetyl-Coenzyme A carboxylase: crucial metabolic enzyme and attractive target for drug discovery. *Cell Mol. Life Sci.* 62:1784-1803.

Toyoda H., Mizushima T., Satoh T., Izuka N., Nomoto A., Chiba H., Mita M., Naganuma A., Siu L.L., Banerjee D., Khurana R.J., Pan X., Pflueger R., Tannock I.F.; (1998). The prognostic role of p53, metallothionein, P-glycoprotein, and MIB-1 in muslce-invasive urothelial transitional cell carcinoma. *Clin Cancer Res.* 4:559–564.

Tseng L.M., Yin P.H., Chi C.W., Hsu C.Y., Wu C.W., Lee L.M., et al.; (2006). Mitochondrial DNA mutations and mitochondrial DNA depletion in breast cancer. *Genes Chromosomes Cancer*: 45:629-38.

Vander Heiden M.G., Cantley L.C., Thompson C.B.; (2009). Understanding the Warburg Effect: The Metabolic Requirements of Cell Proliferation. Science: 324:1029-1033.

Vella N., Aiello M. et al.; (2011). 'Genetic profiling'and ovarian cancer therapy (Review) *Molecular medicine reports*: 4:771–777.

Viniegra J.G., Losa J.H., Sánchez-Arévalo V.J., et al.; (2002). Modulation of PI3K/Akt pathway by E1a mediates sensitivity to cisplatin. *Oncogene*: 21(46):7131–7136.

Vincent T. DeVita SHSAR, (2001). Principles and Practice of Oncology Single Volume. *Cancer*.

Wallace D.C.; (2011). Bioenergetic origins of complexity and disease. *Cold Spring Harb Symp Quant Biol.* 76:1-16.

Wang D and Lippard S.; (2005)**.** Cellular processing of platinum anticancer drugs. *Nature Reviews Drug Discovery:* 4(4):307–320.

Warburg O., Wind F., Negelein E.; (1927). The metabolism of tumors in the body. *J Gen Physiol.* 8(6):519-530

Warburg O.; (1956). On the origin of cancer cells. *Science*: 123(3191):309-314.].

Weber K., Ridderskamp D., Alfert M., Hoyer S., Wiesner R.J.; (2002). Cultivation in glucosedeprived medium stimulates mitochondrial biogenesis and oxidative metabolism in HepG2 hepatoma cells. *Biol Chem*. 383:283-90.

Weinberg F., Hamanaka R., Wheaton W.W., Weinberg S., Joseph J., Lopez M., Kalyanaraman B., Weinhouse S.; (1976). The Warburg hypothesis fifty years later. Z. *Krebsforsch. Klin. Onkol. Cancer Res. Clin. Oncol.* 87:115–126.

Welsh C., Day R., McGurk C., Masters J.R.,Wood R.D., Koberle B.; (2004). Reduced levels of XPA, ERCC1 and XPF DNA repair proteins in testis tumor cell lines. *IntJ Cancer:* 110:352-61.

Whittemore A.S, Harris R., Itnyre J.; (1992). Characteristics relating to ovarian cancer risk: collaborative analysis of 12 US case-control studies. II. Invasive epithelial ovarian cancers in white women. Collaborative Ovarian Cancer Group. *Am J Epidemiol.* 136(10): 1184-203.

Wise D.R., Ward P.S., Shay J.E., Cross J.R., Gruber J.J., Sachdeva U.M., Platt J.M., Dematteo R.G., Simon M.C., Thompson C.B.; (2011). Hypoxia promotes isocitrate dehydrogenase-dependent carboxylation of α-ketoglutarate to citrate to support cell growth and viability. *Proc Natl Acad Sci.* 108: 19611–19616.

Witte A.B., (2005). Inhibition of thioredoxin reductase but not of glutathione reductase by the major classes of alkylating and platinum-containing anticancer compounds. *Free Radic Biol Med.* 2005;39(5):696–703.

Wokolorczyk D., Gliniewicz B., Sikorski A., et al.; (2008). A range of cancers is associated with the **Testa J.R. and Tsichlis P.N.;** (2005). AKT signaling in normal and malignant cells. *Oncogene:* 24(50):7391-7393.rs6983267 marker on chromosome 8. *Cancer Res*. 68(23):9982-9986.

Wu C.W., Yin P.H., Hung W.Y., Li A.F., Li S.H., Chi C.W., et al.; (2005). Mitochondrial DNA mutations and mitochondrial DNA depletion in gastric cancer. *Genes Chromosomes Cancer:* 44:19-28.

Xia J., Psychogios N., Young N., Wishart D.S.; (2009). MetaboAnalyst: a web server for metabolomic data analysis and interpretation. *Nucl. Acids Res.* 37: W652-660.

Xia J. and Wishart D.S.; (2011). Web-based inference of biological patterns, functions and pathways from metabolomic data using MetaboAnalyst. *Nat Protoc.* 6(6):743-760.

Xiao H., Verdier-Pinard P. et al.; (2006). Insights into the mechanism of microtubule stabilization by Taxol. Proc Natl Acad Sci U S A: 103(27):10166–10173.

Yang D. Wang M.T., Tang Y., et al.; (2010). Impairment of mitochondrial respiration in mouse fibroblasts by oncogenic H-R AS (Q61L). *Cancer Biol Ther.* 9(2):122-133.

Yin P.H., Lee H.C., Chau G.Y., Wu Y.T., Li S.H., Lui W.Y., et al.; (2004). Alteration of the copy number and deletion of mitochondrial DNA in human hepatocellular carcinoma. *Br J Cancer:* 90:2390-6.

Yu M., Zhou Y., Shi Y., Ning L., Yang Y., Wei X., et al.; (2007). Reduced mitochondrial DNA copy number is correlated with tumor progression and prognosis in Chinese breast cancer patients. *IUBMB Life* 59:450-7.

Zamble D.B., Mu D., Reardon J.T., Sancar A., Lippard S.J.; (1996). Repair of cisplatin--DNA adducts by the mammalian excision nuclease. *Biochemistry:* 35(31):10004–13.

Zorbas H. and Keppler B.K.; (2005). Cisplatin damage: are DNA repair proteins saviors or traitors to the cell? *Chembiochem.* 6(7):1157–66.